NASA Technical Memorandum 82764

Computational Methods for Internal Flows with Emphasis on Turbomachinery

William D. McNally and Peter M. Sockol
Lewis Research Center
Cleveland, Ohio

Presented at the
Symposium on Computers in Flow Predictions
and Fluid Dynamics Experiments at the
ASME Winter Annual Meeting
Washington, D.C., November 15-20, 1981

NASA

COMPUTATIONAL METHODS FOR INTERNAL FLOWS WITH EMPHASIS ON TURBOMACHINERY

By

William D. McNally and Peter M. Sockol
NASA Lewis Research Center
Cleveland, Ohio

ABSTRACT

A review is given of current computational methods for analyzing flows in turbomachinery and other related internal propulsion components. The methods are divided primarily into two classes, inviscid and viscous. The inviscid methods deal specifically with turbomachinery applications. Viscous methods, on the other hand, due to the state-of-the-art, deal with generalized duct flows as well as flows in turbomachinery passages. Inviscid methods are categorized into the potential, stream function, and Euler approaches. Viscous methods are treated in terms of parabolic, partially parabolic, and elliptic procedures. Various grids used in association with these procedures are also discussed.

INTRODUCTION

The subject of internal flows is a very broad and complex one, encompassing a wide variety of geometries and flow situations. There are many examples of machinery in which internal flows play an important part. One such example is the modern turbofan engine, such as that depicted in Figure 1. Here the understanding of internal flows is very important in predicting the performance of many key components. These include the inlets and exhaust nozzles at the extremeties of the engine, the rotating and stationary turbomachinery blade rows in both the compressor and turbine sections of the engine, the interconnecting ducts, and the combustor portion of the engine. Another significant type of machinery in which internal flows are extremely important is the internal combustion engine. Here the flows to the various inlet and exhaust ducts, ports, and cylinders are extremely complex and basically unsteady. These complex flows must be understood before the performance of such engines can be predicted. Another situation where complex internal flows play a large role in the performance of machinery is that of nuclear reactors. Here the flows through a maze of tubes and passages interact to influence the performance and reliability of the entire system. In addition, the steam generator portion of the nuclear reactor has all complexity of the gas turbine engine described previously, as well as the complexities brought on by a two phase flow situation.

In this paper, in order to make the subject more manageable, we have chosen to treat in detail a subset of the total class of internal flows. We will be speaking specifically about flows through turbomachinery blade rows of all types, as well as viscous flows through ducts of various geometries.

The paper will be divided primarily into descriptions of inviscid flow methods and then viscous flow methods. Inviscid flow methods will be described in the context of turbomachinery blade row applications because a large number of

analyses have been developed for these situations. For viscous flow methods the state-of-the-art is less well advanced. Here the treatment will be expanded beyond turbomachinery to also encompass duct flows. The analyses discussed in the paper will also be limited to steady flows. Although some do have the capability to predict unsteady flow phenomena, they have been developed primarily as predictors for steady flows. They generally are not used in their present form in order to solve unsteady flow problems in turbomachinery.

In describing the analyses, a variety of different geometries will be discussed. We will be describing analyses which apply first of all to axial blade geometries in both compressor and turbine blade rows. Some of these analyses are also designed to predict mixed flow situations, which are encountered in both centrifugal compressors and radial inflow turbines. There are also some analyses designed for pure radial situations, such as those encountered in radial diffusers as well as the inlet pre-swirl vanes in radial turbine situations. Some of the above analyses also apply to geometries which have no blades, such as the interconnecting ducts and bends in turbomachinery. Another differentiation is that between rotating and stationary blade rows, with most of the analyses applying to both. Finally, some types of analyses apply only in certain flow ranges. Most will handle the subsonic flow regime, while emphasis in the recent past has been upon analyses for the transonic and supersonic flow regimes.

A wide variety of flow characteristics exist in the various types of turbomachinery just described. The objective of the analyses to be discussed later will be to predict as many of these flow features as is possible. Figure 2 illustrates for a turbomachinery blade row situation many of the important flow features which we will ideally be trying to compute with the methods described in this paper. First of all, large axial, radial and centrifugal pressure gradients exist within the flow passages due to the turning of the fluid within the blade rows. Secondly, this turning of the fluid within the passages redistributes the incoming vorticity field and generates cross flows. At higher velocities strong shocks exist within the blade passages. These can be complex and interacting, and they in turn can generate their own additional vorticity fields. These shocks, of course, interact with the blade surfaces and endwall boundary layers, often causing separation and additional blade loss.

There are also a wide variety of viscous flow phenomena existing in the blade passages. Primarily there are the boundary layers which exist on all blade and endwall surfaces as well as on the surfaces of midspan dampers which may exist within the blade passages. Such boundary layers can have laminar, transitional, and turbulent regions. When pressure gradients are strong, of course, separation can also occur. Some separations may experience reattachment. Finally, there are the wakes which exist downstream of all blade rows.

In addition to these common flow features, there are other more complex viscous flows which serve to redistribute the internal vorticity in the blade passages. The first of these, commonly encountered in turbines, is the horseshoe vortex which is generated at the junction of the blunt leading edge and the endwall. Such vortices curl up, flow across the passage, and are shed downstream off the endwall or the surface of the adjacent blade row. Another complex flow phenomenon is the tip clearance flow in which a vortical flow is induced by the leakage of fluid across the unshrouded tip of a rotating or a

stationary blade. Finally, the fact that half the blade rows operate in a rotating reference frame introduces the effects of centrifugal and Coriolis forces on both the mean flow and turbulence in these flow passages.

The resultant flow picture is an extremely complex one, particularly in the multi-stage environment that exists in modern turbomachinery. No single analysis can hope to model all of these flow phenomenon at the same time. In the analyses to be described here, a number of different approaches are used to divide this overall problem into one of manageable size. We have chosen here to separate these models into two major groups, inviscid analyses and viscous analyses. Within these classifications there are many other types of modeling assumptions which are made. First, the assumption is always made to limit these analyses to a single blade row, either stationary or rotating (except in the case of hub-to-shroud stream function analyses, some of which have multi-stage capability). Next, within a given blade row, for a steady state type of solution, the assumption is made that the flow in all blade passages is identical; thus only a single blade passage has to be analyzed. Within a blade passage the next decision to be made is whether a two-dimensional or three-dimensional flow solution will be obtained. Obviously in a three-dimensional flow solution the entire passage is considered; however, many times assumptions are made to eliminate flows over the blade tips or the consideration of dampers which may exist in the blade passage. Two-dimensional flow solutions are typically done on one of two types of flow surfaces. The first of these is a meridional plane solution, treating equations that model flow on an average or mean flow surface between the suction and pressure sides of the blade (Figure 3). This surface is generally formed from the projection of the mean camber line of the blade onto the mid passage, with corrections made at the leading and trailing edges for incidence and deviation. The second type of surface on which 2D analyses can be made is the blade-to-blade surface. This surface is generally formed by rotating around the blade row, in the circumferential direction, one of the calculated streamlines in the meridional plane. Such surfaces, therefore, are axisymmetric and usually have radius change from inlet to outlet. Quasi-3-dimensional effects can also be considered on such a surface by giving it a thickness which varies in the meridional flow direction from inlet to outlet.

Beyond the decision concerning the dimensionality of the solution, a number of decisions can be made in the process of modeling the full flow equations down to a reasonable subset to be solved in the particular analysis being performed. Tradeoffs have to be made between modeling sufficient flow physics to capture the important features of the flow, and reducing the equations and boundary conditions such that exorbitant computer time is not consumed in obtaining a solution. Some of the assumptions and approaches which have been used in the past will be summarized in the historical section which follows.

Historical Perspective

A number of excellent articles have appeared in the literature in the last several years reviewing the different analysis methods and theories which have been used to describe the fluid flow through turbomachinery [1, 2, 3, 4, 5, 6, 8]. These do an excellent job of reviewing the early work in the field, as well as some of the more recent approaches which have been developed.

In the 50's and 60's, singularity methods were often used to compute the two-dimensional incompressible potential flows through cascade blade rows. Such

analyses were primarily applied on blade-to-blade types of flow surfaces. These analyses have been reviewed by Gostelow [1], and Perkins and Horlock [3]. These methods will not be discussed in further detail here.

Also in the 50's and 60's classical secondary flow theory was developed to predict three dimensional incompressible rotational or vortical flow in cascades. Such methods have been reviewed by Horlock and Lakshminarayana [2]. These methods likewise will not be discussed in this paper.

In the 60's and early 70's finite difference approaches began to gain prominence, and were used to calculate two-dimensional, subsonic, inviscid flows in turbomachinery. Both streamline curvature and stream function approaches were used, and were applied on both meridional and blade-to-blade flow surfaces. These approaches are reviewed by Gostelow [1], Perkins and Horlock [3], and Japikse [4]. Stream function methods will be discussed in the inviscid flow sections to follow.

During the 1970's time-marching solutions of the Euler equations began to be used to solve both two-dimensional and three-dimensional transonic flows in blade rows. In the 2D cases such methods were applied on both meridional and blade-to-blade surfaces. Some of these methods are reviewed by Japikse [4], and Habashi [5]. They will be discussed and updated in this paper.

Also during the 1970's numerical solutions to the full potential equations for two dimensional transonic flow in turbomachinery began to appear. A great deal of work has been done to extend such methods up to the present time. Early full potential solutions were reviewed by Habashi [5], and the later approaches will be discussed and updated here.

During the 70's many of the above methods, as well as some early viscous approaches, began to be applied to flows in centrifugal impellers. These methods are reviewed in the paper by Adler [6]. These methods are also discussed and updated here. Finally the state-of-the-art in the computation of a wide variety of turbulent flows was addressed at the recent AFOSR-HTTM-Stanford Conference on Complex Turbulent Flows [7]. The relevant findings from this conference will also be discussed.

The review to be given here begins with the consideration of computational meshes, since to a large degree the success of analysis approaches hinges on the nature of the solution grid which is used. This discussion will include consideration of desirable grid properties, the various mesh topologies in use, and methods of grid generation.

Inviscid flow analysis methods are considered next, the Euler equations are introduced, and the difficulties in solving the primitive variable form are discussed. The stream function formulation for two dimensional flows and the scalar potential approximation are both presented, and the advantages and limitations of each are described. The various methods currently in use for turbomachinery flow analysis are then reviewed.

The next section will consider viscous methods. The time-averaged Navier-Stokes equations are introduced and the many difficulties associated with their solution are discussed. Parabolic and partially parabolic approximations are presented and the advantages and limitations of each are described. The various methods in use for both turbomachinery blade row analyses and for generalized duct flow analyses are then reviewed.

Finally a short discussion on the status of turbulence modelling is given. The paper will conclude with comments on future directions.

COMPUTATIONAL GRIDS

The general approach to numerical solution involves discretizing the fluid equations on a network of points, or grid, throughout the physical domain. The accuracy of the resultant solution can depend to a great degree on the properties of this grid.

Cartesian grids, when used, have generally been used in the physical domain. However, they often create problems. At boundaries not aligned with one of the particular mesh directions, either partial mesh cells must be used or external dummy grid points must be introduced. This results in a cumbersome treatment of the boundary conditions and inaccurate results in some cases. A second problem is the lack of resolution of the grid in regions of high flow gradients. Adequate resolution of the flow in regions adjacent to highly curved boundaries often requires local subgrids to be used. The placement of subgrids within the larger grid structure necessitates increased coding, and the resultant logic problems that come with the interaction between the subgrid and the major grid. A final problem is that boundary layers and wakes, which are not generally aligned with the major directions, are often difficult to resolve.

Recent efforts have been placed on devising methods of generating grids possessing a number of desirable features which provide a much more accurate solution in the important regions of the flow. Some of the characteristics of such grids are the following.

1. At solid surfaces all grid lines should be either parallel or normal to the boundary. This simplifies the boundary condition formulation and thus improves the accuracy of the solution. It can also simplify the modelling of the viscous terms in viscous flow calculations.

2. Away from solid surfaces the mesh should not be highly sheared, as this tends to degrade the accuracy of the solution, especially near shocks and other high flow gradient regions.

3. The grid should provide the ability to cluster lines to a desired density in critical regions such as near solid surfaces, at shocks, near leading and trailing edges, and in other regions of high surface curvature.

4. In steady state turbomachinery blade row calculations the assumption is usually made that the flow is identical in neighboring passages. Therefore mesh periodicity is a requirement to simplify the application of boundary conditions at these locations.

5. At upstream and downstream boundaries, adequate but not excessive mesh density is required in order to resolve the flow at these locations and properly provide for the application of boundary conditions.

6. For numerical stability, some algorithms require mesh aspect ratios which don't depart too far from one.

It is usually not possible to obtain a grid which incorporates all of the above features. In many applications these requirements can be in direct conflict. For example, the requirement for local clustering of the grid may lead to excessive shearing in certain regions. Or, the periodicity requirement can be incompatible with the requirement for near-orthogonality in staggered blade rows. Since no grid can possess all of the above features, obviously compromises have to be made which depend on the particular application.

To satisfy these requirements, several types of grids have been developed for use with different geometries. For duct flow calculations, so-called channel grids are used (Figure 4). These consist of a set of throughflow lines together with a set of lines or surfaces normal to these.

For turbomachinery blading three types of grids have been developed.

1. H-type, which is simply a channel grid which has throughflow grid lines aligned with the blades, and the opposing set of grid lines running in the circumferential direction (Figures 5 and 6).

2. O-type, which has one family of lines forming closed loops about the blades, and a second family crossing the first with grid lines radiating out from the blade surfaces to the periodic boundaries (Figures 7 and 8).

3. C-type, which has one family of grid lines originating at the downstream boundary, progressing upstream parallel to the flow, circling the blade and continuing downstream again parallel to the flow. The second family crosses the first, originating at the blade and wake centerline and progressing out to the periodic boundaries (Figures 9 and 10).

Grid Generation Methods

Three general approaches have been employed to generate such grids: conformal mapping, differential equation techniques, and algebraic techniques. Recent updates on a variety of techniques employing these methods are given in Reference 9.

The conformal mapping approach proceeds generally as follows. The physical domain is transformed into a simpler one using complex variable techniques. A rectangular or near orthogonal grid is then constructed in the transformed region by simple algebriac procedures. The transformation of this simple grid back into the physical domain then produces the desired curvilinear mesh in that domain. This procedure is relatively rapid, but control over the placement of mesh points in somewhat limited. The method only lends itself to the generation of two-dimensional grids, but these in turn can be stacked to give a three-dimensional grid. General conformal mapping techniques are surveyed in Reference 10.

In the differential equation technique, the curvilinear coordinates in physical space are defined to be the solution of a set of coupled Poisson equations, one for each of the coordinate directions (ξ, η, ζ, in three dimensions). These equations, however, are somewhat difficult to solve in the physical space. They are therefore transformed to a quasi-linear elliptic system of equations in the rectangular computational space. In this set of equations the cartesian physical coordinates (x, y, z) are the unknowns. This system is then solved by standard finite difference techniques (relaxation methods) to obtain the locations of grid points (x, y, z) in the physical space.

This procedure is quite flexible, and allows considerable control over the placement of grid points. However, it is more time consuming than other approaches. A good description of this technique is contained in Reference 11.

Finally, in the algebraic techniques, curvilinear coordinates are constructed in the physical space through the use of algebraic interpolating functions. Opposing bounding surfaces are represented as algebraic functions of some parameter, ξ . These opposing surfaces form the first and last members of one family of coordinate curves. The second family of coordinate curves is formed by connecting points of equal ξ with interpolating functions in the common parameter η . The remaining members of the first family of coordinate curves are formed by connecting points of equal η . This method is potentially the fastest and the most flexible of all the grid generation techniques. However, the greater flexibility does require more interaction from the user, and the technique may be slightly difficult to master at first. Reference 12 describes one of the more advanced algebraic grid generation techniques.

INVISCID METHODS

Euler Equations

The ultimate equations we would like to solve in any internal flow situation through ducts or turbomachinery are the Navier-Stokes equations which govern general viscous fluid flows. However, solving these equations in their full form on modern day computers is still quite time consuming.

A great deal of information can be gained in most flow situations through solving a simplified form of the Navier Stokes equations, in which all of the viscous terms have been neglected. These are the governing equations for inviscid flows known as the Euler equations. These equations in vector form are as follows:

$$\frac{\partial U}{\partial t} + \frac{\partial F}{\partial x} + \frac{\partial G}{\partial y} = 0 \tag{1}$$

where

$$U = \begin{Bmatrix} \rho \\ \rho u \\ \rho v \\ e \end{Bmatrix} \quad F = \begin{Bmatrix} \rho u \\ \rho u^2 + p \\ \rho u v \\ (e+p)u \end{Bmatrix} \quad G = \begin{Bmatrix} \rho v \\ \rho u v \\ \rho v^2 + p \\ (e+p)v \end{Bmatrix} \tag{2}$$

and ρ and p are the static density and pressure, u and v are the Cartesian velocity components in the x and y directions, and e is the total energy per unit volume. The total energy, e , is related to the internal energy per unit mass, ε , by the following relation

$$\varepsilon = \frac{e}{\rho} - \frac{u^2+v^2}{2} \tag{3}$$

The internal energy, ε , can be related to the pressure and density by the ideal gas relation

$$\varepsilon = \frac{1}{\gamma - 1}\frac{p}{\rho} \tag{4}$$

where γ denotes the ratio of specific heats.

These equations are presented in terms of the conservation variables of mass, momentum, and total energy, and these are commonly the terms for which the equations are solved. The equations are also presented in terms of two-dimensional cartesian components of velocity for the sake of simplicity. Most of the comments made in terms of the equations to be presented in this paper can be extended easily to apply to three-dimensional flows, unless otherwise noted.

In most instances the solution desired is that to the steady state Euler equations, with the time terms not included. This system of equations is a first-order system of partial differential equations. That fact is the source of much of the difficulty in obtaining solutions to these equations in their present form. The equations change in form depending upon the local flow regime. In subsonic flow their character or type is elliptic, whereas in supersonic flow regimes they are of hyperbolic type. This leads to major difficulties in numerically solving the equations, since the locations of the particular flow regimes are not known a priori. In a totally supersonic flow field, where the equations are hyperbolic everywhere, some very efficient methods exist for their solution. Employing the method of characteristics or a simple marching procedure are two common approaches used with supersonic flows. In subsonic domains, however, no good general solution method has been devised for solving this system of elliptic first order equations. One common approach that has been devised for solving these equations in either a subsonic flow field or a mixed subsonic-supersonic flow field is to reintroduce the time terms to the equations. The resultant set of first order partial differential equations is hyperbolic throughout the flow field. A steady-state solution can be obtained by marching these equations from some initial guessed flow field through time until an asymptotic steady-state solution is achieved.

Over the past fifteen years, a large number of algorithms have been developed for the solution of the time-dependent Euler equations to a steady state. The principal disadvantage in approaching a steady state solution in this manner lies in the long computational times which are required to wash out of the flow field all of the initial transients which are introduced due to the initial assumed solution. These initial conditions generally have included within them large perturbations away from the final solution. These give rise to perturbation waves which move through the solution domain as the solution progresses in time. Steady state convergence is reached only when all of these perturbations have completely died out. The Euler equations with the time terms included do not inherently have any dissipative effect. Therefore the discretization of the equations is the only source of damping introduced, and this source is rather small. Generally, to reach a steady state requires a large number of iterations, and thus a long computational time.

A second problem inherent in numerically solving the primative-variable Euler equations is the fact that storage on the computer is quite excessive. In these equations there are four primative variables in 2D, five in 3D. Whether they be the density, velocity components, and energy, or the more common

conservation variables, there are still four or five to be stored at each grid point. This is a major disadvantage compared to alternative methods, to be described shortly, in which only a single parameter must be stored at each grid point.

A third and final source of difficulty in solving the Euler equations is in the boundary conditions that are required by this system. Essentially boundary conditions are required for all of the primative variables on each of the boundaries. Some natural boundary conditions are supplied easily by the physics of the problem; however, other auxiliary boundary conditions must be obtained, generally through application of the method of characteristics at the boundary. Typically this leads to a rather cumbersome treatment, and in most methods approximations are made to the full characteristic relationships. As an example we generally require some sort of compatibility relation obtained from the method of characteristics to get the pressure at solid surfaces. This relationship is often replaced by a more approximate relation which can adversely effect the stability and accuracy of the overall numerical scheme.

A number of approaches to solving the full set of Euler equations will be surveyed later in this paper. The conventional approach to circumventing the problems related to solving the full Euler equations for steady inviscid flow is to define either a stream function or a potential function and solve the resultant second order equations which arise from these definitions.

Stream Function Equation

The stream function equation is derived by postulating that the mass flow components, ρu and ρv, are obtainted from a scalar stream function as follows

$$\rho u = \frac{\partial \psi}{\partial y} \qquad \rho v = -\frac{\partial \psi}{\partial x} \tag{5}$$

where ψ is the stream function. Substitution of these definitions into the continuity equation (1) shows that it is automatically satisfied.

If we introduce these terms into the definition of the vorticity

$$\omega = \frac{\partial v}{\partial x} - \frac{\partial u}{\partial y} \tag{6}$$

we obtain the following

$$\frac{\partial}{\partial x}\left(\frac{1}{\rho}\frac{\partial \psi}{\partial x}\right) + \frac{\partial}{\partial y}\left(\frac{1}{\rho}\frac{\partial \psi}{\partial y}\right) = -\omega \tag{7}$$

where ω is the vorticity component normal to the plane of solution.

To work with this equation we must now obtain relations for the density, ρ, and the vorticity, ω, in terms of the stream function, ψ. From the perfect gas relation we can obtain the following

$$\frac{\rho}{\rho_r} = \left(\frac{a^2}{a_r^2}\right)^{\frac{1}{\gamma-1}} e^{\frac{-S}{R}} \tag{8}$$

where a is the speed of sound, S is the entropy, R is the gas constant, and r refers to a reference state of zero entropy. The quantities ρ_r and a_r are reference conditions. The entropy S can vary from streamline to streamline, but is constant along any given streamline.

In order to relate the speed of sound to the velocity components, we use the equation for conservation of energy as follows:

$$a^2 = a_o^2 - \frac{\gamma-1}{2}\left(u^2+v^2\right) \tag{9}$$

where a_o is speed of sound based on total conditions.

Finally the vorticity can be related to total conditions through Crocco's relation.

$$T\frac{ds}{dn} = \frac{dh_o}{dn} + u\omega \tag{10}$$

where n denotes a direction normal to the streamlines, and h_o is the total enthalpy.

Rearranging we can obtain the following relationship for the vorticity in terms of density, speed of sound, and entropy.

$$\omega = \rho\left(\frac{a^2}{\gamma}\frac{d}{d\psi}\left(\frac{s}{R}\right) - \frac{1}{\gamma-1}\frac{d}{d\psi}\left(a_o^2\right)\right) \tag{11}$$

The stream function equation, Eqn. (7), is a second order partial differential equation, which allows us to use the extensive experience we have with relaxation procedures for the solution of such equations. The stream function formulation retains all of the generality contained in the full Euler equations, so that it does permit variation in entropy, total pressure and temperature throughout the flow field. Likewise the flows which are calculated can be rotational and cover the entire flow range from subsonic through supersonic flows. However, this formulation does bring with it some inherent loss in generality. It is limited to two-dimensional or axisymmetric flows, and is also hampered by the fact that the density in the transonic flow regime is a double-valued function of the unknown ψ. Solution for ψ in the transonic regime is possible, and has recently been obtained by Hafez [13] for an isolated airfoil application. The cascade version of such a development is currently underway. A number of different subsonic stream function solutions have been obtained for meridional plane and blade-to-blade plane regions in turbomachinery applications. These will be surveyed shortly.

Working in terms of the stream function solves many of the problems cited previously for the full Euler equations. The stream function gives a single second order partial differential equation, for which robust and well under-

stood relaxation solution methods exist. These solutions can therefore be obtained in much less computer time than those for the first order Euler systems. The computer storage required for this equation is likewise much lower, necessitating only the storage of the stream function at each mesh point. Finally, the boundary conditions are more natural and are smaller in number. For the stream function generally Dirichlet boundary conditions are used at all solid surfaces, and either Dirichlet or Neumann boundary conditions are imposed at all the open surfaces. The resultant problem can be solved in at least an order of magnitude less time than the full primative-variable Euler equations.

Full Potential Equation

Another approach to circumventing the problems inherent in solving the full Euler equations is to define a scalar potential function, Φ, such that the vector velocity field is everywhere equal to the gradient of that scalar potential.

$$\vec{V} = \vec{\nabla} \Phi \tag{12}$$

By definition then the curl of that velocity field will be everywhere zero, so that such a flow is automatically irrotational throughout the flow field. This does place a restriction on the flow, but brings with it the advantage of being able to work in terms of a single second-order equation instead of the full primative-variable Euler set.

If the velocity field is the gradient of a scalar potential then by definition the components of velocity u and v are related to the potential as follows.

$$u = \frac{\partial \Phi}{\partial x} \qquad v = \frac{\partial \Phi}{\partial y} \tag{13}$$

where Φ is the scalar potential function. Substituting these definitions into the continuity equation yields the full potential equation in conservation form in two-dimensional Cartesian coordinates.

$$\frac{\partial}{\partial x}\left(\rho \frac{\partial \Phi}{\partial x}\right) + \frac{\partial}{\partial y}\left(\rho \frac{\partial \Phi}{\partial y}\right) = 0 \tag{14}$$

Refering to Crocco's relationship, equation (11), we see that for an irrotational two-dimensional flow, if the vorticity is zero, then the flow must be everywhere isentropic, and have constant total temperature or enthalpy throughout. Through the isentropic relationship, we then relate density to the speed of sound as follows.

$$\frac{\rho}{\rho_0} = \left(\frac{a^2}{a_0^2}\right)^{\frac{1}{\gamma-1}} \tag{15}$$

Furthermore, knowing that total temperature is conserved throughout yields the following relationship between the speed of sound and the velocity components.

$$a^2 = a_0^2 - \frac{\gamma-1}{2}\left(u^2+v^2\right) \tag{16}$$

Elimination of the density from the conservation form of the full potential equation, along with use of the energy relationship given above, leads to the following common non-conservation form of the full potential equation.

$$\left(a^2-u^2\right)\frac{\partial^2\phi}{\partial x^2} + \left(a^2-v^2\right)\frac{\partial^2\phi}{\partial y^2} - 2uv\frac{\partial^2\phi}{\partial x\,\partial y} = 0 \tag{17}$$

Some of the advantages and disadvantages of working with the full potential equation are the following. As with the stream function equation, the full potential equation permits the user to work with a single second-order partial differential equation, for the scalar function ϕ . Furthermore, it does not have the restriction of being limited to two-dimensional flow situations, and full 3D flows can be analyzed, as we will see. The two primary disadvantages of this approach are that the flow is limited to being irrotational everywhere, and it is also isentropic. The isentropic assumption implies that shock waves captured in the transonic regime must be limited in Mach number to a value less than about 1.3 in order to be accurate. The irrotationality condition necessitates a uniform incoming flow in two-dimensional flow situations, and the condition that rV_θ equal a constant in the radial direction in three-dimensional turbomachinery flows.

The solution of the full potential equation will admit the existence of discontinuities in the flow field. However, these discontinuities are isentropic shocks, which do not represent true physical shock waves because they do not satisfy the Rankine-Hugoniot jump conditions. However, these shocks will be approximately of the proper strength and will exist in the proper position in the flow field if the Mach number of the flow approaching the shock is less than or equal to 1.3.

With regard to the irrotationality condition for full potential flows, the question arises as to whether this equation can be applied in the rotating reference frame in turbomachinery applications. In this situation, the user must recognize that the equations describe an irrotational flow in the absolute reference frame, with a solid body rotation imposed on that flow field due to the rotation of the wheel. In two-dimensional flows whether the blade row is stationary or rotating, if there is no radius change in the flow field, then the total pressure and total temperature will be constant throughout. If the flow field does have radius change then the rothalpy and entropy will be constant along these 2-D surfaces. The rothalpy, I , is defined in terms of the relative velocity components which are expressed as follows

$$w_z = \frac{\partial\phi}{\partial z} \qquad w_r = \frac{\partial\phi}{\partial r} \qquad w_\theta = \frac{1}{r}\frac{\partial\phi}{\partial r} - \Omega r \tag{18}$$

where r is the local radius, and w_z , w_r , and w_θ are the relative

velocity components in the axial, radial and tangential directions. The rothalpy is then defined as

$$I = h + \frac{w_z^2 + w_r^2 + w_\theta^2}{2} - \frac{\Omega^2 r^2}{2} \qquad (19)$$

where h is the static enthalpy and Ω is the wheel speed. Similarly in three dimensions, in the absolute frame the total pressure and the total temperature will be constant throughout. In the relative frame again the rothalpy and entropy will be everywhere constant.

As was the case with the stream function, using the potential formulation allows us to work with a single second order partial differential equation and obtain all the advantages of the solution methods that exist for that situation. The same comments that where made prior with regard to computer storage again apply. Finally with regard to boundary conditions, generally for the potential function Neumann boundary conditions will exist at all solid surfaces, and either Dirichlet or Neumann boundary conditions will exist at the open surface boundaries of the flow field. These are much easier to incorporate than the more complicated boundary conditions described earlier for the full Euler equations.

We now describe in detail the analysis that have been devised for the various sorts of equations governing inviscid flow situations. Methods for the full potential equation will be described first, followed by those for the stream function equation, and finally those for the full Euler equations.

FULL POTENTIAL EQUATION ANALYSES

A great deal of progress has been made in the last ten years in the development of solutions to the full potential equation for internal turbomachinery applications. A major development at the beginning of this period was the paper by Murman and Cole [14], in which they demonstrated a way to properly account for the domain of dependence in supersonic flow regions by introducing a special backward or upwind differencing. This had the effect of stabilizing solutions in those regions and permitting the first real transonic flow calculations using the potential equation.

Several major breakthroughs were also made during this period by Jameson. The first of these [15] generalized the concepts introduced by Murman and Cole so that they applied to the full potential equation in non-conservation form. Solutions to the full potential equation in this form now routinely use Jameson's rotated difference scheme, which effectively introduces a higher-order term which acts like an artificial viscosity in the supersonic region. Hafez [16] later introduced the concept of artificial compressibility to accomplish somewhat the same objective when the conservation form of the full potential is used. In this case the density is evaluated upstream of the point at which it is to be applied, which again stabilizes the equation in the supersonic zone. Jameson [17] also proposes a method for upwinding the density when the conservation form of the potential equation is used.

A number of different authors, applying these numerical techniques, and using either finite difference, finite area (or volume), or finite element methods to discretize the full potential equation in either conservation or non-

conservation form, have devised several excellent, stable, and accurate methods for solving 2D transonic flows on the blade-to-blade surfaces of turbomachinery. Many of these blade-to-blade analyses also incoporate quasi-3D effects through radius change and stream channel convergence. We are beginning to see a number of full three-dimensional applications of these methods, not only to turbomachinery problems, but also to propeller, wing-body, and nacelle problems as well.

Discretizing the Equation

One of the principal characteristics that differentiates the manner in which solutions are obtained to either the conservation or non-conversation form of the full potential equation, is the way in which the equation is discretized in order to obtain a series of algebraic equations for solution. There are primarily three major approaches to this problem: the finite difference method, the finite area or volume method, and the finite element approach.

In the finite difference method the terms in the basic partial differential equation, in either untransformed physical space or transformed to a computational space, are discretized using standard central differencing and backward (or upwind) differencing techniques. The resultant discretized equations, written at each of the mesh points, form a linear system of algebraic equations which are solved for the unknowns by standard numerical analysis techniques. This approach was applied in the early work of Dodge [18], Ives [19, 20], and Rae [21]. More recently this method has been used by Caspar [22, 23], who applies it to so-called finite or control areas throughout his physical domain.

The next method for discretizing the partial differential equations is termed the finite volume method (finite area method in two dimensions). This approach is a hybrid between a finite difference method and a finite element method, with more of the flavor of the latter. In many algorithms for solving the full potential equation, it is transformed and subsequently solved in the transformed computational plane. However, this approach has drawbacks, in that the transformations can be quite complex, involving a large amount of computational labor in evaluating the coefficients of the transformation. The desire to have an algorithm which does not depend upon the details of the transformation is what motivated the development of finite volume techniques. In this method, a local transformation is done on each of the small volumes which discretize the flow field, and the transformation metrics are evaluated numerically using the Cartesian coordinates of the corners of each of the mesh cells. The unknowns in the problem are then represented by some sort of functional representation on each of these discrete volumes. This method is described more fully in the paper by Caughey and Jameson [24]. This method has been applied recently in the analyses of Dulikravich [25, 26], Farrell and Adamczyk [27], and Fruhauf [28].

The third approach is the finite element method. In the finite element method the physical space is discretized with a series of triangular or quadrilateral shaped elements generated in a completely arbitrary fashion. The generation can be readily designed to concentrate elements in regions of high surface curvature and where flow gradients are strongest. Once the element grid is formed, the potential function is then approximated within each element by some sort of linear combination of mesh point values for the function based on locally defined shape functions assigned to each mesh point. One of the standard weighted residuals methods, usually the Galerkin method, is then used

to reduce the partial differential equations to a system of algebraic equations which can be solved directly. To apply this method, the continuity equation is multiplied by the nodal weighting functions, and is integrated over the volumes of the finite elements. The approximation for the potential function is then substituted into the continuity equation, and the resulting expression represents the error due to the approximation which is being used within the elements. The algebraic sum of all such contributions in the elements with common nodes are then set equal to zero. This represents the algebraic finite element equation for that particular nodal parameter. This set of linear equations is solved to yield the potential function throughout the flow field.

The order of accuracy of the functional approximation on each element can be enhanced by using more elaborate, higher order elements. Typically linear triangular elements are used, but biquadratic and other types of elements can be used to give higher order discretization.

Finite element methods have been used extensively in the blade-to-blade calculation methods of Laskaris [29, 30], Ecer and Akay [31, 32], and Hirsch and Deconinck [33]. The Laskaris work is primarily subsonic, although a three-dimensional application is presented in [30]. The Ecer and Hirsch algorithms have been extended into the transonic range for turbomachinery applications. Eberle [34] has also done a considerable amount of work applying the finite element method to transonic potential flow computations. He has applied such methods to wings, axisymmetric bodies and nozzles, as well as turbomachinery cascades.

Form of the Potential Equation

As mentioned previously, there are two principal forms of the full potential equation for which solutions are generally obtained, the conservation form (14) and the non-conservation form (17). Each has unique characteristics which require that somewhat different methods be applied in their solutions, but there doesn't seem to be any distinct advantage in solving one form over the other. In fact, the authors cited in this paper are approximately evenly divided between the two approaches, with the later approaches favoring solution of the conservation form coupled with artificial compressibility. The non-conservation form of the equations has been solved most recently by Dulikravich [25], and previously by Ives [19], Rae [21], and Dodge [18]. The conservation form is solved by Caspar [22, 23], Farrell [27], Ecer [31, 32], and Hirsch [33]. Fruhauf [28] has solutions for both the conservation and non-conservation forms of the equation.

Stabilization in the Supersonic Zone

Another characteristic which differentiates among the methods used to solve the full potential equation is the technique used to stabilize the equations in the supersonic zone for transonic types of calculations. As mentioned previously, there are two principal techniques which are used in this regard, the artificial viscosity approach of Jameson [15], and the artificial compressibility approach of Hafez [16].

The intent of both of these approaches is to modify the differencing in the critical flow regions such that the grid points which contribute to the solution at a given field point lie within the zone of influence of that point. The intent is to obtain finite difference information primarily from grid

points which lie within the Mach cone effecting a particular grid point for which the equations are being written. Jameson's rotated scheme identifies both hyperbolic and elliptic operators in supersonic zones. Upwind differences are used for the former and central differences for the latter. This has the effect of introducing an artificial viscosity to the solution procedure, which assures its stability in supersonic regions where the equations are hyperbolic. This artificial viscosity approach is employed principally by investigators using the non-conservation form of the full potential equation. It has been used in the work of Dulikravich [25], Ives [19], Rae [21], and Fruhauf [28]. Dodge [18], who also solves the non-conservation form, constructs hyperbolic and elliptic operators on a near-characteristic grid which is updated during the course of calculation. The artificial compressibility scheme of Hafez, which achieves the same objectives as the artificial viscosity approach, has been employed by all investigators solving the conservation form of the full potential equation, that is, Caspar [22], Farrell [27], Ecer [31], and Hirsch [33].

Solution of the Algebraic Equations

Another distinguishing feature between the various methods for solving the full potential equation is the technique which is used to solve the set of difference equations resulting from either finite differences, finite volumes or finite elements. The first of such techniques, and the most common, is some form of relaxation procedure, generally successive line over relaxation (SLOR). This is a technique employed in the work of Farrell [27], Dulikravich [25, 26], Ives [19, 20], Fruhauf [28], Rae [21], and Hirsch [33]. Other approaches generally employ a form of direct solver to do an inversion of the linearized equations. Gaussian elimination is commonly used here as the non-iterative part of an overall iterative solution scheme. Ecer [31, 32], Laskaris [29, 30], and Caspar [22, 23] all employ this approach. The final method used to solve the difference equations is approximate factorization techniques, such as those developed by Holst [34, 35]. ADI methods are a particular example of these. Such approaches can be up to an order of magnitude faster than traditional relaxation inversion techniques. However, they have not generally been applied as yet to turbomachinery cascade problems, except by Hirsch in reference [33].

Another approach useful for solving the difference equations even more rapidly than the approximate factorization methods is the use of multi-grid techniques. Such techniques were demonstrated for external flow applications, by Jameson [36], who extended the methods initially developed by Brandt [37]. To date Hirsch [33] is the only one to apply the multi-grid approach to the solution of the full potential equation for turbomachinery.

Results for Full Potential Equations

Illustrative results will be presented for some of the latest solutions to the full potential equation. These results are for 2D and quasi-3D blade-to-blade stream surfaces, as well as complete 3D flow passage analyses. Most of the references discussed do an excellent job of predicting transonic flow situations on compressor and turbine blade rows with Mach numbers below the 1.3 level.

To illustrate, results are shown first in Figure 11 for the two-dimensional cascade analysis of Dulikravich [26]. Here flow is computed over a cascade of symmetric NACA 0012 airfoils at zero angle of attack and zero stagger,

gap-to-chord ratio of 3.6, and inlet Mach number of 0.8. These results agree very well with the calculations of Caughey, obtained in private communcation, for the identical case. Caughey's calculations were performed using the methods of Reference [24]. Peak Mach number in this calculation reached a value of 1.31, and the sharpness of the shocks shows the excellent results which can be obtained with the full potential approach. Very similar results for this case have been obtained by Farrell [27], Ecer [31], and others.

Results of Farrell [27] are shown in Figure 12 for a supercritical compressor stator tip section designed for NASA Lewis by Sanz using a hodograph technique based on Bauer, et. al. [38]. The trailing edge of this blade ends in a cusp. The inlet Mach number is 0.71, and inlet flow angle 31.16°. The results show that the rapid compression is captured very accurately without any overreaction or steepening by the potential method to form a shock.

Figure 13, again from Farrell, indicates the importance of quasi-3-dimensional streamtube effects in the transonic flow regime. This figure shows a series of calculations performed on a thick compressor stator hub section, again developed for NASA Lewis by Sanz. Farrell's approach was first used to calculate strict 2D flow over the blade. This agrees very well with the Sanz hodograph solution, except at the trailing edge, where in Farrell's analysis the idealized blade of infinite length was replaced by a blade with constant trailing edge radius. The remaining two curves on the figure show the effects of radius change and streamtube convergence. In the first of the remaining two curves, a streamtube convergence was imposed of approximately 14% (axial velocity density ratio = 1.15), with no radius change on the stream sheet. The streamtube convergence strongly increases the Mach number on the suction surface of the blade, so that the presence of a reasonably strong shock is evident. In the final curve, the opening up of the passage due to a radius change of 5%, entirely relieves the effect which was evident previously. The increasing radius has a strong decelerating effect on the flow since the blade-to-blade passage now diverges in the downstream direction. The differences evident in these three curves indicate very strongly the requirement to consider quasi-3-dimensional effects in transonic design situations.

Finally, two results from Hirsch [33], shown in Figures 14 and 15, indicate typical results obtained with a finite element blade-to-blade code. The first, Figure 14, shows results calculated for a VKI-LS59 gas turbine cascade, calculated on the grid shown in Figure 5. The inlet Mach number is 0.281, inlet flow angle 30.0°, outlet Mach number 0.975, and outlet flow angle -65.89°. The stream channel convergence in the through flow direction is unity. The comparison with experimental data in this accelerating flow situation is extremely good, even in the transonic regime at the rear end of the blade. The compressor results shown in Figure 15 are for a double circular arc 9.5° camber compressor cascade. Inlet Mach number in this case is 1.05, inlet flow angle 58.0°, outlet Mach number 0.761, and outlet angle 49.5°. The stream channel convergence from inlet to outlet has a value of 0.86. The deviations in this case on the suction side of the blade between the computation and experiment are explained by the presence of large boundary layers which exist with compressor flows.

Finally three-dimensional results computed with the 3D code of Dulikravich [26, 39] are presented in Figure 16. These results are for an idealized rotor with the flow conditions illustrated on the figure. The results show regions of supersonic flow on all blade surfaces from hub to shroud, with fairly strong shocks existing in the tip region. Peak Mach numbers at the tip reach

values of approximately 1.5. Two grids were used to obtain this solution, progressing from a rather coarse grid with 24 points around the blade by 6 normal and 6 radial to a final grid with double those mesh dimensions in all directions.

STREAM FUNCTION EQUATION ANALYSES

In the previous section on the full potential equation, it was indicated that major work in the application of that equation to internal turbomachinery flows didn't occur until after the papers by Murman and Cole [14], Jameson [15], and Hafez [16]. These papers appeared in the early and mid 70's, so that all of the major applications to turbomachinery using the full potential equation have occurred from the mid 70's to the present time. A major point driving the development of these analyses was the need to extend the performance of modern day turbomachinery blading so that significant ranges of the flow field were in the transonic regime.

Stream function equation applications to turbomachinery, on the other hand, occured about ten years prior to those for the full potential equation. The earliest applications appeared in the late 60's, and these have continued to be developed and extended throughout the 1970's. It may seem strange that developments of the stream function equation appeared sooner than those for the full potential equation, since stream function analysis permits a more general modeling of the full rotational flow field, incorporating all the generality contained in the full Euler equations. (This capability is, however, limited strictly to subsonic flows, at least up until the present time). A major development paving the way for analyses of turbomachinery flows using the stream function equation was the series of early papers by Wu, particularly [40], which derived the stream function equations for solutions on hub-to-shroud and blade-to-blade stream surfaces of turbomachinery. This paper appeared in 1952, but its application was delayed until the late 60's awaiting the development of larger and faster computers on which the equations could be accurately solved.

In Wu's so-called general theory, the stream function equations are solved on two intersecting families of stream surfaces - the hub-to-shroud and the blade-to-blade. The complete three-dimensional flow field is calculated through an iterative process which involves transfer of information back and forth between these two sets of surfaces. Wu's analysis assumes that the flow relative to the blade rows is steady; however it does not demand that the flow at the exit of the blade row be axisymmetric. Therefore, exit flows can vary circumferentially, and following blade rows are thus subject to time-varying inlet flow. Because of this, Wu's general method of analysis is only applicable to flow through an isolated blade row. To apply it to a multi-stage machine, the time dependence must be removed by circumferentially averaging between each row of blades.

Several principal authors have developed computer codes for quasi-3D calculations in turbomachinery, following the work of Wu [40]. Adopting the nomenclature of Wu, these flows are either solved along meridional types of surfaces, which Wu calls S2, or blade-to-blade surfaces, called S1. Most authors have used the approach of having only a single S2 meridional stream surface along which the through-flow is calculated, interacted with a series of axisymmetric blade-to-blade surfaces from the hub to the shroud. Complications arise in the interaction between these two types of surfaces

from the fact that the shape of the S2 meridional stream surface as well as its thickness can only really be determined from the S1 blade-to-blade solutions. These solutions in turn require the knowledge of the through-flow on the meridional surface in order to provide boundary conditions as well as the thickness of the blade-to-blade stream sheets. Obviously the procedure to approach convergence is iterative, and can be handled in a wide variety of different ways.

Derivation of the stream function equations on the two intersecting surfaces is complex, and the reader is referred to details in Wu and in the other references to be given shortly. Each author approaches derivation in a slightly different way, and the resultant non-conservation equations on the meridional surfaces and blade-to-blade surfaces differ from each other in a variety of ways.

Historical Development and Applications

The two earliest developers of stream function analyses for turbomachinery worked independently of each other, and their methods appeared at approximately the same time. These were Katsanis in the United States and Marsh in England. Oddly enough they worked on different surfaces, Katsanis on blade-to-blade methods, and Marsh on hub-shroud stream surfaces. Katsanis published several NASA TN's for incompressible and high subsonic blade-to-blade applications, and then in 1969 published [41] his TN for what he called transonic blade-to-blade flows. This analysis applied to any fixed or rotating axial, radial or mixed flow turbomachinery blade row. Quasi-3D effects were incorporated through a stream channel thickness. The transonic flow referred to in Katsanis's title was not obtained by the stream function method, but by application of a velocity gradient approach, using information about the shape of the streamlines obtained from the stream function method at reduced weight flow. Wood [42] has since devised methods for extending Katsanis's approaches into the low transonic regime, obtaining more accurate results without having to employ the velocity gradient approach. In 1969 Katsanis and McNally [43] also published a method to analyze blade-to-blade flows through slotted or tandem blade rows, as well as a method [44] to greatly magnify the solution obtained with the methods of [41, 43] around the blade edges or the slot region of a tandem or slotted blade. All of these methods of Katsanis use a regular rectangular mesh on the blade-to-blade flow surface. Such a mesh has non-uniform-length mesh spacing adjacent to the blade surfaces, requiring special treatment of the boundary conditions at these locations.

Marsh [45] was developing at the same time his 2D stream function analysis for hub-shroud surfaces. This was the first such analysis to appear in the literature; and its major contribution, other than the solution method itself, was the development of techniques for applying the method on an irregular grid. This grid was composed of parallel lines in the radial direction in conjunction with through-flow lines which follow the shape of the hub and shroud boundaries. The net result was irregular, or non-rectangular, mesh cells in the solution domain. Marsh's technique applied to axial, radial and mixed flow turbomachines, and the finite difference equations for the stream function were solved by a matrix method; hence the "matrix through-flow" label given to Marsh's techniques and other techniques such as his which followed. Marsh deviated from the "general theory" of Wu, as most other authors were also to do subsequent to him. Marsh developed what he called the "through-flow theory" in which the time dependence was removed by treating the

flow on the midchannel as an axially symmetric flow between each pair of blades in the blade row.

Marsh's code was applied at the National Gas Turbine Establishment, and Smith [46] presented a paper in 1968 contrasting results from that technique to those of the established streamline curvature methods. The major conclusion of the paper was that the matrix through-flow method enabled significant advances to be made in the calculation of quasi-3D flows. It pointed to the need for incorporating a good endwall boundary layer solution and accurate loss mechanisms in this sort or program before adequate comparisons could be made with experimental data.

Smith and his co-workers at N.G.T.E. continued the development of matrix methods and quickly extended them to blade-to-blade surfaces. In 1970 Smith [47] and Frost presented a paper for computing flow fields on blade-to-blade stream surfaces using both a matrix stream function analysis and a streamline curvature technique. This method was applicable to any type of axial or mixed flow compressor or turbine blading with either stationery or rotating blade rows. In 1970 Smith [48] also published a paper describing both the meridional and the blade-to-blade analyses which were in use at that time at N.G.T.E. This was the first paper describing the meridional and blade-to-blade methods being used together in a unified way. However, the paper did not describe in detail the iteration process used between the two approaches.

Another set of codes for both hub-to-shroud and blade-to-blade analyses using the stream function equation was developed in the early 70's at Carleton University in Canada by Davis and Millar. Intially Davis [49] published a thorough analysis of Marsh's approach to generating a curvilinear grid on the hub-shroud stream surface. His paper redeveloped the Marsh technique and again applied it to the hub-shroud stream surface of an axial turbomachine. In 1972 and 1973 Davis and Millar [50, 51] published extensive reports on the development of both blade-to-blade and hub-to-shroud codes at Carleton University. The hub-shroud code, extended the methods originally developed by Marsh. The blade-to-blade analysis was likewise similar to those published earlier by Katsanis and Smith. In 1974 Davis and Millar [52] compared the matrix through-flow technique to streamline curvature methods for calculating flows on hub-shroud surfaces. They applied the two techniques to a duct flow, a transonic fan, and three-stage axial compressor. These comparisons indicated that the two approaches gave similar results, and that there was a small operational advantage with the matrix through-flow method. Both methods were shown to be subject to certain instabilities. The convergence of the stream function from iteration to iteration had to be damped in the matrix through-flow method, while the shift in streamline position had to be carefully damped in the streamline curvature techniques.

In 1975 Davis [53] presented the first hub-to-shroud stream function solution for flow in a centrifugal compressor. To accomplish this he used a special form of through-flow grid which remained quasi-orthogonal throughout the solution domain. He employed two versions of the stream function equation, one for regions where the axial velocity exceeded the radial, and the second in regions were the radial velocity was the larger. Furthermore, Davis incorporated a turbulent endwall calculation, using an integral method based on the entrainment theory of Head [54]. Although the equations derived by Davis were for application to centrifugal turbomachinery, they were only applied in the paper to stationary components: an inlet, a diffuser, and an intra-stage return bend.

In 1973 and 1974 Katsanis and McNally published NASA reports and an accompanying paper [55] describing their hub-to-shroud stream function analysis for use with the blade row analysis of reference [41]. This hub-shroud analysis could handle either axial or mixed flow compressor or turbine blade rows, but was limited to a single blade row. Later, in 1977, the same authors [56, 57] extended this code so that it also applied to radial or centrifugal blade rows. Mild transonic flows were treated with the same velocity gradient method used in the blade-to-blade analysis.

At about this same time, Marsh [58] published a paper similar to earlier papers by Smith [46] and Davis [52], comparing the matrix through-flow analysis approach to streamline curvature techniques for the hub-shroud problem. Like the previous papers, he discussed various loss models which were in use, and the need for a good endwall boundary layer analysis. Marsh concluded that the matrix through-flow and the streamline curvature techniques could be viewed as two different methods for solving the same governing equations on the same mean stream surface. He did not conclude that there was a definite superiority of one method over the other. He recommended that work be pursued to develop more accurate methods for estimating the losses within blade rows, to calculate the development of the endwall boundary layers, and to predict secondary flows.

Iterative Approaches and Finite Element Methods

In 1976 the first paper was published, by Bosman [59], giving significant detail concerning an iterative approach to couple hub-to-shroud and blade-to-blade stream function analyses. Bosman presents equations applicable to any type of stationery or rotating turbomachinery geometry including centrifugals. He described the following iterative procedure: The initial S2 stream surface is assumed to coincide with a mean blade shape. From the calculated S2 streamlines, S1 stream sheets are generated by revolution about the axis of rotation. S1 solutions are then obtained and from these mass-averaged streamlines are defined, thus giving a re-definition of the S2 stream surface. Another S2 solution is then obtained, and the process repeated until convergence is obtained. Thus the shape of the S2 stream surface evolves from S1 solutions and is not constructed by any sort of corrections to the mean camber surface for incidence and deviation angles as is done in several other techniques. Bosman applied his techniques to calculate flows in a low speed centrifugal compressor, and in a radial inflow turbine. A meridional view showing the hub and shroud profile for the low speed compressor as well as the grid used in Boman's calculation is indicated in Figure 17. This is an eight bladed compressor with a very short inducer section. In Figure 18 the S1 mean streamlines calculated by Bosman at the hub, mid-section and shroud for approximately zero incidence are shown. It is unlikely that a user trying to predict the stream surface to satisfy given incidence and slip conditions would have produced streamlines at all approximating those calculated by Bosman. Figures 19 and 20 show the calculated hub and shroud S2 velocity distributions, and illustrate the effect of the stream surface shape upon these. These figures show that there is a major influence on the hub and shroud velocities due to the graduated slip that occurs in the exit sections of the impeller.

A second, more elaborate iterative procedure was described by Adler and Krimerman [60] in 1978. Their meridional and blade-to-blade computer codes, based on finite element methods, are described in references [61, 62]. Adler's iterative process occurs in four distinct steps. The first two are

normal applications of meridional and blade-to-blade calculations on axisymmetric stream surfaces. In the initial hub-shroud solution the mean camber surface is adjusted at the loading edge to be aligned to the inlet relative flow velocity and at the trailing edge to be parallel to an assumed deviation angle. After these initial two solutions a number of different hub-to-shroud stream surfaces are calculated from corresponding streamlines in the blade-to-blade surfaces. These hub-shroud surfaces are no longer axisymmetric. From these multiple hub-shroud solutions, blade-to-blade surfaces are finally calculated by connecting corresponding streamlines. These blade-to-blade surfaces are therefore no longer surfaces of revolution. Iteration is continued back and forth between the third and forth steps until convergence is obtained. Adler applies this technique to a centrifugal impeller, and shows that the results clearly deviate from results obtained using a single axisymmetric meridional surface. He claims that these deviations are significant enough to justify this type of flow field calculation in highly-loaded compressors with back-swept blading where the flow is very three- dimensional. Since the four corner streamlines in Adler's analysis are forced to remain within the corners, one can argue whether the results obtained here are worth the extra effort.

Hirsch [63] in 1976 published the first numerical solution of the meridional through-flow stream function equation based on the finite element method. The method was applied to axial flow machines, but was also developed for radial machinery. The method was shown to be applicable to transonic stages in cases where the tangential velocity distribution was given, as long as the meridional velocity remained subsonic. Several years later, Hirsch published an iterated analysis [64] in which meridional and blade-to-blade finite element stream function analyses were combined for application to axial turbomachinery. Again the flow in the S2 surface was replaced by the calculation of the exact mass-averaged pitch-averaged flow on the meridional (z , r) plane. Hirsch uses second-order isoparametric quadrilaterial elements which allow an accurate simulation of blade curvature even in highly curved regions such as leading and trailing edges. Even though Hirsch's meridional calculation permits transonic relative flows as long as the merdional Mach number is lower than 1, the blade-to-blade code used in this combined analysis permits only subsonic velocities throughout the flow field. Results of this analysis were compared favorably with the LDV data obtained by DFVLR in Germany [65]. In 1980 Hirsch [66] again presented a combined iterative analysis, this time for centrifugal compressors. Results were computed for the radial compressor mapped with LDV by Eckardt [67]. Hirsch concluded that the viscous and secondary flow effects were not well reproduced with the through-flow calculations particularly in the back end of the compressor. Hirsch also presented a quasi-3D calculation on the so-called Type-B centrifugal compressor described in reference [68]. Figure 21 shows the shape of this compressor in the meridional plane and indicates the finite element mesh as well as the calculated meridional streamlines obtained for a flow coefficient of 0.2. Figures 22 and 23 show the static pressure distributions on the hub and shroud sections for a flow coefficient of 0.5. The experimental results from [68] are compared here to the calculated blade pressure distributions. The inviscid calculations predict a stronger local acceleration along the shroud suction surface than experimentally determined. Figures 24 and 25 show the calculated Mach number distributions along the hub and shroud. The figure at the hub indicates a local low velocity region in the outlet portion of the blade near the pressure side of the passage. The shroud profiles indicate details of a local acceleration region found near the front end of the suction surface of the blade. The differences between data and calculation indicate

that the secondary flows existing in the passage create velocity components which give a better behavior to the real flow than that found in the calculations. These differences illustrate the limitations of the quasi-3D approach were secondary flows are not taken into account.

Finally, in 1980 Goulas [69] presented a stream function analysis for the blade-to-blade flow in a centrifugal compressor which contains splitter blades. He derived his analysis so it could either calculate isentropically, or simulate turbulent flows with the addition of a simple turbulence model and zero velocity conditions at the wall. He adapted the method to handle stagnation points as well as the formation of small re-circulation zones at the front end of the splitter blades which sometimes occur in the analysis. His method was applied to a centrifugal compressor in which he studied various axial locations for the leading edge of the splitter.

Multi-Stage Meridional Capability

Of the methods just described for analyzing hub-shroud flow with stream function analyses, the methods of Marsh [45], Smith [48], Davis [49, 51], and Hirsch [63, 64] all permit the analysis of multi-stage machines. The method of Davis, however, was only demonstrated [49, 51] for a single full stage machine. On the other hand, the methods of Katsanis [55, 56], and Bosman [59] only apply to a single blade row.

Generation of Algebraic Equations

Most of the methods described above for both meridional and blade-to-blade types of stream function analyses have used finite difference techniques to generate the algebraic equations from the partial differential equation. The methods of Marsh, Smith, Davis, Bosman, Katsanis, and Hafez all fall within this class. Only the more recent methods of Hirsch and Adler use finite element techniques to discretize the equations. As time goes by and more and more automatic grid generators are developed for finite elements in turbomachinery applications, this approach will no doubt be used more heavily.

Iteration Between Hub-Shroud and Blade-to-Blade Solutions

Most of the authors referenced above, except Marsh who developed the first through-flow method, have developed codes for both meridional and blade-to-blade analyses. In some of these references details were given concerning automated interactions between the S1 and S2 surfaces. Marsh, Smith, Davis, and Katsanis described no such interactions. Bosman [59], Adler [60], and Hirsch [64, 66] all described such an interaction between the two types of surfaces. In cases where no interaction occurs, the midchannel stream surface is either formed as a midchannel projection of the mean camber line of the blade, or by altering that projection to accommodate at the leading edge for incidence and at the trailing edge for deviation angle. Where interaction does occur, the shape of the meridional stream surface is obtained from some sort of integration or mass averaging of the flow on the blade-to-blade surfaces from hub to shroud.

Type of Finite Difference Mesh

In all of the hub-to-shroud analyses mentioned above, there is a fair degree of uniformity in the grids, with most using a form of quasi-orthogonal grid similar to those originally chosen by Marsh in the first meridional analysis.

None are rectangular, and all have some sort of through-flow streamlines which match the hub and shroud geometries coupled with a grid of lines nearly orthogonal to these passing from hub to shroud. Generally details are not presented concerning the generation schemes used for these grids, except by Katsanis who uses the method of reference [70]. In some of the later methods, particularly those due to Bosman, Adler and Hirsch, the grids coincide with the blade edges giving a more accurate solution in those regions.

On the blade-to-blade surfaces a wider variety of meshes are used. In the blade-to-blade methods of Katsanis [41], and Bosman [59] rectangular grids are used with the inherent problems these bring near the boundaries. Rectangular grids provide a great advantage in the interior regions of the flow domain. Because of their regularity, the finite difference expressions are very simple and uniform throughout such a grid. However, at the boundaries such grids pose difficulties because of the irregularly sized mesh legs which intercept the boundaries in both directions. In other methods, noteably Smith's [47,48] and Davis [50], a channel or H-type grid is used with straight lines running in the θ direction and through-flow streamlines adhering to the shape of the blade surfaces on the suction and pressure sides of the channel. Finally, for the finite element methods, Hirsch uses second-order isoparametric quadrilaterial elements in both his meridional and blade-to-blade solutions. Adler, on the other hand, uses linear triangular finite elements.

Solution of the Algebraic Equations

Two principal techniques were used to solve the algebraic equations in most of the references. The first involved classical matrix inversion techniques and the second relaxation procedures. Of those that mentioned their methods for solving the equations, only Katsanis used a relaxation method. Most of the authors using direct inversion factored their matrices to lower and upper triangular banded matrices. Once this is done, and the banded matrices are stored, they can be applied efficiently from iteration to iteration without any large expenditure of computer time.

Viscous Loss Corrections

A number of different approaches are used with both the meridional and blade-to-blade stream function analyses to simulate the effects of viscous loss in these inviscid calculations. The first of these involves correlation for loss as a function of various blade geometry, setting angle and loading parameters. The second method involves a pre-specification of a distribution of total pressure from inlet to outlet through the blade row. This total pressure is incorporated into the solution procedure and effects the velocity accordingly. The final method employs the calculation of either endwall or blade surface boundary layers. These boundary layers then alter the shape of either the meridional or blade-to-blade channel thus effecting the internal flow solution.

Transonic and Three-Dimensional Flows

The stream function method has always traditionally been applied to two-dimensional and subsonic flows. Recently Hafez [13] has approached the solution of the stream function equation in conservation form using techniques traditionally applied to the full potential equation in that form. He has found that traditional methods such as artificial compressibility can be extended to the stream function equation. He has investigated methods to

overcome the fact that the density is not uniquely determined in terms of the mass flux, having instead both subsonic and supersonic solutions on either side of the sonic point. He has applied the resultant method to flows over a NACA 0012 airfoil at a variety of inlet Mach numbers in the transonic range. He has also performed calculations about a 10% parabolic airfoil, as well as transonic flows about a cylinder. These results have been compared to both potential and Euler solutions. Hafez has likewise investigated the application of stream function methods to three-dimensional flows through the use of two different stream functions for this problem. This work is ongoing, and as yet has not been applied to turbomachinery situations.

FULL EULER EQUATION ANALYSES

Explicit Time Marching Methods

Explicit solutions to the Euler equations have been under development for a number of years, with applications for internal flow situations dating back to the 1950's. An explicit method is one in which all spatial derivatives are evaluated using known conditions at an old time level. Futhermore, information at the new time level depends on information obtained from only a small number of points. The resultant methods are simple and easy to code. All such methods, however, are limited by the so-called Courant, Friedrichs, and Lewy (CFL) stability limit, which states that the domain of dependence of the numerical finite difference scheme must contain the complete domain of dependence of the original hyperbolic differential equations.

A major milestone in the development of explicit methods was the paper by MacCormack [71]. This method has second order accuracy in both time and space. It is a two-step predictor-corrector method, which alternates between forward and backward differencing on the two steps. The ease with which this method can be applied has led to many applications in the turbomachinery field. One of the first applications of the MacCormack scheme to turbomachinery was by Gopalakrishnan and Bozzola [72]. Gopalakrishnan applied the basic MacCormack algorithm without modification to a transonic compressor cascade with supersonic inlet flow shocking down in a blade row to subsonic outlet flow.

Another application of the same scheme to turbomachinery was that of Kurzrock and Novick [73]. This solution was obtained for a rotating blade-to-blade stream surface, with radius change and stream channel convergence included. The authors retained the viscous terms from the Navier-Stokes equations, with an artifically enlarged viscosity coefficient in order to capture shocks. They applied the method to transonic flow in a 2D compressor cascade and also to the quasi-3D stream surface of a compressor rotor. Comparisons between computed and experimental exit conditions were presented.

Thompkins [74] has applied the MacCormack algorithm to flow through a three-dimensional transonic compressor rotor. This method can be applied to any general compressor blade shape, including those with part-span shrouds. Computer results applying this method to a transonic compressor will be presented later.

Another set of explicit methods is obtained by writing the conservation laws in integral form and applying them to local control volumes surrounding each grid point. The fluxes of mass, momentum and energy crossing the control

surfaces are evaluated using the values from surrounding points. A first order integration in time is then used to advance the dependent variables forward to a steady state.

The first major application of this technique for turbomachinery was by McDonald [75], who applied the method to 2D transonic flow in axial turbine cascades. His approach includes the use of hexagonal elements surrounding each grid point, as well as the replacement of the energy equation by a statement of constant total enthalpy throughout the field. Computed and experimental results were compared for a number of high-turning turbine cascades with supersonic exits.

Denton [76, 77, 78] has developed a somewhat simpler method for both 2D and 3D turbomachinery flows. Denton employs quadrilaterial elements in two dimensions and six-sided elements in 3D, which lead to simpler expressions for his surface flux integrals. In order to ensure stability he uses upwind differencing in the streamwise direction for the fluxes of mass and momentum, while using downwind differencing for pressure. Central differencing is used for all quantities in the pitchwise direction. This scheme has the property that stability depends only on the axial Mach number, not on the absolute Mach number which is more usual. This method has been successfully applied to a wide variety of both axial and mixed flow compressor and turbine geometries.

Another first-order explicit method has been developed recently by Bosman and Highton [79] for three-dimensional flow situations. The method employs two separate overlapping grids on which density and internal energy are evaluated at one set of nodes, and velocities are evaluated at the second set. This overlapping scheme facilitates the evaluation of fluxes for the corresponding control surfaces. Bosman updates his primative variables in a sequential fashion. First, he evaluates the velocities, then density and pressure. A new set of velocities is then obtained using the new pressures. Next, internal energy and temperature are updated, which leads to a final update of the pressure. At each stage in this process, the most recent values of all primative variables are used to update the fluxes. The method has been applied to both radial inflow turbines [79] and to centrifugal compressor impellers [80]. Results from the radial turbine example will be presented later.

Recent efforts have been devoted to improving both the accuracy and the speed of explicit methods. A significant example of the former is Moretti's λ -scheme [81] which exploits concepts from the method of characteristics for hyperbolic systems. In Moretti's scheme he rewrites the Euler equation so that the right-hand sides involve derivatives of one-dimensional Riemann invariants only. These derivatives are then replaced by one-sided differences in directions corresponding to the projection of the associated bicharacteristics onto the previous time plane. The equations are then updated in time by a two-step predictor-corrector scheme similar to that of MacCormack's. The result seems to be improved accuracy as evidenced by very sharp shocks captured with modest numbers of grid points. The λ -scheme by itself only produces isentropic shocks unless it is corrected with a shock fitting procedure, as is done in De Neef and Moretti [82]. The λ -scheme has been modified and applied to simple compressor and turbine cascades by Pandolfi and Zannetti [83]. A similar method to the λ -scheme has been developed by Chakravarthy, et al. [84].

Ni [85] has developed a new explicit method which is both accurate and quite fast. He begins with a scheme that appears to be equivalent to the second-order Lax-Wendroff procedure, (see Richtmyer and Morton [86]). However, by using a spatially varying time-step, which is taken to be everywhere near the CFL limit, he obtains a method which operates with the largest possible time step in all regions. More importantly, this effectively biases the differencing in such a way that the finite difference scheme has a domain of dependence which approximates that of the underlying hyperbolic system. Ni's method has been coupled with a multi-grid procedure which greatly speeds convergence to a final steady state. The method was applied in [85] to transonic flow in a turbine cascade as well as to an axisymmetric nacelle with centerbody.

Another approach to speeding convergence of the explicit methods to a steady state is to add purely artifical unsteady terms to the steady equations. When properly constructed, these artificial terms can introduce a strong internal damping into the resulting unsteady system. Such approaches are called pseudo-unsteady. One such method has been employed by Essers [87] to compute 2D steady irrotational transonic flows. In this approach the artificial unsteady terms are added to the continuity equation and to the irrotationality condition. This results in two equations in the unknown velocities, with density obtained from the isentropic relationship. These equations are solved by an adaption of MacCormack's predictor-corrector scheme. Results are presented by Essers for two-dimensional flow through a turbine rotor blade section with supersonic exit. Effects of various treatments of the blunt trailing edge are also presented.

Another pseudo-unsteady method has been developed by Viviand and Veuillot [88, 89]. In this technique the energy equation is replaced by the statement of constant total enthalpy, and the pressure is then expressed as a simple function of density and velocity. The resultant system includes the unsteady continuity and momentum equations. These are solved by a generalization of MacCormack's predictor-corrector scheme. Since the system has no unusual damping mechanism beyond the normal damping due to truncation errors and simple artificial viscosity, it relies on careful treatment of waves at the boundaries in order to reach a steady state. A three-dimensional version of this method has been developed by Brochet [90, 91] and applied to flow in a supersonic compressor cascade with converging endwalls and to transonic flow in a fan rotor. Results from the cascade will be presented later.

Implicit Time Marching Methods

Implicit time-marching methods for both the Euler and the Navier-Stokes equations date from the mid-1970's. In implicit methods the equations are backward differenced in time, and the non-linear terms at the new time are Taylor-expanded about their values at the previous time level. This produces a system which is linear in the unknowns at the new time level. The spatial derivatives are then approximated by finite differences, resulting in a large system of coupled linear algebraic equations for the unknowns at the new time level. In each of the methods to be discussed here, these equations are solved by block alternating-direction-implicit (block ADI) techniques. In this approach the matrices are first factored into a sequence of matrices for one-dimensional problems, each of which can be inverted by a tri-diagonal routine. The matrix elements in these one-dimensional problems are in turn simple block matrices whose size is equal to the number of unknowns at each grid point. The solution at each time-step proceeds non-iteratively by first

moving along the grid lines in one direction, inverting a tri-diagonal matrix for each line. It then proceeds similarly in each of the other physical grid directions of the problem.

The first of these methods was introduced by Briley and McDonald [92, 93], primarily for the compressible Navier-Stokes equations. Beam and Warming [94] independently developed a very similar method for the Euler equations. Briley and McDonald [95] have since shown that when the Beam and Warming algorithm is written in the "delta" form to solve for the corrections to the unknowns at the new time levels, the two methods have identical linearized block implicit matrices.

Steger [96, 97] has developed a curvilinear coordinate version of the Beam-Warming algorithm for viscous as well as inviscid flows, and has applied it to both isolated airfoils and cascades in two dimensions. Shamroth, et al. [98] has applied the Briley-McDonald procedure to laminar and turbulent flow through a cascade. Finally, Fruhauf [28] has applied the Beam-Warming algorithm to solve the Euler equations for both subsonic and supercritical flow through cascades.

In all of the time-marching explicit and implicit methods some form of numerical damping is present in the solution procedure which smoothes the oscillations that occur in the vicinity of strong shock waves. Most of the methods have added the damping explicitly in the form of a higher-order differencing term. However, in all of these cases the natural truncation errors that occur as the result of any finite difference procedure will add their own damping. Since the form of these damping terms varies considerably from method to method we will not discuss the details for any particular application.

New Methods Under Development

A number of methods are under development in order to achieve more accurate and faster solutions for the Euler equations. Delaney [99] is developing a hopscotch method for solving the Euler equations for application to cascades. The method appears to be significantly faster than the original MacCormack algorithm.

Denton [100] has extended his earlier Euler method by employing a simpler more accurate differencing scheme. He has also increased the convergence speed through the use of a simple multi-grid procedure. He has applied the method to 2D transonic flow in both compressor and turbine blade rows.

Johnson [101], in order obtain the benefits of existing rapid solution procedures for second-order partial differential equations, has developed a new technique in which the first-order steady Euler equations are imbedded in a second-order system. Published results to date have been for the transonic small disturbance equations and the full Euler equations in subcritical flow.

Both Ecer and Akay [102] and Lacor and Hirsch [103] have developed methods which are the equivalent of solving the full steady Euler equations. In these two approaches the velocity is split into potential and rotational parts. The resultant system of equations includes a second order equation for a potential function which is obtained from the continuity equation, and a pair of first order convective equations describing the evolution of two scalars which together determine the rotational part of the velocity field. These are

solved as a coupled system. Both of these methods have used finite element formulations. Ecer has applied his technique to 2D transonic flow in a channel with a bump and to flow around a 2D cylinder. Hirsch applies his method to calculate 3D flow in a rectangular elbow with 90° of turning.

Finally Chang and Adamczyk [104] have developed a new semi-direct algorithm for computing three-dimensional inviscid shear flows. This algorithm is composed of two iteration loops. In the inner loop, the velocity and density fields are evaluated for specified vorticity, total enthalpy and entropy fields. This evaluation is reduced to the solution of a pair of Poisson equations in the computational domain which are solved by three-dimensional, fast, direct Poisson solvers. In the outer loop, the vorticity, total enthalpy and entropy are obtained by solving convective equations for a pair of scalars in a manner similar to that of the previous two references. In the present work, finite difference procedures are used throughout. To date the method has been applied to study the development of inviscid shear flows in turning channels.

Applications of Euler Methods

Several results will be presented to indicate the kinds of calculations which are being performed with the various Euler equation methods. The method of Thompkins [74] has been applied at NASA by Chima and Strazisar [105] to calculate the three-dimensional flow field within a transonic axial compressor rotor at design speed, and to compare those results to laser anemometer measurements at maximum-flow and near-stall operating points. Figure 26 indicates Mach number contours for the measured laser anemometer results at a section 15% from the tip of the blade. These results can be compared to the calculated contours in Figure 27 at the same location. These figures indicate a pronounced bowwave and passage shock system, and show excellent agreement between the measured and calculated results.

The method of Bosman [79] has been applied to a radial inflow turbine which turns through 90° of deflection in the meridional plane and has a 70° deflection in the m-θ plane at the blade tip. Such a geometry will naturally produce large three-dimensional secondary flows, and one of the strong points of the Bosman technique is that it picks up these natural inviscid vortex motions in such a three-dimensional geometry. Figure 28 indicates for the design point condition the calculated streakline pattern on the hub section of the blade. Some of these streaklines have been joined to form a streamline which is seen to migrate from mid-passage over to the suction surface of the blade. A migration in the opposite direction was calculated by Bosman along the tip. Similar calculated patterns are indicated for the suction and pressure sides of this turbine rotor in Figure 29. Figure 30 compares the mid-passage-flow shroud static pressure distribution with experimental results and with two-dimensional calculations using a blade-like hub-shroud stream surface. The two-dimensional results have strong deviation from the experiments, especially in the trailing edge region, while the three-dimensional calculation agrees with the experiments quite well.

Brochet [90] applies his method to the calculation of flow through a supersonic compressor cascade with subsonic axial velocity. This cascade has converging sidewalls in the throughflow direction, with a contraction ratio of 0.7. The calculation was obtained for an upstream Mach number of 1.5 and a compression ratio of 2.0. Calculated pressure contours, related to upstream stagnation pressure, are presented in Figures 31 and 32 for the plane of

symmetry section and for the converging wall blade section. For the back pressure chosen, a shock is calculated which spans the entire passage from one converging wall to the other. At mid-passage the calculated flow field and shock structure agree quite well with two-dimensional calculations obtained by taking into account the stream channel convergence. This is no longer true, however, near the converging wall where only the truely three-dimensional model appears capable of representing phenomena correctly.

Finally, the method of Ni [85] has been applied to flow past a VKI gas turbine rotor blade, and compared to data by Sieverding [106]. Figure 33 presents calculated and experimental surface Mach numbers for this turbine rotor. The agreement is excellent on both blade surfaces except for small deviations very close to the shock impingement point on the suction side of the blade. Figure 34 indicates the mesh used in the calculation and shows the calculated Mach number contours. It also indicates the experimentally determined shock locations, showing that the shock is generated at the trailing edge. Calculated and experimental shock locations are in good agreement.

VISCOUS METHODS

Full Viscous Equations

Most flows of engineering interest are adequately described by the compressible Navier-Stokes equations. These equations, in two-dimensional conservation form and Cartesian (x, y) coordinates, are written

$$\frac{\partial U}{\partial t} + \frac{\partial F}{\partial x} + \frac{\partial G}{\partial y} = \frac{\partial R}{\partial x} + \frac{\partial S}{\partial y} \tag{20}$$

where U, F, and G are the same as for the Euler equations, and

$$R = \begin{Bmatrix} 0 \\ \tau_{xx} \\ \tau_{xy} \\ R_4 \end{Bmatrix} \qquad S = \begin{Bmatrix} 0 \\ \tau_{yx} \\ \tau_{yy} \\ S_4 \end{Bmatrix} \tag{21}$$

with

$$\begin{aligned} \tau_{xx} &= 2\mu\frac{\partial u}{\partial x} - \frac{2}{3}\mu\Theta & \tau_{yy} &= 2\mu\frac{\partial v}{\partial y} - \frac{2}{3}\mu\Theta \\ \tau_{xy} &= \tau_{yx} = \mu\left(\frac{\partial u}{\partial y} + \frac{\partial v}{\partial x}\right) & \Theta &= \frac{\partial u}{\partial x} + \frac{\partial v}{\partial y} \\ R_4 &= \tau_{xx}u + \tau_{yx}v + \chi\frac{\partial \varepsilon}{\partial x} & S_4 &= \tau_{xy}u + \tau_{yy}v + \chi\frac{\partial \varepsilon}{\partial y} \end{aligned} \tag{22}$$

Here μ is the viscosity coefficient and χ is the coefficient of thermal conductivity.

The above equations are valid for turbulent flows, but such computations are impractical today due to the large range of length scales in the turbulent spectra. The above equations are replaced by time-averaged equations and the Reynolds stresses, e.g. $-\rho\overline{u'v'}$, are modelled through the addition of auxiliary algebraic or differential relations. If a Boussinesq or "eddy viscosity" model is adopted for the Reynolds stresses, the above equations

will hold for the mean fluid variables $\bar{\rho}$, $\bar{u}$, $\bar{v}$, $\bar{E}$, with μ and k replaced by their effective turbulent values.

For practical engineering flows with curved boundaries, the above Cartesian equations are transformed to curvilinear body-fitted coordinates. This adds considerable complexity to the equations, especially so for the viscous terms.

For steady flows the time derivatives are often retained as an aid in the solution process. The resulting time-averaged Navier-Stokes equations in curvilinear coordinates are quite difficult to solve for a number of reasons. First, there are many disparate length scales which must be resolved. These may be associated with boundary layers, wakes, vortices and shock waves. For complex flows this requires a very large number of grid points even for a minimum description of important phenomena. Second, a large number of quantities are needed at every grid point in the field. For example, in three-dimensional flow, one might need five primative variables, two turbulence properties, and nine or more metric derivatives. The above requirements lead to the need for a very large computer memory and associated long running times to achieve a solution. If sufficient computer core is not available, the metric derivatives may have to be re-computed at every time step or iteration, which adds to the overall run time. Third, the numerical problems associated with the solution of the first order inviscid Euler equations are still present in viscous problems especially for high Reynolds numbers. One such problem often occurs when the local cell Reynolds number, $\rho u \Delta x/\mu$, exceeds 2 and the solution becomes either unstable or highly inaccurate. The common "fix" of locally switching from central to first order upwind differencing of the convective term can introduce excessive numerical diffusion. Finally, we note in some cases with steady boundary conditions a steady solution may not even exist.

Many techniques have been developed over the years for viscous problems which solve simplier sets of equations. We consider only those for steady flows, and group them into two categories.

Partially Parabolic Approximation

The first of these is the so-called partially parabolic approximation. This assumes the existence of a predominant flow direction, which is known a priori. Therefore, flow separation is excluded. The viscous terms are simplified by neglecting diffusion in the main flow direction. This is much like the boundary layer approximation. In two dimensions, if x is the flow direction, the vector R is dropped from Eq. (20) and $\partial v/\partial x$ is dropped from τ_{yx}. Both terms in Θ are retained as they are comparable in magnitude for compressible flow. For three dimensions see Caretto, Curr, and Spalding [107]. One variable, usually the pressure, is treated as elliptic and stored at every grid point. The remaining variables, eg. u, v, E in 2D, are treated as parabolic and stored on only two or three cross-sections at a time. Starting from an approximate pressure field the momentum and energy equations are marched in the flow direction. The variables are corrected locally to satisfy continuity. After each marching sweep, the pressure field is updated by solving an elliptic (Poisson) equation on the entire grid. This sequence of marching followed by the pressure update procedure is repeated until convergence. This type of analysis is applicable to many internal flows in the absence of streamwise separation. This includes those in turning ducts and turbomachinery blade rows provided that the details of the flow in the leading and trailing edge regions can be glossed over. The efficiency of such

computations should compare quite favorably with those of time marching procedures if convergence can be obtained in a moderate number of marching sweeps, perhaps under 50 for a three-dimensional problem. This would be especially true if some rapid procedure such as multi-grid is used to solve the elliptic equation for the pressure.

Fully Parabolic Approximation

Next we consider the fully parabolic approximation. This uses the same assumptions as the above with regard to the predominant flow direction and the neglect of viscous diffusion in this direction. In addition, upstream transmission of pressure disturbances generated during the calculation is assumed to be negligible. An initial pressure field, which is stored on the full grid, is assumed to contain all of the effects of boundary curvature. The remaining variables, including the pressure correction, are stored on only two or three cross sections at a time. The momentum and energy equations, or an equivalent set, are marched a single time in the flow direction. The variables are corrected locally at each cross section in order to satisfy continuity. This type of procedure should be applicable to flows in duct-like geometries with moderate turning in the absence of streamwise separation. Since only a single marching sweep in employed, these computations should be orders of magnitude faster than for any time marching procedure.

Both of these parabolic approximations are capable in principle of predicting strong secondary flows provided that local continuity is well satisfied on each cross section. Both of these can even treat modest amounts of streamwise separation if the Flugge-Lotz and Rehyner approximation is adopted, i.e. streamwise velocity is artificially prevented from going negative in the convective term only.

We now proceed to discuss methods in each of the above categories starting with the fully parabolic approximation. Within each category, we consider the main elements of a solution procedure and in so doing present what in our view are the significant distinguishing features of each method.

FULLY PARABOLIC METHODS

Main Parabolizing Assumption

All of the methods in this category require an additional assumption, beyond the neglect of streamwise viscous diffusion, in order to obtain a fully parabolic system of equations. In the usual procedure a bulk pressure correction, $\overline{p_c}$, assumed uniform over each cross section, is introduced into the streamwise momentum equations. This correction is determined so as to ensure the correct mass flux through each cross section. The cross flow equations, on the other hand, retain a separate pressure correction p_c which is permitted to vary over the cross section. This procedure is employed by Patankar and Spalding [108], Briley [109], Ghia et. al. [110], Roberts and Forester [111], and Briley and McDonald [112].

A different procedure is employed by Anderson [113] in 2D and Anderson and Hankins [114] in 3D. The equations are parabolized by writing them in an approximate intrinsic coordinate system which could be obtained for example from an incompressible potential flow solution. The assumption of small velocities normal to the streamwise grid lines eliminates convective

derivatives and viscous terms in the transverse momentum equations. The resulting system is fully parabolic with characteristic surfaces coincident with the cross-planes. Hence, no bulk pressure correction is required.

Satisfaction of Local Continuity

We next consider the technique for satisfying local continuity over a cross-section. Patankar and Spalding [108] introduce approximate relations between the velocities and pressure corrections which are obtained from the transverse momentum equations. Substitution of these into continuity yields a 2D elliptic equation which is solved over the cross-section. Another approach, adopted by Briley [109] and Ghia et. al. [110], assumes a 2D potential Φ for the transverse velocity corrections. Substitution of this potential into continuity yields a 2D elliptic equation for Φ in the cross-plane. The divergence of the transverse momentum equations provides a second elliptic equation for the pressure correction. Roberts and Forester [111] work directly with the divergence of the transverse momentum equations which gives a 2D elliptic equation with a source term related to the non-satisfaction of local continuity. This equation is solved iteratively with the momentum equations until continuity is also satisfied. This technique is related to that of Harlow and Welch [115] for 2D time-dependent flows. Briley and McDonald [112] split the transverse velocity into irrotational and rotational parts described by a 2D potential Φ and stream function Ψ, respectively. Substitution into continuity gives a 2D elliptic equation for Φ. Substitution into the definition of streamwise vorticity ω_s gives a 2D elliptic equation for Ψ. This is solved coupled with the transport equation for ω_s which replaces both transverse momentum equations. Anderson [114] uses the same splitting as Briley and McDonald and solves for Φ, Ψ, and ω_s. However, the Poisson equation for pressure p is added to the system.

Approximation by Algebraic System

All of the methods considered here use finite difference techniques to approximate the viscous equations with an algebraic system. First order upwind differences are used in the main flow direction and second order central differences in the cross-plane. Within this common framework, a few variations deserve comment. Patankar and Spalding [108] use a staggered grid similar to that of Harlow and Welch [115]. Velocity components and pressures are stored at different locations within a grid cell in order to simplify the differencing of the convective terms. The other methods store all variables at common locations within the grid. For large transverse velocities both Patankar and Spalding [108] and Ghia et. al. [110] switch to upwind differencing in the cross-plane. Roberts and Forester [111] add explicit local damping to deal with this problem. The other methods have not as yet encountered this problem. Anderson [113] in his 2D method applied Keller's box scheme to a system of first order partial differential equations. In the current version [114] for 3D flows, he goes back to a system of second order equations and uses differencings similar to the other methods.

Solution of Algebraic System

Finally, we consider the techniques for solving the algebraic system of equations at each cross-section. Patankar and Spalding [108] use a completely non-iterative scheme. Provisional velocity components are obtained from the momentum equations by an ADI marching technique. The bulk correction $\overline{p_c}$ is

obtained by satisfying a global mass balance over the cross-section. The local correction p_c is obtained from the 2D elliptic equation by several ADI sweeps. All velocities are next corrected using the approximate relationships between velocity and pressure corrections. Finally, the energy equation is solved again by ADI. The procedures of Briley [109] and Ghia et. al. [110] are similar to the above, except that p_c is determined iteratively with the streamwise velocity and the 2D elliptic equations for Φ and p_c are solved by point SOR. The overall process still is essentially non-iterative at each cross-section. Roberts and Forester [111] follow a sequence similar to that of Briley, without the equation for Φ. However, the entire sequence is repeated iteratively at each cross-section using updated pressures in the momentum equations until convergence is achieved. Briley and McDonald [112] solve for the streamwise velocity, density, and total enthalpy with a coupled block ADI technique and iterate to determine $\bar{p}_c$. Next scalar ADI is used to find the potential Φ. Finally, a coupled block ADI scheme is used to find Ψ and ω_s while satisfying the no-slip condition at the wall. Anderson [114] solves a fully coupled system for primary velocity, Φ, Ψ, ω_s, p, and total enthalpy. At present point SOR is used with a 6 x 6 block inversion at each point.

Application of Methods

The methods of this section have been applied to a variety of flows. The method of Patankar and Spalding [108] has been used for developing laminar flow in a square duct with a moving wall [108] and a round turning duct [116]. Briley [109] calculated the developing laminar flow in rectangular ducts and included the effects of transverse buoyancy. The method of Ghia et. al. [110] has been applied to the developing laminar flow in straight ducts of polar cross-section [110] and to turning ducts of rectangular cross-section [117]. Roberts and Forester [111] computed the turbulent flow in a rectangular-to-round diffusing transition duct. The method of Briley and McDonald [112] has been used for laminar flows in a turning duct similar to a turbine blade passage [112] and for turbulent flow in a rectangular turning duct [118]. Finally, Anderson [113] has computed several 2D turbulent flows in axisymmetric ducts with curved walls and Anderson and Hankins [114] have applied their 3D method to the hot turbulent flow in a turbofan forced mixer nozzle.

To illustrate the capability of these methods we present results obtained by Kreskovsky, Briley, and McDonald [118] for turbulent flow in a rectangular duct with a 90^0 bend. Figures (35) and (36) show computed primary and radial velocity profiles, for a cross-section 77.5^0 around the bend, compared with the LDV measurements of Taylor et. al. [119]. Note the very large radial velocity near the suction side of the channel. The quantitative disagreement with the data may be due in part to the large streamwise step used in the computation.

Two general comments would seem in order at this point. First, all of the methods in this section seem promising provided that small enough streamwise steps are used in the computation and sufficient pains are taken to ensure that local continuity is satisfied accurately enough for correct secondary velocities to form. Second, from the standpoint of efficiency a non-iterative procedure would seem to be preferable.

Finally, we note that Baker and Orzechowski [120] have developed a finite element parabolic method. Like the methods of Briley and Ghia et. al., it

solves 2D elliptic equations for Φ and p. Like that of Anderson it uses the small transverse velocity assumption to parabolize the system. As of this writing, however, we are not sufficiently familiar with the operation of the method to discuss it further.

PARTIALLY PARABOLIC METHODS

Satisfaction of Local Continuity

Three of the four methods considered in this section are similar to fully parabolic methods and hence our discussion can be somewhat abbreviated. We first consider the satisfaction of local continuity. Both Pratap and Spalding [121] and Moore and Moore [122] employ approximate relations between the velocity and pressure corrections and adjust these variables at each cross-section in the same manner as Patankar and Spalding. However, in successive passes, as the pressure field is refined, these approximate corrections should approach zero. Chilukuri and Pletcher [123] correct the velocity field at each cross-section through a potential Φ in a manner similar to that of Briley and Ghia et. al. By assuming Φ to be zero at the downstream station the method simultaneously corrects the primary velocity without the need for a bulk pressure correction. As the pressure field is refined in successive passes Φ should approach zero. Dodge [124] splits the velocity into viscous and potential parts by setting

$$\vec{V} = \nabla\Phi + \vec{U} \qquad (23)$$

In this expression $\vec{U}$ is obtained by marching the momentum equations. Φ is updated after each full sweep by substituting the above expression into the continuity equation and solving the resulting three-dimensional elliptic equation. Unlike the other methods, however, Φ does not approach zero with successive passes through the grid.

Elliptic Pressure Update

The technique for updating the elliptic pressure field is the main distinguishing feature of these methods. Pratap and Spalding [121] use the pressure field obtained from the continuity corrections during the march. An ad hoc means of distributing these corrections upstream is mentioned in the paper but not discussed. Moore and Moore [122] obtained an elliptic pressure correction equation from an approximation to the divergence of the vector momentum equation. This is solved after each march of the viscous equations using source terms calculated and stored during the march. The source terms and therefore the corrections approach zero after many marching passes through the field. Chilukuri and Pletcher [123] use the pressure Poisson equation obtained from the divergence of the full momentum equation. This is solved after each march with source terms again evaluated and stored during the march. The new pressure replaces the old. Dodge [124, 125] introduces an approximate inviscid relation between the pressure and the velocity potential Φ. Once the 3D elliptic equation is solved for Φ, after each march, the pressure p is obtained from the algebraic relation.

Approximation by Algebraic System

As in the previous section, finite difference techniques are used in each method to approximate the differential system by a large algebraic system. In

the marching equations first or second order upwind differences are used in the primary flow direction and second order central differences in the cross-plane. The main distinguishing features are discussed briefly. Both Pratap and Spalding [121] and Chilukuri and Pletcher [123] use the same staggered grid employed by Patankar and Spalding. The velocity components and the pressure are each stored at different locations in a grid cell. Moore and Moore [122] use a different staggered scheme with all velocity components stored at common locations and only the pressure corrections stored at different places in the grid. Dodge [125] stores all variables at common grid locations. In addition he introduces finer subgrids near the walls in order to resolve the viscous layers. The elliptic pressure update equations of both Moore and Moore [122] and Chilukuri and Pletcher [123] use central differences in all directions. The global potential equation of Dodge [125] uses the mixed upwind-central differencing of reference [18].

Solution of Algebraic System

The solution techniques for the algebraic systems are also similar to those of the preceding section. All methods use an ADI technique to obtain the velocity components from the momentum equations during the march. Since Chilukuri and Pletcher [123] solve 2D problems, they only need to perform a tridiagonal matrix inversion in one direction. Pratap and Spalding [121] and Moore and Moore [122] use ADI to solve the pressure correction equations at each cross-plane. Only the Moore's, however, iterate with the momentum equations until the pressure corrections are acceptably small. Both Moore and Moore [122] and Chilukuri and Pletcher [123] use point relaxation procedures to solve the elliptic pressure equations. The Moore's omit points in the near wall region of the boundary layer in their method. Dodge [124, 125] obtains separate marching solutions on each of his near wall subgrids and couples these to the interior marching solution at their common boundaries. The global potential equation for Φ is solved by the transonic relaxation technique of reference [18], with the near wall subgrid points omitted from the field. Thus, Dodge is the only method able to compute viscous transonic flows with shocks.

Application of Methods

The partially parabolic methods have been applied to a somewhat broader range of flows than those of the previous section. The method of Pratap and Spalding [121] has been used for 3D turbulent flow in rectangular turning ducts [126]. Moore and Moore have computed 3D turbulent flow in an accelerating rectangular elbow [127] and two centrifugal impellers [128, 129]. Chilukuri and Pletcher [123] computed 2D laminar flow in the inlet of a straight channel over a broad range of Reynolds numbers. Dodge [125] has calculated 3D turbulent flow in a rectangular diffuser and a low aspect ratio turbine stator. We show results from two of these computations as examples of the state-to-the-art.

Stanitz et al. [130] measured the turbulent flow in an accelerating rectangular elbow designed by means of potential flow theory. The planform is shown in figure (37). Moore and Moore [127] computed this flow for cases with exit Mach numbers of 0.26 and 0.4 in which spoilers were used to thicken the incoming endwall boundary layers. Figure (38) shows computed and measured wall static pressure on four potential surfaces from inlet to exit. Figure (39) shows computed and measured total pressure loss contours at the exit plane downstream of the bend.

Dodge [125] has computed 3D turbulent flow through a highly-loaded low-solidity high-aspect-ratio turbine stator. His results are compared to the measurements of Waterman [131]. Figure (40) shows computed contours of static pressure ratio on the blade suction surface. Figures (41) and (42) show computed and measured static pressures for the hub and tip blade sections, respectively.

In both of these cases there is good qualitative and fair quantitative agreement between the computations and the measurements. These results are encouraging, but much work remains to be done. In particular, the development of an accurate and efficient global pressure update procedure for transonic viscous flows with shock waves would be a major accomplishment.

ELLIPTIC METHODS

All of the methods in this category are capable of computing separated flows. Some of them employ parabolic approximations in the viscous terms only. The utility of these methods in the analysis of separated flows justifies their inclusion in the present section. The methods which solve the compressible equations in conservation-law form have shock-capturing capability. This is not generally available in the parabolic methods to date. In the absence of separation or shock waves, the elliptic methods may or may not be more accurate than the parabolic ones. This is primarily dependent on the accuracy of the differencing of the inviscid terms in the equations. Most of the methods now in use for internal flows are adaptions of techniques discussed here. However, other methods, especially those now under development for external aerodynamic applications, will undoubtedly be adapted for internal flows in the near future.

Methods for Steady Equations

We consider first, techniques for solving the steady viscous equations. A popular method introduced by Caretto et al. [132] is based on that of Patankar and Spalding [109]. The method uses the so-called SIMPLE algorithm which stands for Semi Implicit Method for Pressure Linked Equations. In this technique an initial pressure field is substituted into the momentum equations which are in turn solved for provisional values of the velocities. An approximate velocity-pressure correction relation is then substituted into continuity to give a 3D equation for pressure corrections. The corrected pressure field, underrelaxed for stability, is then substituted into the momentum equations to continue the process. Many variants of this method have been studied by Raithby and Schneider [133]. They found that reintroduction of the time derivatives, with backward time differencing, into the momentum equations increased the convergence rate of the algorithm. Of course, this converts the method to an implicit time marching procedure.

A different procedure has been used by Walitt et al. [134]. The 3D steady equations are transformed to a 2D unsteady system by treating one direction of the problem as time-like and evaluating the spatial derivatives in this direction from a previous solution. The equations are solved by marching through the field in the time-like direction. After one complete sweep, the time-like direction is switched and the equations are marched in a new direction. Since an explicit procedure is used to solve the equations on each cross-plane, very small steps in the marching direction are required in order to assure stability. This method has been applied to a centrifugal impeller [134] and to flow in a supersonic compressor cascade with splitter vanes [135].

Methods for Unsteady Equations

We next consider techniques for solving the unsteady viscous equations. These are closely related to explicit and implicit time marching methods for the Euler equations, although in some cases the viscous method came first. In an explicit technique all spatial derivatives are evaluated at a previous time. Hence, the solution procedure is unchanged by the addition of viscous terms. The boundary conditions on the velocity are changed in order to enforce no-slip at solid walls. The close mesh spacing, necessary to resolve the boundary layers, imposes severe time step restrictions in order to maintain numerical stability (CFL limit). Bosman and Highton [136] have developed an explicit viscous method closely related to the Euler method of reference [79]. The intended application here was to 3D subsonic flow in rotating machinery. Shang et al. [137] have implemented a 3D version of MacCormack's explicit predictor-corrector scheme [71] on a vector computer. The application here was to supersonic shocked flow in a rectangular wind tunnel. Spradley et al. [38] have also implemented a 3D explicit method on a vector computer. The time updating was quite similar to the MacCormack scheme. However, the spatial discretization was obtained by means of the general interpolants method (GIM), [139]. The application here was to supersonic flow in an exhaust nozzle.

In an implicit technique, the non-linear spatial derivative terms are linearized about the previous time, and backward differencing is used on the time derivative. The resulting coupled linear system is modified by the addition of the viscous terms. However, for central differencing of both inviscid and viscous terms, the matrix structure remains the same as for the Euler equations. These implicit techniques permit high resolution of the viscous layers without severe time-step restrictions. Briley and McDonald [92, 93] and Beam and Warming [94] have developed similar implicit techniques which were described earlier. Briley and McDonald have concentrated on viscous flows from the outset. Steger [96] has implemented the Beam and Warming procedure in a 2D curvilinear-coordinate, viscous code, which is applicable to a broad range of flow conditions including those in turbomachinery. In addition, Steger drops the streamwise viscous diffusion terms in the equations.

Ghia et al. [140] have developed what is termed a semi-elliptic implicit method for 2D incompressible flow. They first present a fully elliptic method that solves the complete momentum equations together with a Poisson equation for the pressure. Continuity is enforced by driving one of the source terms in the Poisson equation to zero in the manner of Harlow and Welch [115]. The semi-elliptic method is obtained by dropping the streamwise viscous diffusion terms. This in turn permits a simpler solution procedure for the momentum equations.

Approximation by Algebraic System

All but one of the elliptic methods use finite difference techniques to approximate the differential equations by a large algebraic system. Spradley et al. [138] use the GIM formulation which is similar to the finite volume approaches discussed earlier. In this approach the dependent variables are represented by interpolating functions over the interior of local mesh volumes. The algebraic system is obtained from weighted integrals of the differential equation over each mesh volume. Only Caretto et al. [132] use the staggered grid differencing scheme discussed earlier in reference to

Patankar and Spalding [108]. Bosman and Highton [136] employ the staggered arrangement discussed earlier as part of their Euler method [79]. All the other methods store all of the dependent variables at common grid locations. The hybrid central-upwind differencing used by Patankar and Spalding has also been used by Caretto et al. [132] and Briley and McDonald [93]. Ghia et al. [140] has used upwind differencing of the streamwise convective term everywhere in the flow field.

Solution of Algebraic System

The techniques for solving the algebraic system of equations have been discussed earlier, either in connection with the associated Euler methods or in the two sections on parabolic methods. Only a few comments are made here. All of the explicit time marching procedures as well as the explicit spatial marching method of Walitt et al. [134] use local update schemes somewhat akin to point Jacobi relaxation. Values at the new time depend only on a few surrounding values at the previous time. This is a slowly converging process, but it is easily coded. All of the implicit time marching procedures as well as the steady method of Caretto et al. [132] use ADI techniques to solve at least the momentum equations. These techniques can be made very fast, especially if the time-step is permitted to vary both in time and space, see e.g. McDonald and Briley [141]. Finally, for completeness, we note that the elliptic pressure equation has been solved by ADI, Caretto et al. [132], and by point SOR, Ghia et al. [140].

Application of Elliptic Methods

To illustrate the state-of-the-art for elliptic methods in internal viscous flows, we present results from four of the analyses discussed above. The actual range of applications of the methods is too broad to be covered here.

Humphrey et al. [142] have computed laminar flow in a square turning duct using a method based on that of Caretto et al. [132]. Results were compared with LDV measurements by the same authors. Figure (43) compares calculated and measured (circles) streamwise velocity profiles at mid-span and quarter-span for several cross-sections progressing from upstream to completion of the 90^{o} bend. The disagreement at the last three stations may be due to inadequate grid resolution (10 x 15) over the cross-section. A similar computation and comparison with data for turbulent flow in the same duct is presented in reference [143].

Buggeln et al. [144] have used the method of Briley and McDonald [93] to compute both laminar and turbulent flow in curved ducts, channels and pipes. We present comparisons with the data of Taylor et al. [119] for the same turbulent flow case computed by Kreskovsky et al. [118] with the parabolic method of Briley and McDonald [112]. This also is the same duct used for the studies reported in references [142] and [143]. Figure (44) shows comparisons for streamwise velocity profiles at the symmetry plane for several stations upstream of, around, and downstream of the bend. Figure (45) shows comparisons for several radial velocity profiles at the 77.5^{o} station. Comparing Figure (45) with Figure (36) shows considerable agreement between the two methods.

Shang et al. [137] have computed the 3D flow in a square wind-tunnel diffuser for a case with a normal shock wave system interacting with the turbulent tunnel-wall boundary layer, Figure (46). Figure (47) shows computed Mach

number contours in the plane of symmetry. Figure (48) shows comparisons with the LDV measurements of Abbiss et al. [145] for the streamwise velocity in the symmetry plane through the interaction region. The agreement is quite good.

Finally, Ghia et al. [140] have computed 2D laminar flow in a channel with a large constriction using both their fully elliptic and semi-elliptic methods. Figure (49) shows computed streamline contours for a case with a large separation zone on the downstream side of the constriction. The upper part of the figure shows an enlargement of the central portion of the full channel shown below. Figures (50) and (51) show computed results of both methods for wall shear and wall static pressure, respectively. The agreement between both methods is excellent even for the wall shear in the separated region on the lower wall.

In general these methods all perform quite well. The disagreement with experiment where it exists is probably due to inadequate grid resolution. However, much work remains to be done to determine the numerical accuarcy of all these methods. For 3D flows this can be a very expensive process.

TURBULENCE MODELING

The recently completed AFOSR-HTTM-Stanford Conference on Complex Turbulent Flows was organized for the purpose of providing an assessment of the state-of-the-art in turbulent flow prediction, especially that of turbulence modeling. A wide range of test flows with reliable experimental data was assembled and computational groups were invited to submit computed results for these flows to the Conference. The comparisons of these results with the data together with the findings of the Evaluation Committee will be presented in reference [7]. We confine ourselves to a few observations on these proceedings.

The current focus in turbulent modeling seems to have shifted from the one and two equation eddy viscosity models of a few years ago to methods which predict the Reynolds stresses themselves. Many results obtained with these models were presented at the Conference. However, while the promise of these models is considerable, at the present they show little or no advantage over the simpler treatments. This finding is especially true for separated flows.

The results of any turbulent flow prediction depend at least as much on the numerical technique as they do on the turbulence model. For most of the flows included in the conference, it was not possible to separate the limitations of the numerics from those of the turbulence models. Grid refinement studies were presented in only a few cases and many of these were inadequate. Hence, in judging the merit of any turbulent flow computation, the method had to be considered as an amalgam of numerical procedure and turbulence model.

In many internal flows, and especially in those through turbomachinery components, as a result of the rapid turning of the fluid, the evolution of the flow is dominated by the balance between strong pressure gradients and centrifugal forces. Turbulent mixing, though present, plays a lesser role. Indeed the development of complex secondary flows in these components, while dependent on the presence of shear layers due to upstream viscous effects, is an essentially inviscid phenomenon. Hence, if one can develop a sufficiently accurate and efficient numerical technique for solving the partial differential equations of fluid dynamics, good predictions of such flows should be possible

even with a relatively simple turbulence model. This view is supported by the observations of Humphrey et al. [143] in their studies of turbulent flow in turning ducts.

CONCLUDING REMARKS

The current status of potential flow methods for turbomachinery is quite advanced. A large number of codes have been developed for analyzing two-dimensional transonic flow with shocks on blade-to-blade surfaces. While an order of magnitude speed up in computing time may be possible with the latest procedures, many of these codes run fast enough for routine use by designers. In addition, we are aware of three codes which can compute three-dimensional potential flow in rotors. One of these has demonstrated transonic shock-capturing ability. Most of the stream function codes for turbomachinery applications are based on classical relaxation or matrix inversion techniques. They solve for subcritical flow on blade-to-blade or hub-to-shroud surfaces. Recently, however, a transonic stream function method has been developed and one application to a cascade is under development. In the case of the primitive variable Euler equations a large number of codes have been developed for turbomachinery applications. Most of these solve for two-dimensional, blade-to-blade flow with shocks. There are, in addition, at least three codes which analyze three-dimensional shocked flows in rotors. With few exceptions, however, these codes utilize older long-running numerical algorithms whose accuracy is not up to current standards. Since solution of the Euler equations is now one of the most active areas of research in computational fluid mechanics and since a number of promising new methods are under development, this situation should be much improved in a few years.

The state-of-the-art for viscous methods is much less developed than for inviscid ones. A few single-pass parabolic marching codes have been developed for three-dimensional flows in ducts and turning passages. These methods are relatively fast and fairly accurate in the absence of strong secondary flows. When strong secondary flows are present at high Reynolds numbers, either excessive grid or implicit numerical dissipation may be needed to maintain stability in inviscid regions of the flow. A few multi-pass partially parabolic codes have been developed for three-dimensional flows in turning passages and at least two of these have been applied to turbomachinery rotors. In these methods the pressure field is treated as elliptic and is updated as the computation proceeds. Much work remains to be done to speed up these methods and to extend the pressure correction techniques into the transonic regime. A number of codes have been developed which solve the full time-averaged Navier-Stokes equations in either two or three dimensions, in both ducts and turbomachinery, for both subsonic and transonic flow. The comments on accuracy and computational efficiency which were made for the Euler equation methods are equally valid here except that the computer times are even longer. It is likely that the status of Navier-Stokes codes will be improved substantially with the advent of new improved Euler solvers since most regions of viscous flows are dominated by inviscid effects. Finally, we come to the question of turbulence models for all the viscous methods. Here we can close on a more hopeful note. Although it is not true that turbulence models are getting much more accurate, in many flows in turning passages and turbomachinery the velocity field is determined primarily by the balance between centrifugal forces and pressure gradients and the effects of turbulence are relatively weak. Hence, if one has a sufficiently accurate numerical procedure, one can hope to adequately compute such flows even with a relatively simple turbulence model.

REFERENCES

1. Gostelow, J. P.: "Review of Compressible Flow Theories for Airfoil Cascades," ASME Journal of Engineering for Power, October, 1973, pp. 281-292.

2. Horlock, J. H.; and Lakshminarayana, B.: "Secondary Flows: Theory, Experiment, and Application in Turbomachinery Aerodynamics," Annual Review of Fluid Mechanics, Volume 5, 1973, pp. 247-280.

3. Perkins, H. J.; and Horlock, J. H.: "Computation of Flows in Turbomachines," Finite Elements in Fluids - Volume 2, Gallagher, et. al., eds., John Wiley, 1975, pp. 141-157.

4. Japikse, D.: "REVIEW-Progress in Numerical Turbomachinery Analysis," ASME Journal of Fluids Engineering, December, 1976, pp. 592-606.

5. Habashi, W. G.: "Numerical Methods of Turbomachinery," Recent Advances in Numerical Methods in Fluids, Volume 1, Pineridge Press, Ltd., 1980, pp. 245-287.

6. Adler, D.: "Status of Centrifugal Impeller Internal Aerodynamics, Part I: Inviscid Flow Prediction Methods," ASME Journal of Engineering for Power, July, 1980, pp. 728-737; Part II: Experiments and Influence of Viscosity, ASME Journal of Engineering for Power, July, 1980, pp. 738-746.

7. Kline, S. J.; Cantwell, B. J.; and Ferziger, J. H.: "Proceedings of the 1980-81 AFOSR-HTTM-Stanford Conference on Complex Turbulent Flows: Comparison of Computation and Experiment," Volume II: Taxonomies, Methods and Conclusions, Stanford University Press (to be published), 1982.

8. Klein, A.: "Aerodynamics of Cascades," AGARD-AG-220, 1977.

9. Smith, R. E., Ed.: "Numerical Grid Generation Techniques," NASA CP 2166, 1980.

10. Moretti, G.: "Grid Generation Using Classical Techniques," Numerical Grid Generation Techniques, NASA CP 2166, 1980, pp. 1-36.

11. Thompson, J. F.; Thames, F. C.; and Mastin, C. W.: "Automatic Numercial Generation of Body-Fitted Curvilinear Coordinate System for Field Containing any Number of Arbitrary 2-Dimensional Bodies," Journal of Computational Physics, Volume 15, 1974, pp. 299-319.

12. Eiseman, P. R.: "A Multi-Surface Method of Coordinate Generation," Journal of Computational Physics, Volume 33, 1979, pp. 118-150.

13. Hafez, M.; and Lovell, D.: "Numerical Solution of Transonic Stream Function Equation," AIAA Paper 81-1017, AIAA Computational Fluid Dynamics Conference, Palo Alto, 1981.

14. Murman, E. M.; and Cole, J. D.: "Calculation of Plane, Steady Transonic Flows," AIAA Journal, Volume 9, 1971, pp. 114.

15. Jameson, A.: "Iterative Solution of Transonic Flows Over Airfoils and Wings Including Flows at Mach 1," Communications of Pure and Math, Volume 27, 1974, pp. 283.

16. Hafez, M.; South, J.; and Murman, E.: "Artifical Compressibility Methods for Numerical Solution of Transonic Full Potential Equations," AIAA Journal, Volume 17, 1979, pp. 838.

17. Jameson, A.: "Transonic Potential Flow Calculations in Conservation Form," Proceedings AIAA Second Computational Fluid Dynamics Conference, Hartford, Connecticut, 1975, pp. 148.

18. Dodge, P. R.: "A Non-Orthogonal Numerical Method for Solving Transonic Cascade Flows," ASME Paper 76-GT-63, 1976.

19. Ives, D. C.; and Liutermoza, J. F.: "Second-Order Accurate Calculation of Transonic Flow Over Turbomachinery Cascades," AIAA Journal, Volume 17, 1978, pp. 870; also AIAA Paper 78-1149.

20. Ives, D. C.; and Liutermoza, J. F.: "Analysis of Transonic Cascade Flow Using Conformal Mapping and Relaxation Techniques," AIAA Paper 76-370, AIAA Ninth Fluid and Plasma Dynamics Conference, San Diego, 1976.

21. Rae, W. J.; and Homicz, G. F.: "A Rectangular-Coordinate Method for Calculating Nonlinear Transonic Potential Flow Fields in Compressor Cascades," AIAA Paper 78-248, AIAA Sixteenth Aerospace Sciences Meeting, Huntsville, Alabama, 1978.

22. Caspar, J. R.: "Unconditionally Stable Calculation of Transonic Potential Flow Through Cascades Using An Adaptive Mesh for Shock Capture," to be presented at ASME 27th International Gas Turbine Conference, London, England, April, 1982.

23. Caspar, J. R.; Hobbs, D. E.; and Davis, R. L.: "The Calculation of Two-Dimensional Compressible Potential Flow in Cascades Using Finite Area Techniques," AIAA Paper 79-0077, 17th Aerospace Sciences Meeting, New Orleans, Louisiana, 1979.

24. Caughey, D. A.; and Jameson, A.: "Numerical Calculation of Transonic Potential Flow About Wing-Body Combinations," AIAA Journal, Volume 17-Number 2, pp. 175, 1979; also AIAA paper 77-677.

25. Dulikravich, D. S.: "Numerical Calculation of Transonic Axial Turbomachinery Flows," Proceedings of Seventh International Conference on Numerical Methods in Fluid Dynamics, Stanford, California, 1980, pp. 164.

26. Dulikravich, D. S.; and Caughey, D. A.: "Finite Volume Calculation of Transonic Potential Flow Through Rotors and Fans," FDA-80-03 Report, Cornell University, March, 1980.

27. Farrell, C. A.; and Adamczyk, J. J.: "Full Potential Solution of Transonic Quasi-3-Dimensional Flow Through A Cascade Using Artificial Compressibility," ASME Paper 81-GT-70, ASME Gas Turbine Conference, Houston, Texas, March, 1981.

28. Fruhauf, H. H.: "Numerical Computation of Compressible Cascade Flows," Fifth International Symposium on Airbreathing Engines, Bangalore, India, February, 1981.

29. Laskaris, T. E.: "Finite-Element Analysis of Compressible and Incompressible Viscous Flow and Heat Transfer Problems," The Physics of Fluids, Volume 18, 1975, pp. 1639.

30. Laskaris, T. E.: "Finite-Element Analysis of 3-Dimensional Potential Flow in Turbomachines," AIAA Journal, Volume 16, 1978, pp. 717.

31. Akay, H. U.; and Ecer, A.: "Transonic Flow Computations in Cascades Using Finite Element Method," ASME Paper 81-GT-4, ASME International Gas Turbine Conference, Houston, Texas, 1981.

32. Ecer, A.; and Akay, H. U.: "Investigation of Transonic Flow in a Cascade Using An Adaptive Mesh," AIAA Paper 80-1430, AIAA 13th Fluid and Plasma Dynamics Conference, Snowmass, Colorado, 1980.

33. Deconinck, H.; and Hirsch C.: "Finite Element Methods for Transonic Blade-to-Blade Calculation in Turbomachines," ASME Paper 81-GT-5, ASME International Gas Turbine Conference, Houston, Texas, 1981.

34. Holst, T. L.: "Implicit Algorithm for Conservative Transonic Full Potential Equation Using An Arbitrary Mesh," AIAA Journal, Volume 17, 1979, pp. 1038.

35. Holst, T. L.; and Ballhaus, W. F.: "Conservative Implicit Schemes for the Full Potential Equation Applied to Transonic Flows," AIAA Journal, Volume 17, 1979, pp. 145.

36. Jameson, A.: "A Multi-Grid Scheme for Transonic Potential Calculations on Arbitrary Grids," Proceedings of AIAA Fourth Computational Fluid Dynamics Conference, Williamsburg, Virginia, 1979, pp. 122.

37. Brandt, A.: "Multi-Level Adaptive Grid Technique (MALT) for Fast Numerical Solution to Boundary Value Problems," Proceedings of Third International Conference on Numerical Methods and Fluid Mechanics, Paris, France, 1972, pp. 82.

38. Bauer, F.; Garabedian, P.; Korn, D.; and Jameson, A.: "Supercritical Wing Sections II," Lecture Notes in Economics and Mathematical Systems, Volume 108, Springer-Verlag, New York, 1975.

39. Dulikravich, D. S.: "CAS3D - FORTRAN Program for Analysis of 3D, Steady, Transonic, Potential, Axial Turbomachinery Flows Using O-Type Grids," to be published as NASA CR, 1982.

40. Wu, C. H.: "A General Theory of Three-Dimensional Flow In Subsonic and Supersonic Turbomachines of Axial, Radial and Mixed-Flow Types," NASA TN 2604, 1952.

41. Katsanis, T.: "FORTRAN Program for Calculating Transonic Velocities on a Blade-to-Blade Stream Surface of a Turbomachine," NASA TN D-5427, 1969.

42. Wood, J. R.: "Improved Method for Calculating Transonic Velocities on Blade-to-Blade Stream Surfaces of a Turbomachine," NASA Technical Paper 1772, 1981.

43. Katsanis, T.; and McNally, W. D.: "FORTRAN Program for Calculating Velocities and Stream Lines on a Blade-to-Blade Stream Surface of a Tandem Blade Turbomachine," NASA TN D-5044, 1969.

44. Katsanis, T.; and McNally W. D.: "FORTRAN Program for Calculating Velocities in a Magnified Region on a Blade-to-Blade Stream Surface of a Turbomachine," NASA TN D-5091, 1969.

45. Marsh, H.: "A Digital Computer Program for the Through-Flow Fluid Mechanics in an Arbitrary Turbomachine using a Matrix Method," Aeronautical Research Council R&M 3509, 1968.

46. Smith, D. J. L.; and Barnes, J. F.: "Calculation of Fluid Motion in Axial Flow Turbomachines," ASME Paper 68-GT-12, 1968.

47. Smith, D. J. L.; and Frost, D. H.: "Calculation of the Flow Past Turbomachine Blades," Proceedings of the Institution of Mechanical Engineers, Volume 184, 1970, pp. 72.

48. Smith, D. J. L.: "Computer Solutions of Wu's Equations for the Compressible Flow Through Turbomachines," Fluid Mechanics, Acoustics, and Design of Turbomachinery, Part I, NASA SP-304, 1974.

49. Davis, W. R.; and Millar, D. A. J.: "A Discussion of the Marsh Matrix Technique Applied to Fluid Flow Problems," Canadian Aeronautics and Space Journal, Volume 5, 1972, pp. 64.

50. Davis, W. R.; and Millar, D. A. J.: "A Matrix Method Applied to the Analysis of the Flow Past Turbomachine Blades," Carleton University Report ME/A72-7, 1972.

51. Davis, W. R.; and Millar, D. A. J.: "Axial Flow Compressor Analysis Using a Matrix Method," Carleton University Report ME/A73-1, 1973.

52. Davis, W. R.; and Millar, D. A. J.: "A Comparison of the Matrix and Stream Line Curvature Methods of Axial Flow Turbomachinery Analysis, from a User's Point of View," ASME Paper 74-WA/GT-4, ASME Journal of Engineering for Power, 1974.

53. Davis, W. R.: "A General Finite Difference Technique for the Compressible Flow in the Meridional Plane of Centrifugal Turbomachinery," ASME Paper 75-GT-121, 1975.

54. Head, M. R.: "Entrainment in the Turbulent Boundary Layer," Aeronautical Research Council R&M 3152, 1958.

55. Katsanis, T.; and McNally, W. D.: "Quasi-3-Dimensional Flow Solution by Meridional Plane Analysis," SAE Paper 740850, 1974.

56. Katsanis, T.; and McNally, W. D.: "Revised FORTRAN Program for Calculating Velocities and Streamlines on the Hub-Shroud Midchannel Stream Surface of an Axial, Radial, or Mixed-Flow Turbomachine or Annular Duct, I - User's Manual," NASA TN D-8430, 1977.

57. Katsanis, T.; and McNally, W. D.: "Revised FORTRAN Program for Calculating Velocities and Streamlines on the Hub-Shroud Midchannel Stream Surface of Axial, Radial, or Mixed-Flow Turbomachine or Annular Duct, II - Programmer's Manual," NASA TN D-8431, 1977.

58. Marsh, H.: "Through-Flow Calculation in Axial Turbomachinery: A Technical Point of View," AGARD Propulsion and Energetics Panel, 47th Meeting, Paper Number 2, 1976.

59. Bosman, C.; and El-Shaarawi, M. A. I.: "Quasi-3-Dimensional Numerical Solution of Flow in Turbomachines," ASME Paper 76-FE-23, 1976.

60. Adler, D.; and Krimerman, Y.: "The Complete 3-Dimensional Calculation of the Compressible Flow Field in Turbo Impellers," Journal of Mechanical Engineering Science, Volume 20, 1978, pp. 149.

61. Adler, D.; and Krimerman, Y.: "The Numerical Calculation of the Meridional Flow Field in Turbomachines Using the Finite Element Method," Israel Journal of Technology, Volume 12, No. 3/4, 1974.

62. Adler, D.; and Krimerman, Y.: "The Numerical Calculation of the Blade-to-Blade Flow Field in Turbo Impellers Using the Finite Element Method," Journal of Mechanical Engineering Sciences, Volume 19, 1977, pp. 108.

63. Hirsch, C.; and Warzee, G.: "A Finite Element Method for Through-Flow Calculation in Turbomachines," ASME Paper 76-FE-12, 1976.

64. Hirsch, C.; and Warzee, G.: "An Integrated Quasi-3-D Finite Element Calculation Program for Turbomachinery Flows," ASME Journal of Engineering for Power, Volume 101, 1979, pp. 141.

65. Dunker, R. J.; Strinning, P. E.; and Weyer, H. B.: "Experimental Study of the Flow Field within a Transonic Axial Compressor Rotor by Laser Velocimetry and Comparison with Through-Flow Calculation," ASME Paper 77-GT-28, 1977.

66. Hirsch, C.; and Warzee, G.: "Quasi-3-D Finite Element Computation of Flows In Centrifugal Compressors," Symposium on Performance Prediction of Centrifugal Pumps in Compressors, pp. 69, ASME 25th International Gas Turbine Conference, New Orleans, Louisiana, March, 1980.

67. Eckardt, D.: "Detailed Flow Investigations within a High-Speed Centrifugal Compressor Impeller," ASME paper 76-FE-13, ASME Journal of Fluids Engineering, Volume 98, 1976, pp. 390.

68. Mizuki, S.; Ariga, I.; and Watanabe, I: "Investigation Concerning the Blade Loading of Centrifugal Impellers," ASME Paper 74-GT-143, 1974.

69. Goulas, A.: "A Blade-to-Blade Solution of the Flow in a Centrifugal Compressor Impeller with Splitters," ASME Journal of Engineering for Power, Volume 102, 1980, pp. 632.

70. McNally, W. D.: "FORTRAN Program for Generating a Two-Dimensional Orthogonal Mesh Between Arbitrary Boundaries," NASA TN D-6766, 1972.

71. MacCormack, R. W.: "The Effect of Viscosity in Hypervelocity Impact Cratering," AIAA Paper 69-345, 1969.

72. Gopalakrishnan, S.; and Bozzola, R.: " Computation of Shocked Flows in Compressor Cascades," AIAA Paper 72-GT-31, 1972.

73. Kurzrock, J. W.; and Novick, A. S.: "Transonic Flow Around Rotor Blade Elements," Journal of Fluids Engineering, 1975, pp. 598.

74. Thompkins, W. T.: "A FORTRAN Program for Calculating Three-Dimensional, Inviscid, Rotational Flows with Shock Waves in Axial Compressor Blade Rows. I-User's Manual," Proposed NASA CR, 1982.

75. McDonald, P. W.: "The Computation of Transonic Flow Through Two-Dimensional Gas Turbine Cascades," ASME Paper 71-GT-89, 1971.

76. Denton, J. D.: "A Time Marching Method for Two- and Three-Dimensional Blade-to-Blade Flow," Aeronautical Research Council R&M 3775, 1975.

77. Denton, J. D.: "Extension of the Finite Area Time Marching Method to Three Dimensions," VKI Lecture Series, Volume 84, 1976.

78. Denton, J. D.; and Singh, U. K.: "Time Marching Methods for Turbomachinery Flow Calculation. Part I Basic Principles and 2D Applications, and Part II Three-Dimensional Flows," VKI Lecture Series, 1979-7, 1979.

79. Bosman, C.; and Highton, J.: "A Calculation Procedure for Three-Dimensional, Time-Dependent, Inviscid, Compressible Flow Through Turbomachine Blades of Any Geometry," Journal of Mechanical Engineering Science, Volume 21, 1979, pp. 39.

80. Bosman, C.: "An Analysis of Three-Dimensional Flow in a Centrifugal Compressor Impeller," Journal of Engineering for Power, Volume 102, 1980, pp. 619.

81. Moretti, G.: "The λ -Scheme," Computers and Fluids, Volume 7, 1979, pp. 191.

82. De Neef, T.; and Moretti, G.: "Shock Fitting for Everybody," Computers and Fluids, Volume 8, 1980, pp. 327.

83. Pandolfi, M.; and Zannetti, L.: "A Physical Approach to Solve Numerically Complicated Hyperbolic Flow Problems," Proceedings of Seventh International Conference on Numerical Methods in Fluid Mechanics, Palo Alto, Springer-Verlag, 1980.

84. Chakravarthy, S. R.; Anderson, D. A.; and Salas, M. D.: "The Split-Coefficient Matrix Method for Hyperbolic Systems of Gas Dynamic Equations," AIAA Paper 80-0268, AIAA 18th Aerospace Sciences Meeting, Pasadena, 1980.

85. Ni, R. H.: "A Multiple Grid Scheme for Solving the Euler Equations," AIAA 5th Computational Fluid Dynamics Conference, Palo Alto, AIAA Paper 81-1025, 1981.

86. Richtmyer, R. D.; and Morton, K. W.: Difference Methods for Initial-Value Problems, 2nd Edition, Interscience Publishers, New York, 1967.

87. Essers, J. A.; and Kafyeke, F.: "Application of Fast Pseudo-Unsteady Method to Steady Transonic Flows in Turbine Cascades," ASME Paper 81-GT-124, 1981.

88. Viviand, H.; and Veuillot, J. P.: "Methodes Pseudo-Instation-Naires Pour Le Calcul D'Ecoulements Transsoniques," ONERA Publication 1978-4, English Translation ESA.TT.561, 1978.

89. Veuillot, J. P.; and Viviand, H.: "A Pseudo-Unsteady Method for the Computation of Transonic Potential Flows," AIAA Journal, Volume 17, Number 7, July, 1979.

90. Brochet, J.: "Numerical Computation of Three-Dimensional Transonic Internal Flows," Rech. Aerosp. Number 1980-5, 1980.

91. Enselme, M.; Brochet, J.; and Boisseau, J. P.: "Low Cost Three-Dimensional Flow Computations Using a Mini-System," AIAA 5th Computational Fluid Dynamics Conference, Palo Alto, AIAA Paper 81-1013, 1981.

92. Briley, W. R.; and McDonald, H.: "Solution of the Three-Dimensional Compressible Navier-Stokes Equations By An Implicit Techniques," Proceedings 4th International Conference on Numerical Methods In Fluid Dynamics, Boulder, Springer-Verlag, 1975, pp. 105.

93. Briley, W. R.; and McDonald, H.: "Solution of the Multidimensional Compressible Navier-Stokes Equations by a Generalized Implicit Method," Journal of Computational Physics, Volume 24, 1977, pp. 372.

94. Beam, R. M.; and Warming, R. F.: "An Implicit Finite-Difference Algorithm for Hyperbolic Systems in Conservation-Law Form," Journal of Computational Physcis, Volume 22, 1976, pp. 87.

95. Briley, W. R.; and McDonald, H.: "On the Structure and Use of Linearized Block Implicit Schemes," Journal of Computational Physics, Volume 34, 1980, pp. 54.

96. Steger, J. L.: "Implicit Finite-Difference Simulation of Flow About Arbitrary Two-Dimensional Geometries," AIAA Journal, Volume 16, 1978, pp. 679.

97. Steger, J. L.; Pulliam, T. H.; and Chima, R. V.: "An Implicit Finite Difference Code for Inviscid and Viscous Cascade Flow," AIAA Paper 80-1427, AIAA 13th Fluid and Plasma Dynamics Conference, Snowmass, 1980.

98. Shamroth, S.; Gibeling, H. J.; and McDonald, H.: "A Navier-Stokes Solution for Laminar and Turbulent Flow Through a Cascade of Airfoils," AIAA Paper 80-1426, AIAA 13th Fluid and Plasma Dynamics Conference, Snowmass, 1980.

99. Delaney, R. A.: "Time-Marching Analysis of Steady Transonic Flow in Turbomachinery Cascades Using the Hopscotch Method," to be presented ASME Gas Turbine Conference, London, 1982.

100. Denton, J. D.: "An Improved Time-Marching Method for Turbomachinery Flow Calcultion," to be presented ASME Gas Turbine Conference, London, 1982.

101. Johnson, G. M.: "Surrogate-Equation Technique for Simulation of Steady Inviscid Flow," NASA TP 1866, 1981.

102. Ecer, A.; and Akay, H. U.: "Solution of Steady Euler Equations for Flows Using a Variational Finite Element Formulation," Open Form, AIAA 5th Computational Fluid Dynamics Conference, Palo Alto, 1981.

103. Lacor, C.; and Hirsch, C.: "Rotational Flow Calculations In Three-Dimensional Blade Passages," to be presented ASME Gas Turbine Conference, London, 1982.

104. Chang, S. C.; and Adamczyk, J. J.: "A Semi-Direct Algorithm for Computing 3-D Inviscid Shear Flows," AIAA 5th Computational Fluid Dynamics Conference, Palo Alto, 1981.

105. Chima, R. V.; and Strazisar, A. J.: "Comparison of Two- and Three-Dimensional Flow Computations with Laser Anemometer Measurements in a Transonic Compressor Rotor," NASA TP 1931, 1982.

106. Sieverding, C. H.: "Experimental Data on Two Transonic Turbine Blade Sections in Comparison with Various Theoretical Methods," von Karman Institute, LS 59, 1973.

107. Caretto, L. S.; Curr, R. M.; and Spalding, D. B.: "Two Numerical Methods for Three-Dimensional Boundary Layers," Computer Methods in Applied Mechanics and Engineering, Volume 1, 1972, pp. 39-57.

108. Patankar, S. V.; and Spalding, D. B.: "A Calculation Procedure for Heat, Mass and Momentum Transfer In Three-Dimensional Parabolic Flows," International Journal of Heat and Mass Transfer, Volume 15, 1972, pp. 1787-1806.

109. Briley, W. R.: "Numerical Method for Predicting Three-Dimensional Steady Viscous Flow in Ducts," Journal of Computational Physics, Volume 14, Number 1, 1974, pp. 8-28.

110. Ghia, U.; Ghia, K. N.; and Studerus, C. J.: "Three-Dimensional Laminar Incompressible Flow In Straight Polar Ducts," Computers and Fluids, Volume 5, 1977, pp. 205-218.

111. Roberts, D. W.; and Forester, C. K.: "Parabolic Procedure for Flows In Ducts with Arbitrary Cross-Sections," AIAA Journal, Volume 17, Number 1, 1979, pp. 33-40.

112. Briley, W. R.; and McDonald, H.: "Analysis and Computation of Viscous Subsonic Primary and Secondary Flows," AIAA Paper 79-1453, July, 1979.

113. Anderson, O. L.: "Calculation of Internal Viscous Flows in Axisymmetric Ducts at Moderate to High Reynolds Numbers," Computers and Fluids, Volume 8, 1980, pp. 391-411.

114. Anderson, O. L.; and Hankins, G. B., Jr.: "Development of a Parabolic Finite Difference Method for 3-D High Reynolds Number Viscous Internal Flows," ASME Paper Winter Annual Meeting, November, 1981.

115. Harlow, F. H.; and Welch, J. E.: "Numerical Calculation of Time-Dependent Viscous Incompressible Flow of Fluid with Free Surface," Physics of Fluids, Volume 8, 1965, pp. 2182-2189.

116. Patankar, S. V.; Pratap, V. S.; and Spalding, D. B.: "Prediction of Laminar Flow and Heat Transfer in Helically-Coiled Pipes," Journal of Fluid Mechanics, Volume 62, Part III, 1974, pp. 539-551.

117. Ghia, K. N.; and Sokhey, J. S.: "Laminar Incompressible Viscous Flow in Curved Ducts of Regular Cross-Sections," Journal of Fluids Engineering, Volume 99, 1977, pp. 640-648.

118. Kreskovsky, J. P.; Briley, W. R.; and McDonald, H.: "Prediction of Laminar and Turbulent Primary and Secondary Flows in Strongly Curved Ducts," NASA CR-3388, February, 1981.

119. Taylor, A. M. K. P.; Whitelaw, J. H.; and Yianneskis, M.: "Measurements of Laminar and Turbulent Flow in a Curved Duct with Thin Inlet Boundary Layers," NASA CR-3367, January, 1981.

120. Baker, A. J.; and Orzechowski, J. A.: "A Continuity-Constraint Finite Element Algorithm for Three-Dimensional Parabolic Flow Prediction," ASME Paper, Winter Annual Meeting, November 1981.

121. Pratap, V. S.; and Spalding, D. B.: "Fluid Flow and Heat Transfer and Three-Dimensional Duct Flows," International Journal of Heat and Mass Transfer, Volume 19, 1976, pp. 1183-1188.

122. Moore, J.; and Moore, J. G.: "A Calculation Procedure for Three-Dimensional, Viscous, Compressible Duct Flow. Part I-Inviscid Flow Considerations," ASME Paper 79-WA/FE-4, December, 1979.

123. Chilukuri, R.; and Pletcher, R. H.: "Numerical Solutions to the Partially Parabolized Navier-Stokes Equations for Developing Flow in a Channel," Numerical Heat Transfer, Volume 3, 1980, pp. 169-188.

124. Dodge, P. R.: "Numerical Method for 2D and 3D Viscous Flows," AIAA Journal, Volume 15, Number 7, 1977, pp. 961-965.

125. Dodge, P. R.: "3-D Heat Transfer Analysis Program," AFAPL-TR-77-64, October, 1977.

126. Pratap, V. S.; and Spalding, D. B.: "Numerical Computations of the Flow In Curved Ducts," The Aeronautical Quarterly, Volume 26, 1975, pp. 219-228.

127. Moore, J.; and Moore, J. G.: "A Calculation Procedure for Three-Dimensional, Viscous, Compressible Duct Flow. Part II-Stagnation Pressure Losses in a Rectangular Elbow," ASME Paper 79-WA/FE-5, December, 1978.

128. Moore, J.; and Moore, J. G.: "Calculations of Three-Dimensional, Viscous Flow and Wake Development in a Centrifugal Impeller," Symposium on Performance Prediction of Centrifugal Pumps and Compressors, ASME 25th International Gas Turbine Conference, New Orleans, 1980.

129. Moore, J.; and Moore, J. G.: "Three-Dimensional, Viscous Flow Calculations for Assessing the Thermodynamic Performance of Centrifugal Compressors - Study of the Eckardt Compressor," AGARD Conference, Brussels, May, 1980.

130. Stanitz, J. D.; Osborn, W. M.; and Mizisin, J.: "An Experimental Investigation of Secondary Flow in An Accelerating Rectangular Elbow with 90° of Turning," NACA TN-3015, October, 1953.

131. Waterman, W. F.: "Low-Aspect-Ratio Turbine Technology Program-Final Report for Phase II," AiResearch Report 75-211701 (2), March, 1977.

132. Caretto, L. S.; Gosman, A. D.; Patankar, S. V.; and Spalding, D. B.: "Two Calculation Procedures for Steady, Three-Dimensional Flows with Recirculation," Third International Conference on Numerical Methods in Fluid Mechanics, Paris, 1972, Springer-Verlag, New York.

133. Rathby, G. D.; and Schneider, G. E.: "Numerical Solution of Problems in Incompressible Fluid Flow: Treatment of the Velocity-Pressure Coupling," Numerical Heat Transfer, Volume 2, 1979, pp. 417-440.

134. Walitt, L.; Harp, J. L., Jr.; and Liu, C. Y.: "Numerical Calculation of the Internal Flow Field in a Centrifugal Compressor Impeller," NASA CR-134984, December, 1975.

135. Walitt, L.; and Liu, C. Y,: "Numerical Calculations of the Viscous Flow In a Supersonic Compressor Cascade with Splitter Vanes," AFAPL-TR-78-2, February, 1978.

136. Bosman, C.; and Highton, J.: "The Computation of Three-Dimensional Viscous, Compressible Flow," Numerical Methods in Laminar and Turbulent Flow, Editors Taylor, C.; Morgan, K.; and Brebbia, C. A., Proceedings of the International Conference, University of Swansea, 1978, Halsted Press, John Wiley and Sons.

137. Shang, J. S.; Buning, P. G.; Hankey, W. L.; and Wirth, M. C.: "Performance of a Vectorized Three-Dimensional Navier-Stokes Code on the CRAY-1 Computer," AIAA Journal, Volume 18, Number 9, 1980, pp. 1073-1079.

138. Spradley, L. W.; Stalnaker, J. F.; and Ratliff, A. W.: "Solution of the Three-Dimensional Navier-Stokes Equations on a Vector Processor," AIAA Journal, Volume 19, Number 10, 1981, pp. 1302-1307.

139. Prozan, R. J.; Spradley, L. W.; Anderson, P. G.; and Pearson, M. L.: "The General Interpolants Method," AIAA Paper 77-642, June, 1977.

140. Ghia, U.; Ghia, K. N.; Rubin, S. G.; and Khosla, P. K.: "Study of Incompressible Flow Separation Using Primitive Variables," Computers and Fluids, Volume 9, 1981, pp. 123-142.

141. McDonald, H.; and Briley, W. R.: "Computational Fluid Dynamic Aspects of Internal Flows," AIAA Paper 79-1445, July, 1979.

142. Humphrey, J. A. C.; Taylor, A. M. K.; and Whitelaw, J. H.: "Laminar Flow In a Square Duct of Strong Curvature," Journal of Fluid Mechanics, Volume 83, Part III, 1977, pp. 509-527.

143. Humphrey, J. A. C.; Whitelaw, J. H.; and Yee, G.: "Turbulent Flow in a Square Duct with Strong Curvature," Journal of Fluid Mechanics, Volume 103, 1981, pp. 443-463.

144. Buggeln, R. C.; Briley, W. R.; and McDonald, H.: "Computation of Laminar and Turbulent Flow in Curved Ducts, Channels, and Pipes Using the Navier-Stokes Equations," ONR Report R80-920006-F, December, 1980.

145. Abbiss, J. B.; East, L. F.; Nash, C. R.; Parker, P.; Pike, E. R.; and Swayer, W. G.: "A Study of the Interaction of a Normal-Shock Wave and Turbulent Boundary Layer Using a Laser Anemometer," Royal Aircraft Establishment, England, TR 75141, February, 1976.

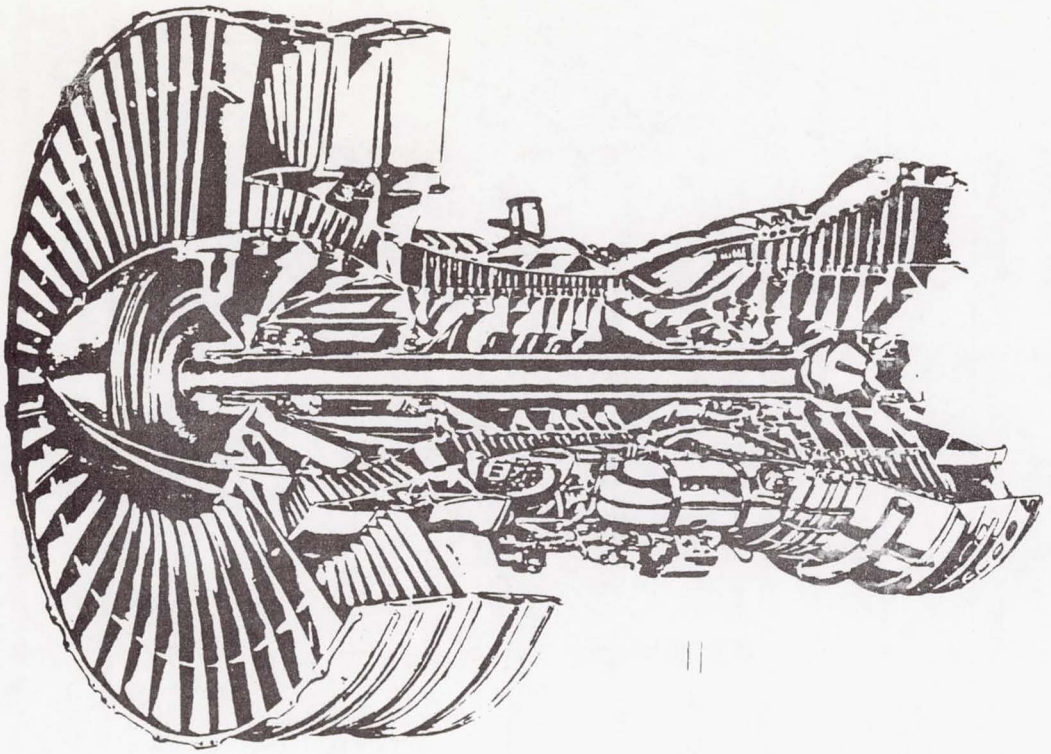

FIG. 1 - PRATT & WHITNEY JT9D TURBOFAN ENGINE

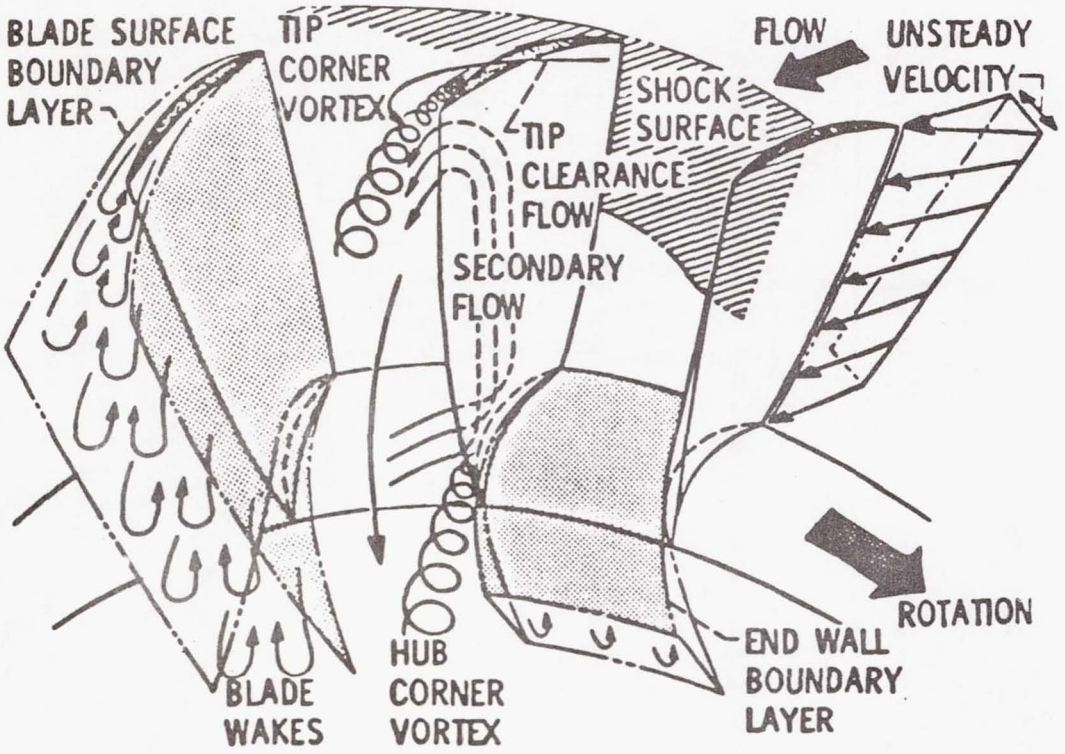

FIG. 2 - TURBOMACHINERY BLADE ROW FLOW FEATURES

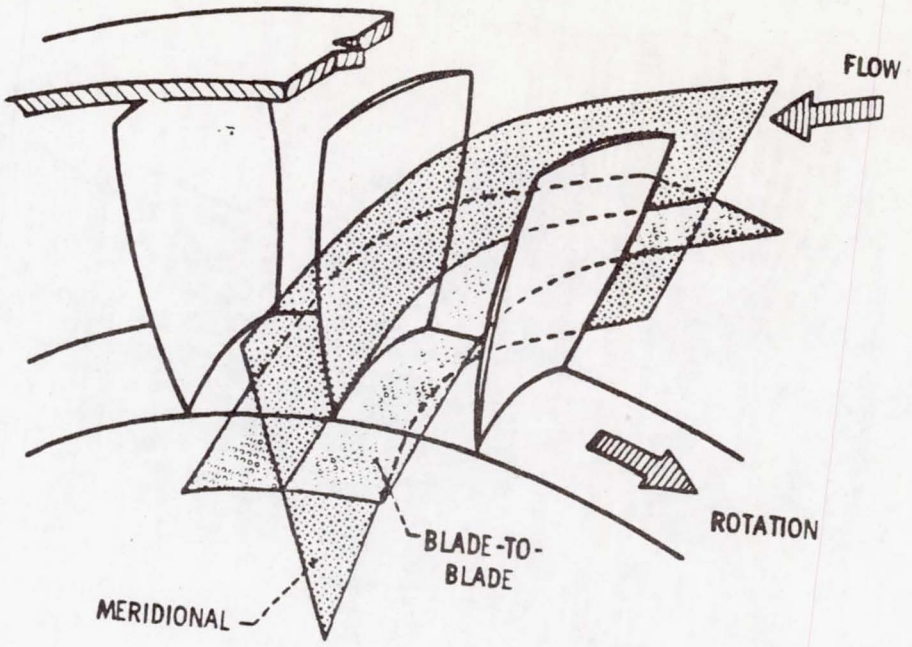

FIG. 3 - TURBOMACHINERY TWO-DIMENSIONAL FLOW SURFACES

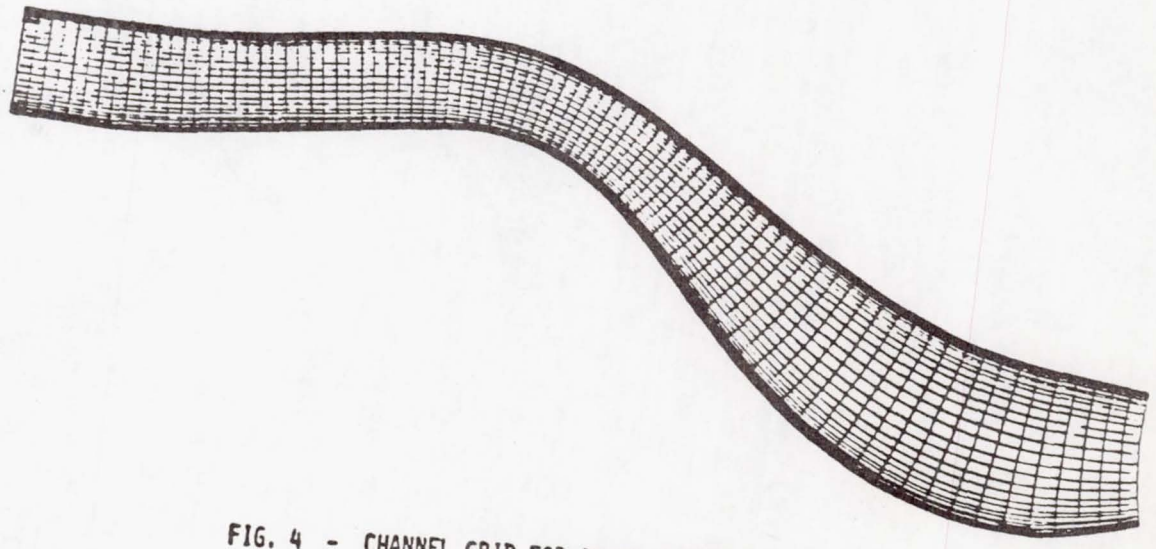

FIG. 4 - CHANNEL GRID FOR INLET TRANSITION DUCT

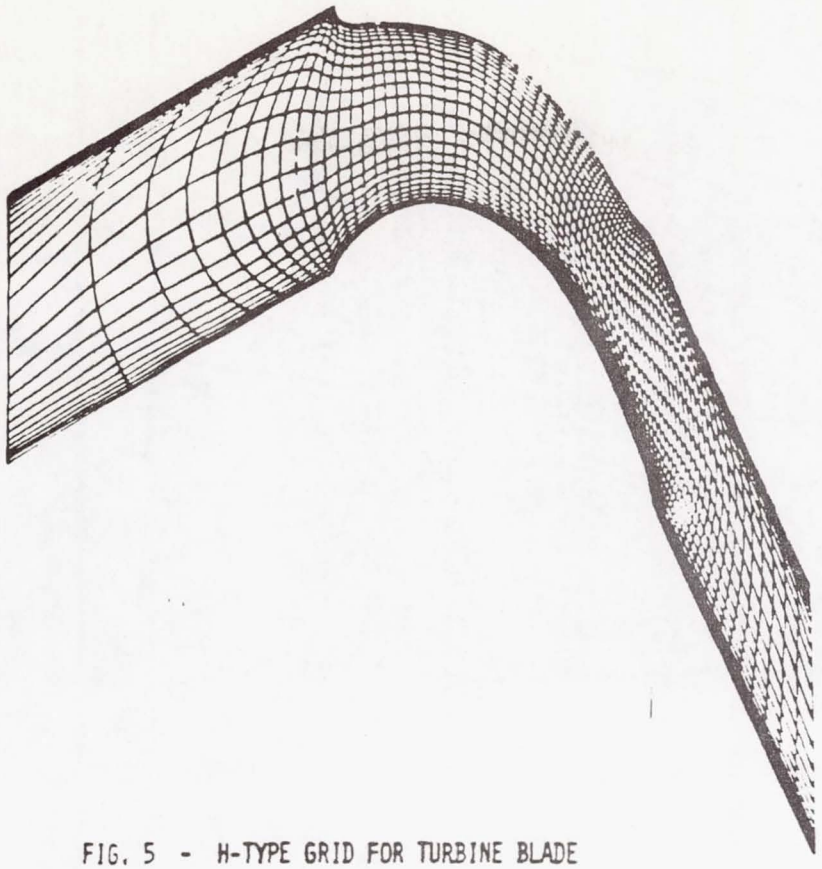

FIG. 5 - H-TYPE GRID FOR TURBINE BLADE

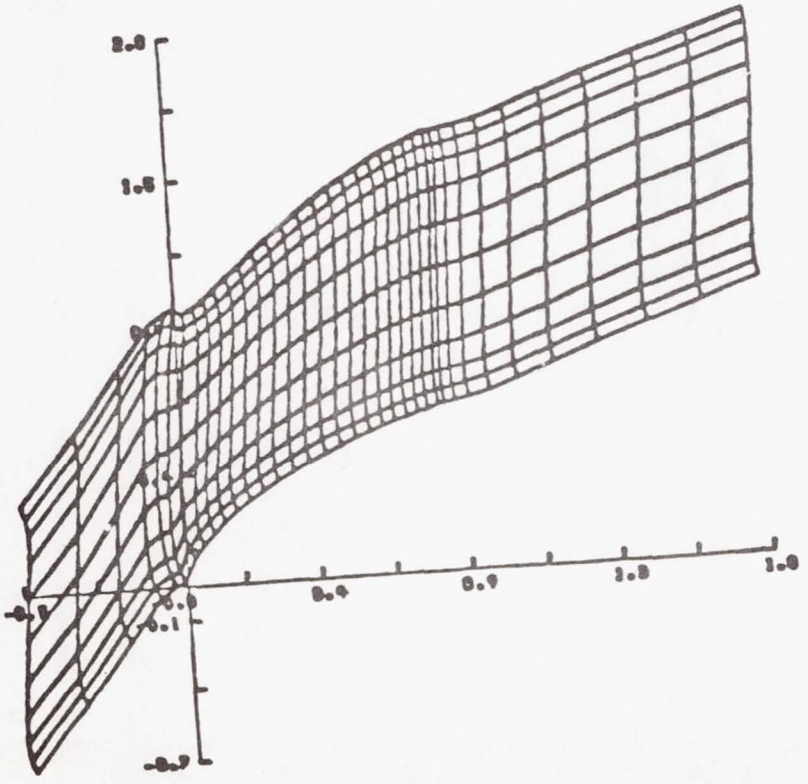

FIG. 6 - H-TYPE GRID FOR GOSTELOW COMPRESSOR

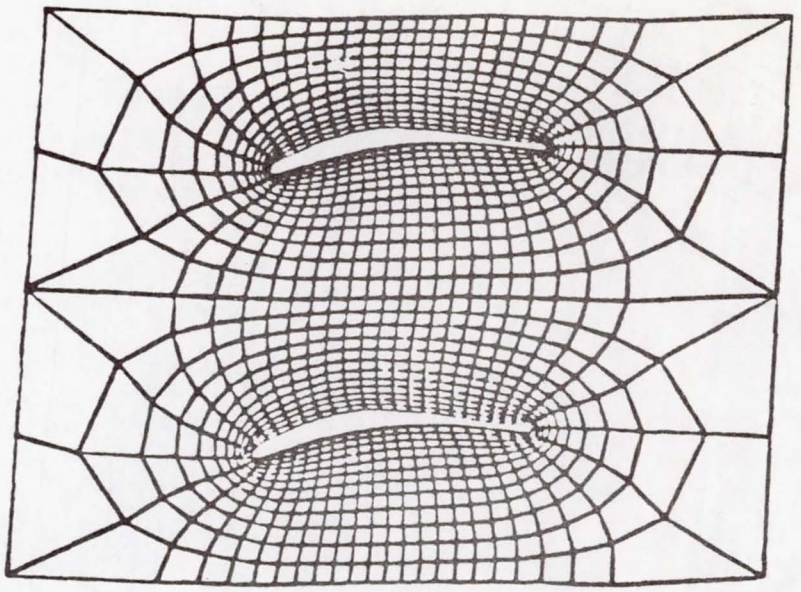

FIG. 7 - O-TYPE GRID FOR COMPRESSOR BLADE ROW

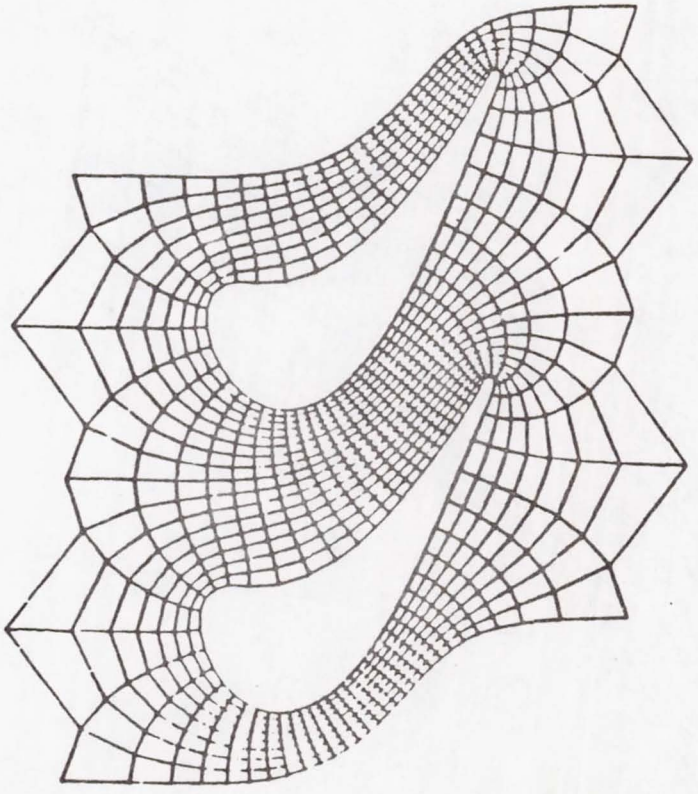

FIG. 8 - O-TYPE GRID FOR TURBINE STATOR BLADE ROW

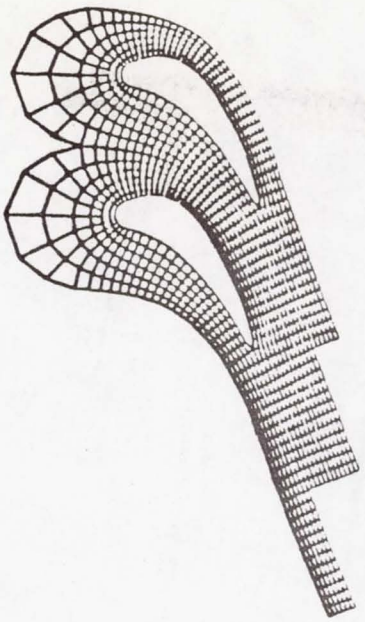

FIG. 9 - C-TYPE GRID FOR TURBINE STATOR BLADE ROW

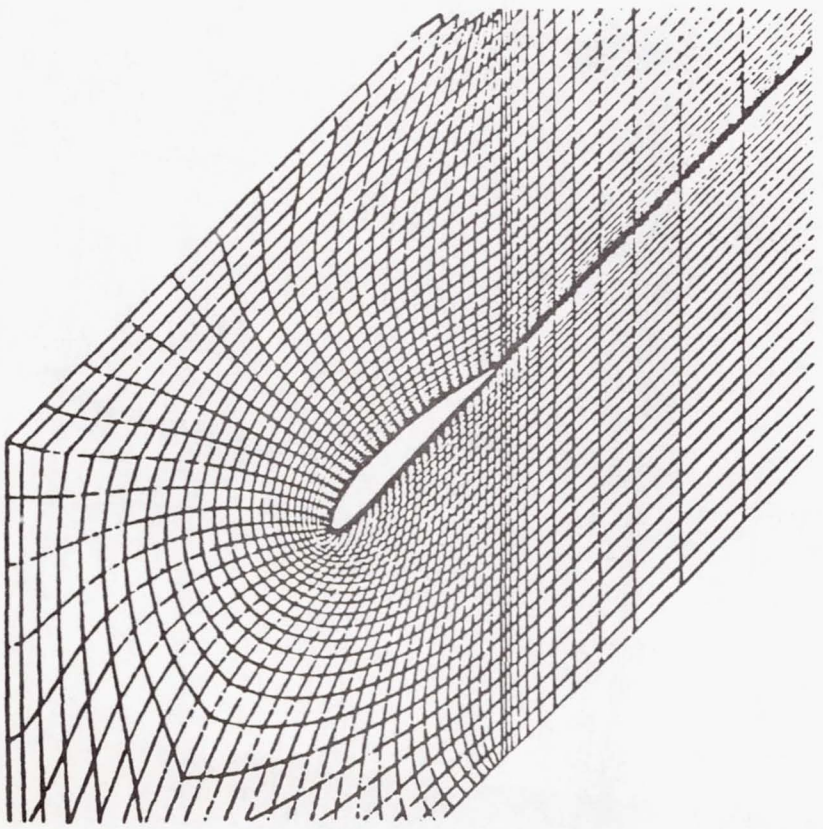

FIG. 10 - C-TYPE GRID FOR COMPRESSOR BLADE

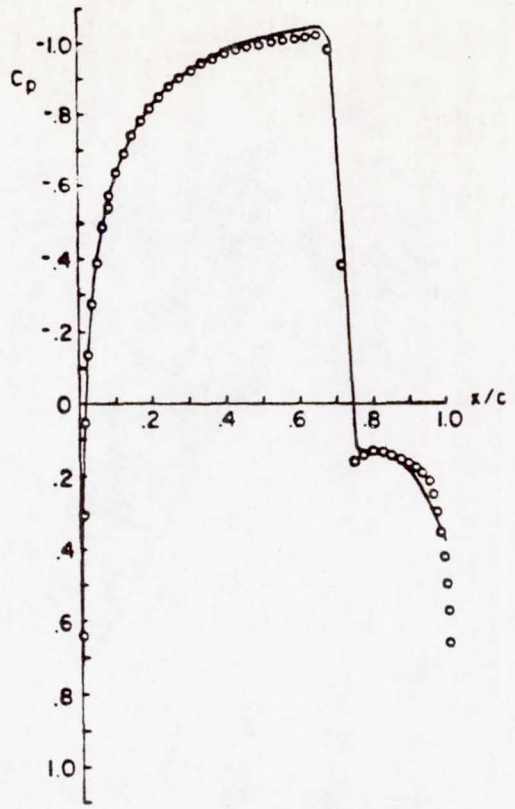

FIG. 11 - DULIKRAVICH - NACA 0012 COMPARISON WITH CAUGHEY

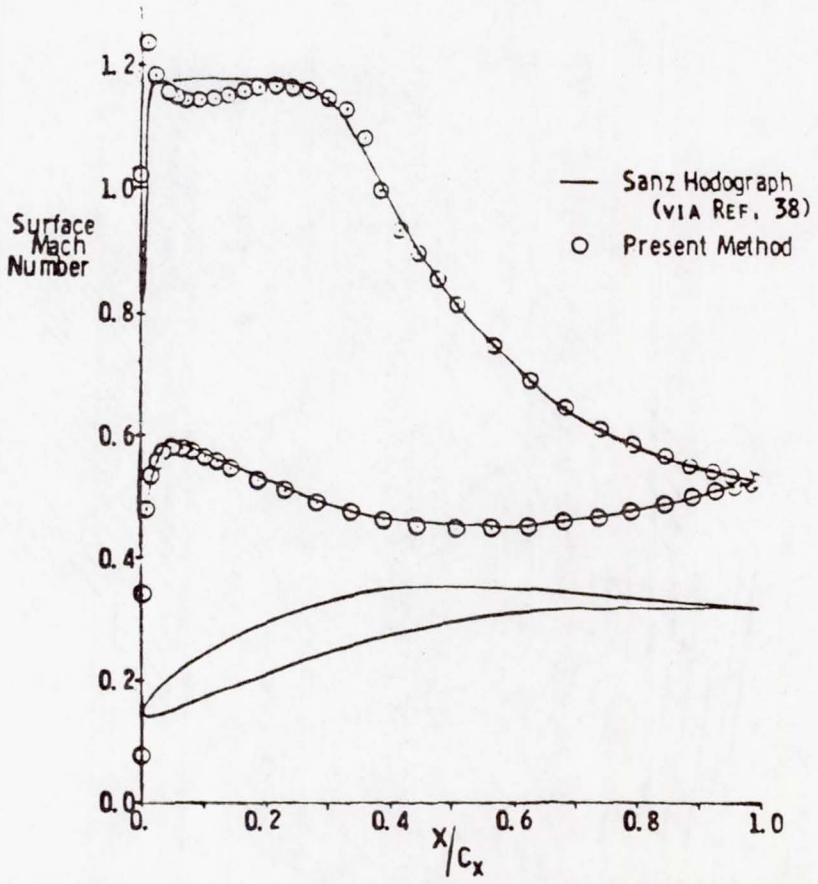

FIG. 12 - FARRELL - SUPERCRITICAL STATOR COMPARISON WITH SANZ

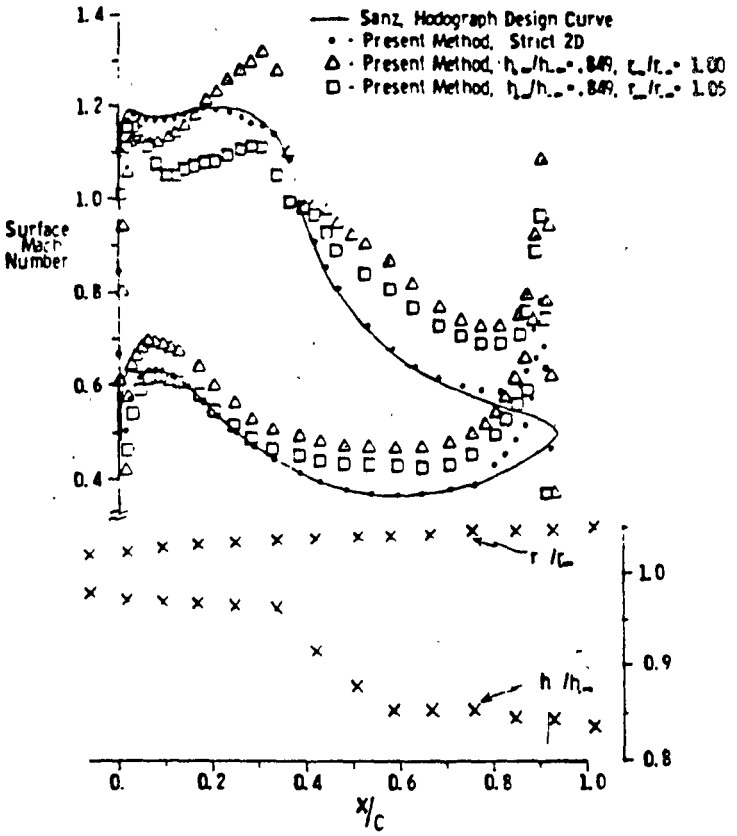

FIG. 13 - EFFECT OF STREAMTUBE THICKNESS AND RADIUS CHANGE ON FLOW ABOUT SUPERCRITICAL STATOR HUB SECTION

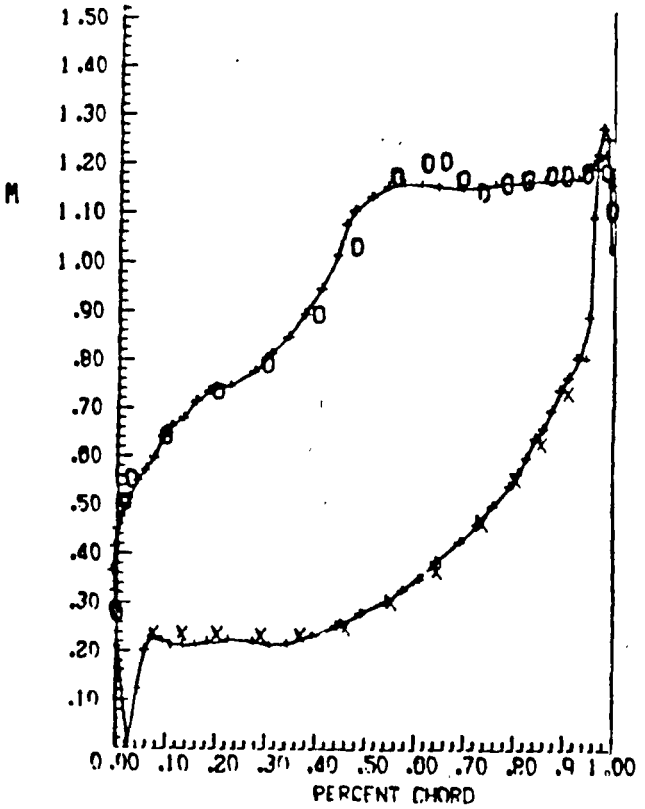

FIG. 14 - HIRSCH - VKI TURBINE CASCADE COMPARISON WITH EXPERIMENT

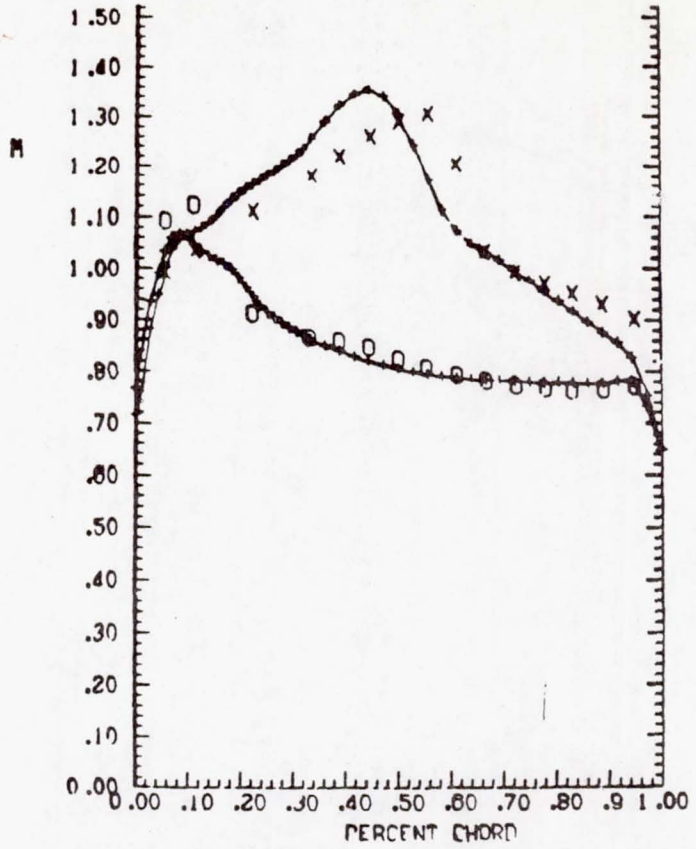

FIG. 15 - HIRSCH - VKI COMPRESSOR CASCADE COMPARISON WITH EXPERIMENT

RELATIVE MACH NUMBER DISTRIBUTION AT A NUMBER OF SPANWISE LOCATIONS

XM1 = 0.62 ROT = 1000. R_H = 1. M R_T = 2. M

MESH = 24 x 6 x 6

MESH = 48 x 12 x 12

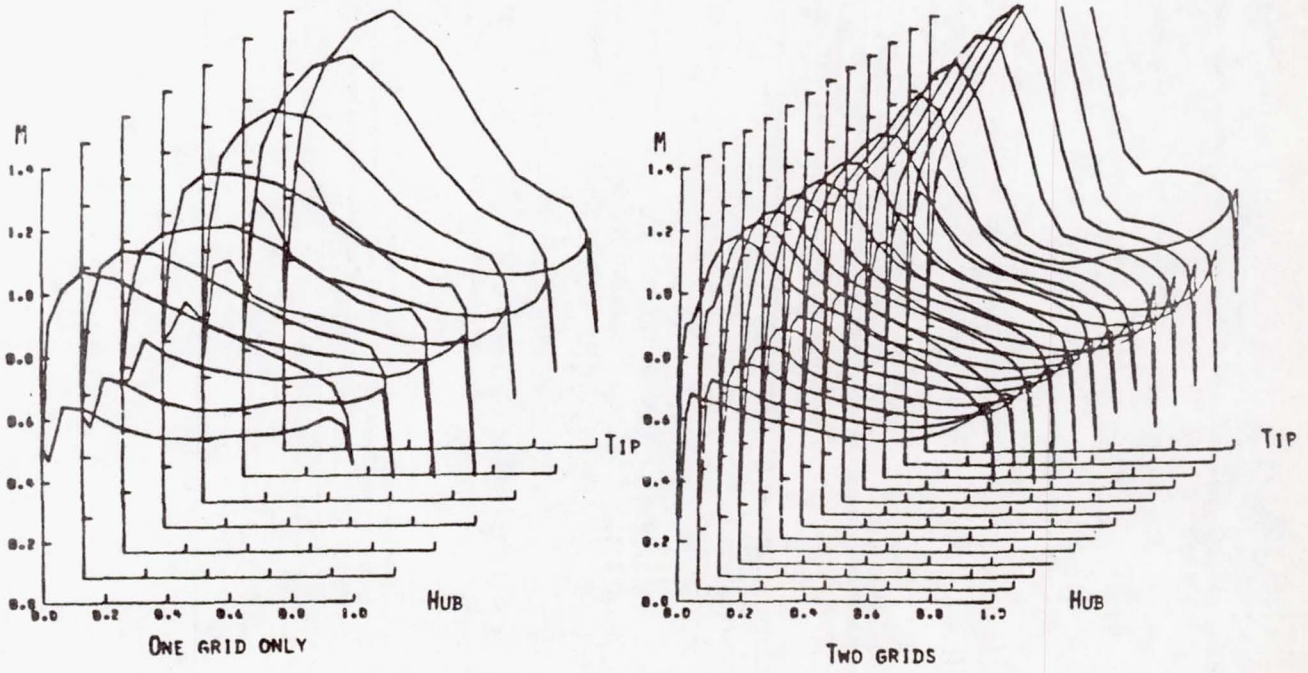

FIG. 16 - DULIKRAVICH - 3D FULL POTENTIAL ROTOR CALCULATION

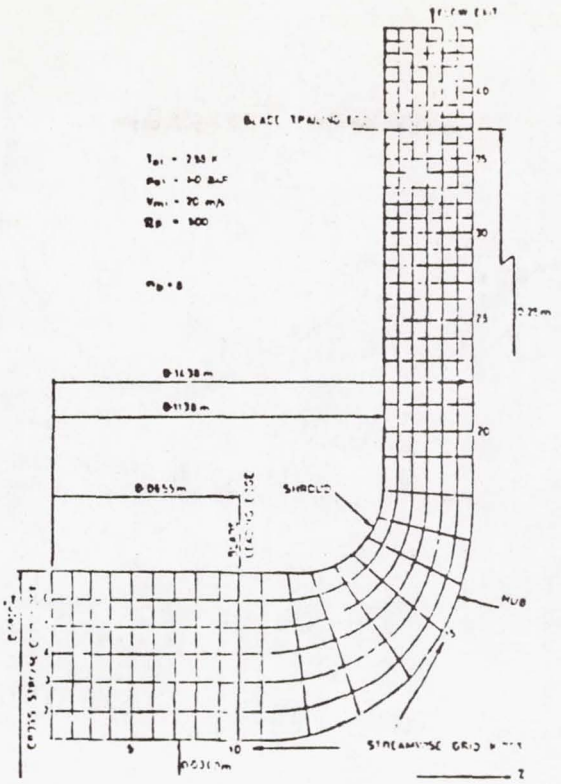

FIG. 17 - BOSMAN - LOW SPEED COMPRESSOR WITH MERIDIONAL GRID

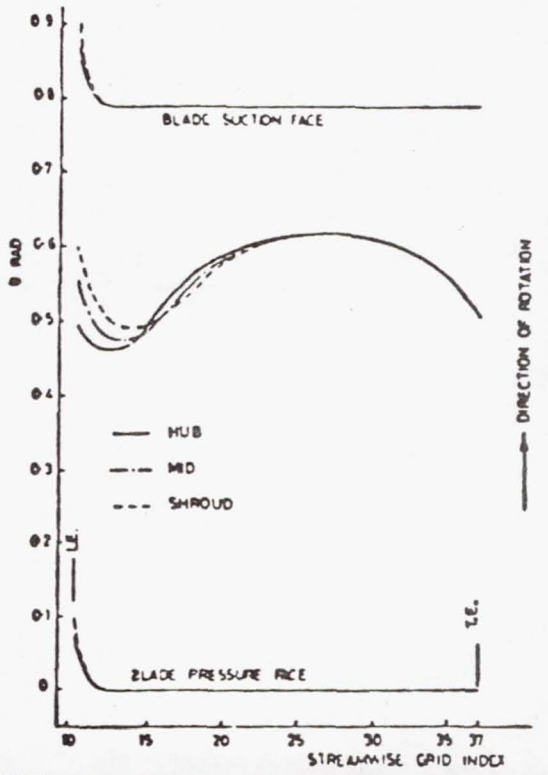

FIG. 18 - BOSMAN - COMPRESSOR BLADE SHAPE WITH S1 MEAN STREAMLINES FROM HUB TO SHROUD

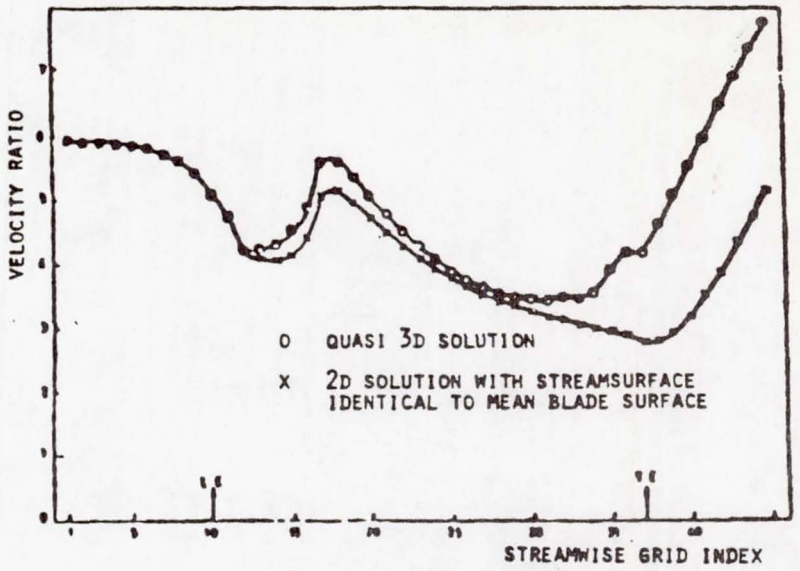

FIG. 19 - RELATIVE VELOCITY DISTRIBUTIONS ON HUB WITH NON-ITERATED AND ITERATED BOSMAN SOLUTIONS

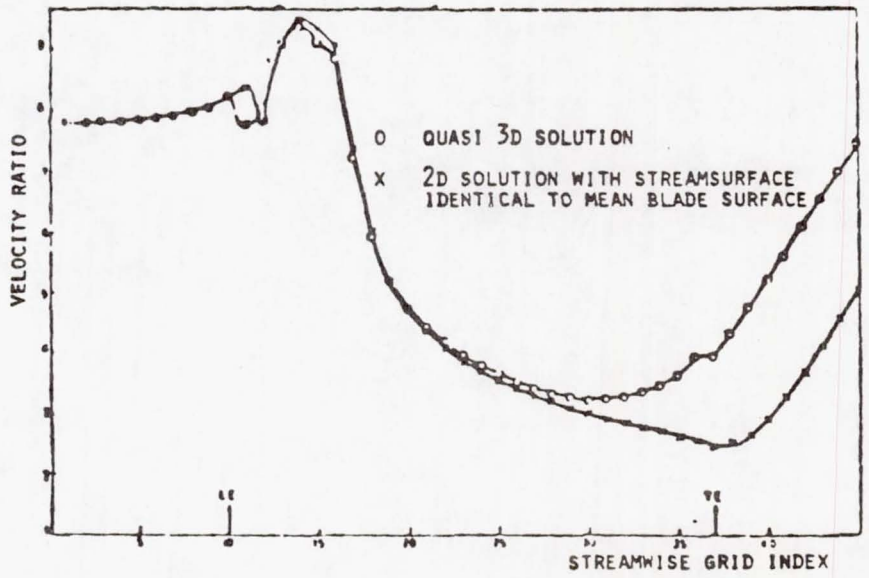

FIG. 20 - RELATIVE VELOCITY DISTRIBUTIONS ON SHROUD WITH NON-ITERATED AND ITERATED BOSMAN SOLUTIONS

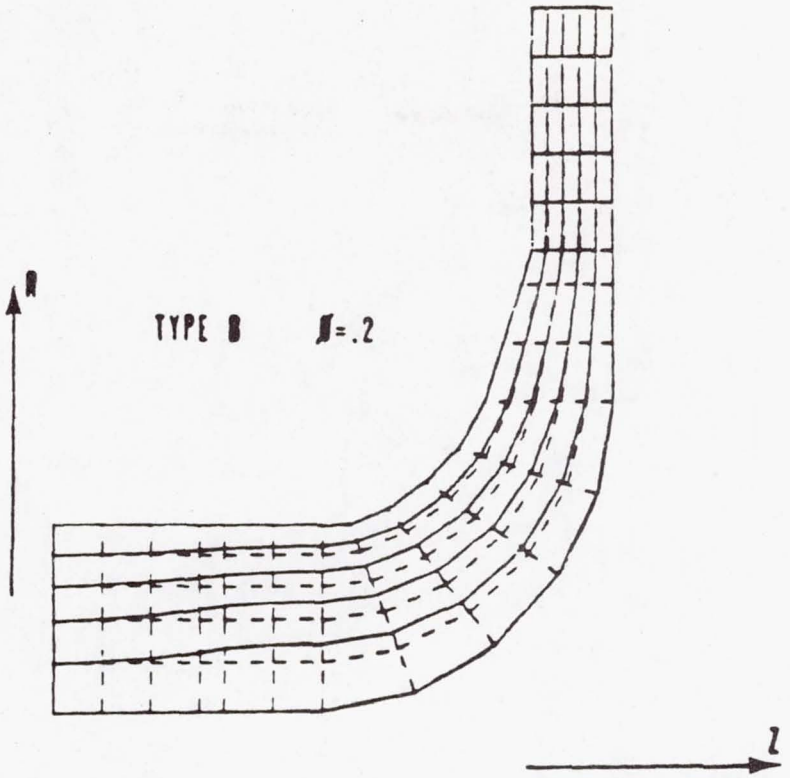

FIG. 21 - HIRSCH - IMPELLER WITH FINITE ELEMENT GRID AND STREAMLINES

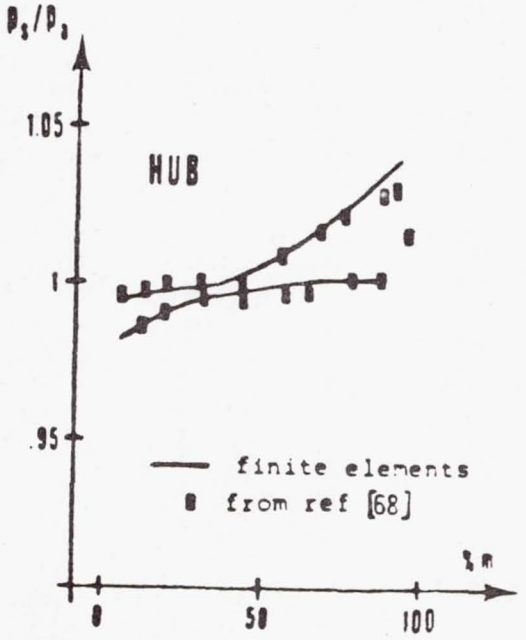

FIG. 22 - HIRSCH - CALCULATED AND EXPERIMENTAL STATIC PRESSURE ON IMPELLER HUB

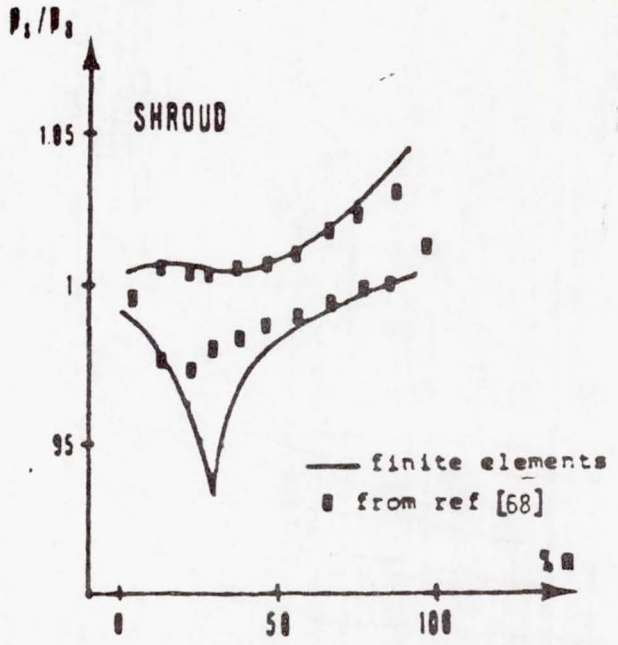

FIG. 23 - HIRSCH - CALCULATED AND EXPERIMENTAL STATIC PRESSURE ON IMPELLER SHROUD

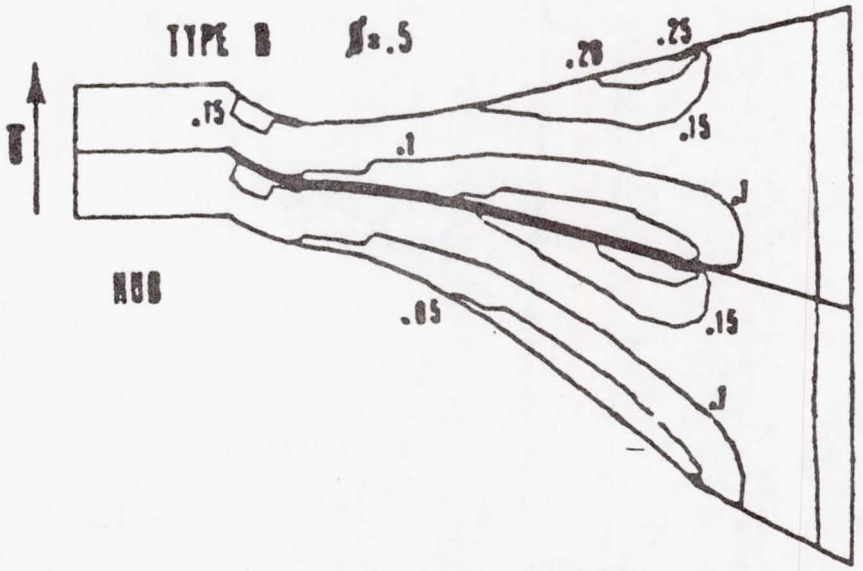

FIG. 24 - HIRSCH - CALCULATED MACH NUMBER CONTOURS ON IMPELLER HUB

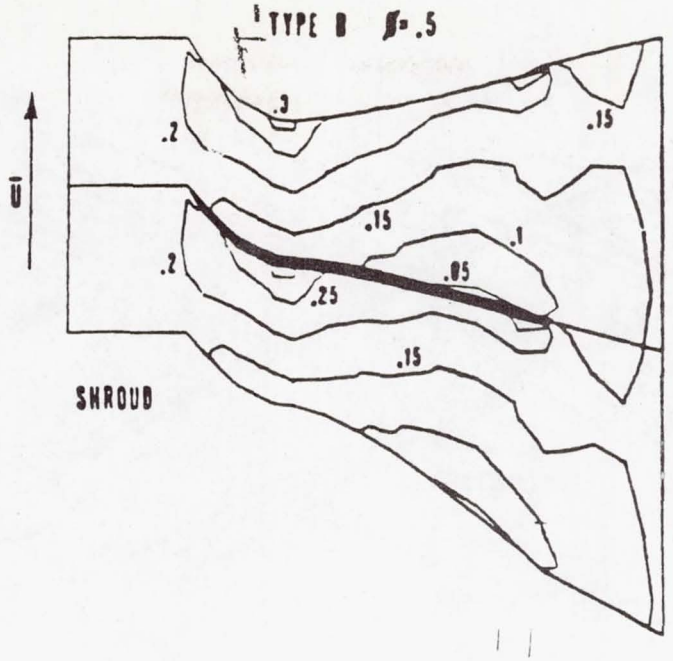

FIG. 25 - HIRSCH - CALCULATED MACH NUMBER CONTOURS ON IMPELLER SHROUD

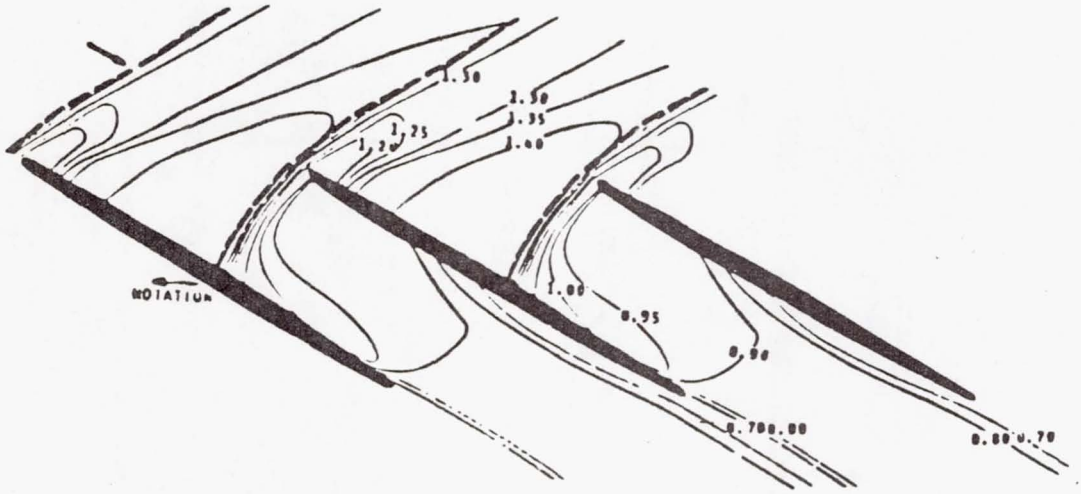

FIG. 26 - MEASURED MACH NUMBER CONTOURS NEAR TIP
OF NASA TRANSONIC COMPRESSOR ROTOR

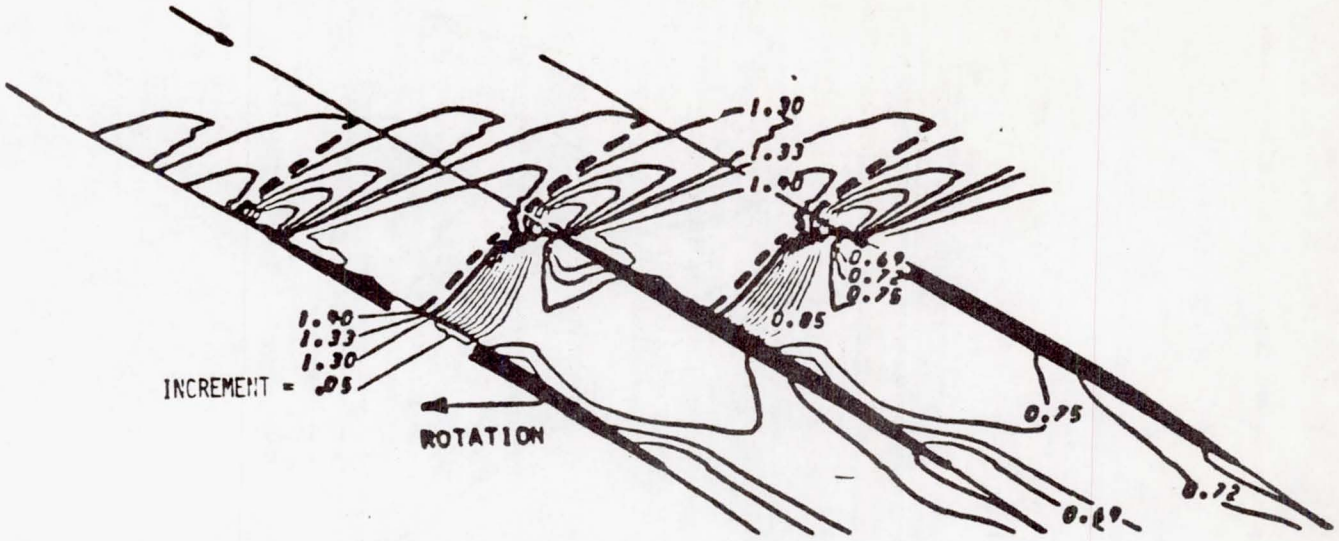

FIG. 27 - CALCULATED MACH NUMBER CONTOURS NEAR TIP OF NASA TRANSONIC COMPRESSOR ROTOR - THOMPKINS METHOD

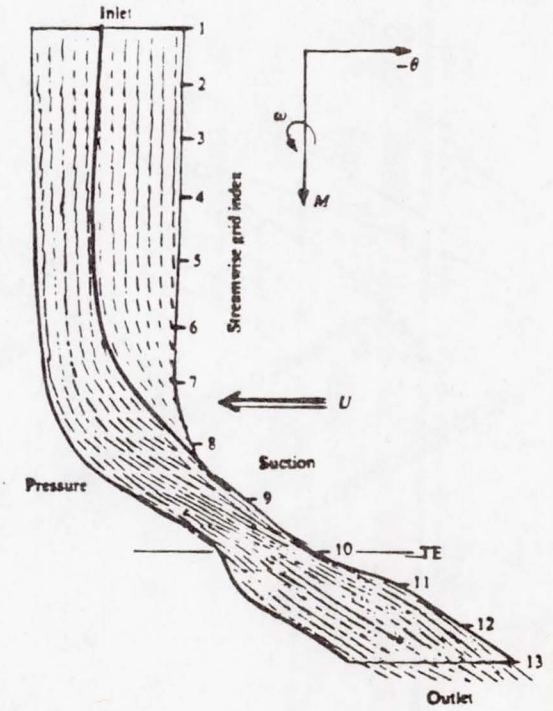

FIG. 28 - BOSMAN - RADIAL INFLOW TURBINE HUB WITH CALCULATED PATHLINES

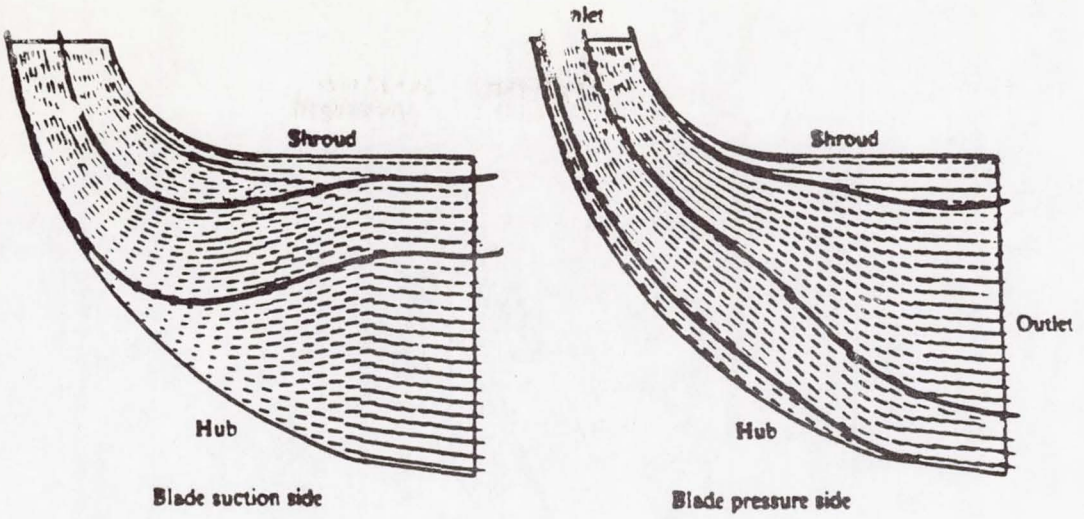

FIG. 29 - BOSMAN - RADIAL INFLOW TURBINE BLADE SURFACES WITH CALCULATED PATHLINES

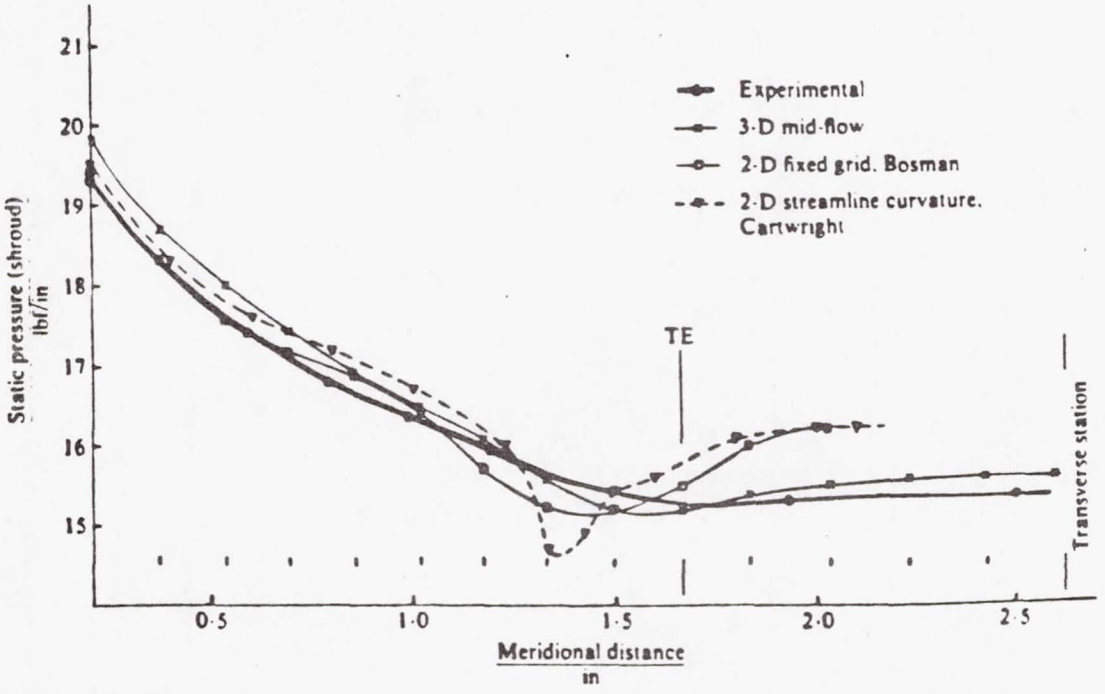

FIG. 30 - BOSMAN - RADIAL INFLOW TURBINE SHROUD STATIC PRESSURES - 2D vs. 3D

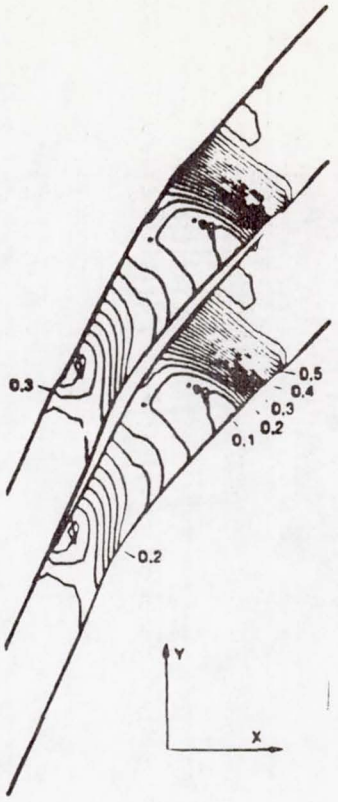

FIG. 31 - BROCHET - PRESSURE CONTOURS IN PLANE OF SYMMETRY FOR CONVERGING SIDEWALL COMPRESSOR CASCADE

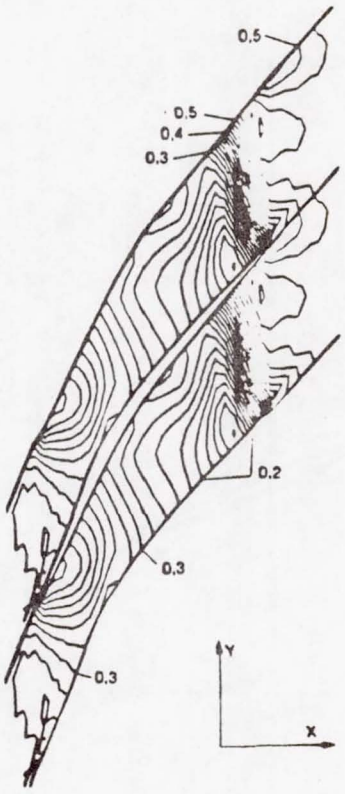

FIG. 32 - BROCHET - PRESSURE CONTOURS ALONG CONTOURED SIDEWALL OF COMPRESSOR CASCADE

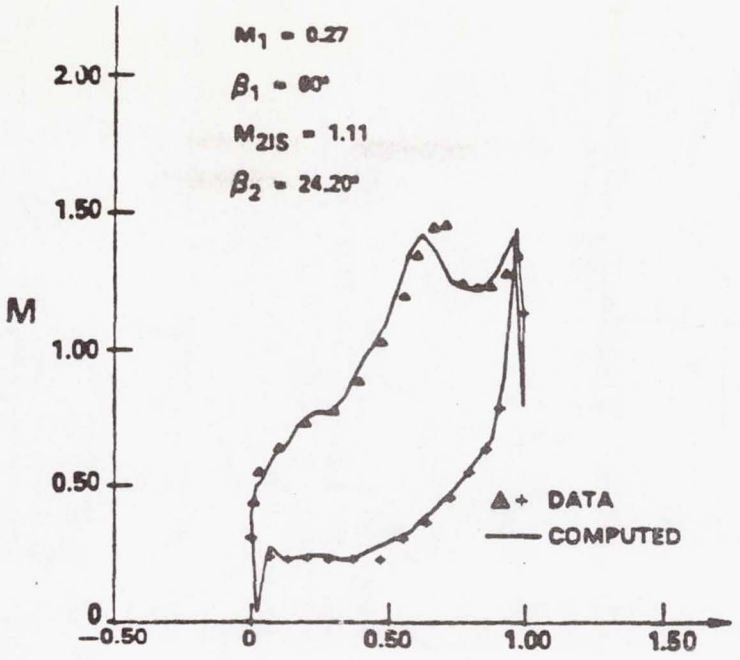

FIG. 33 - NI - CALCULATED AND MEASURED SURFACE MACH NUMBER ON VKI TURBINE ROTOR

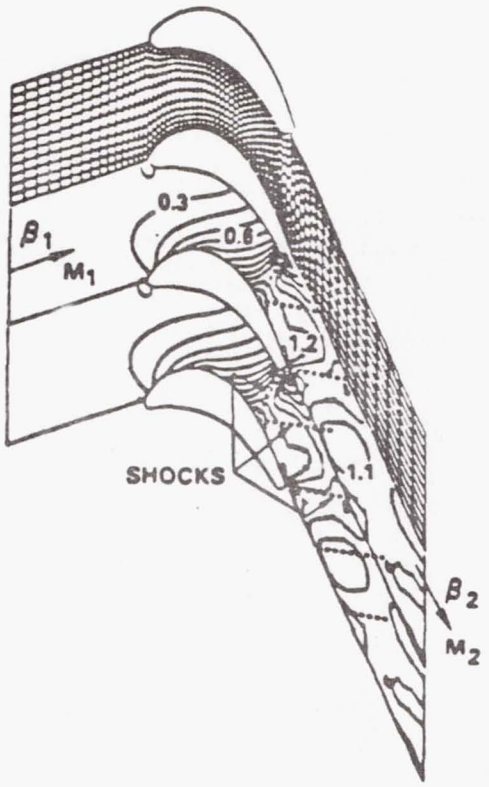

FIG. 34 - NI - MACH NUMBER CONTOURS FOR VKI TURBINE ROTOR

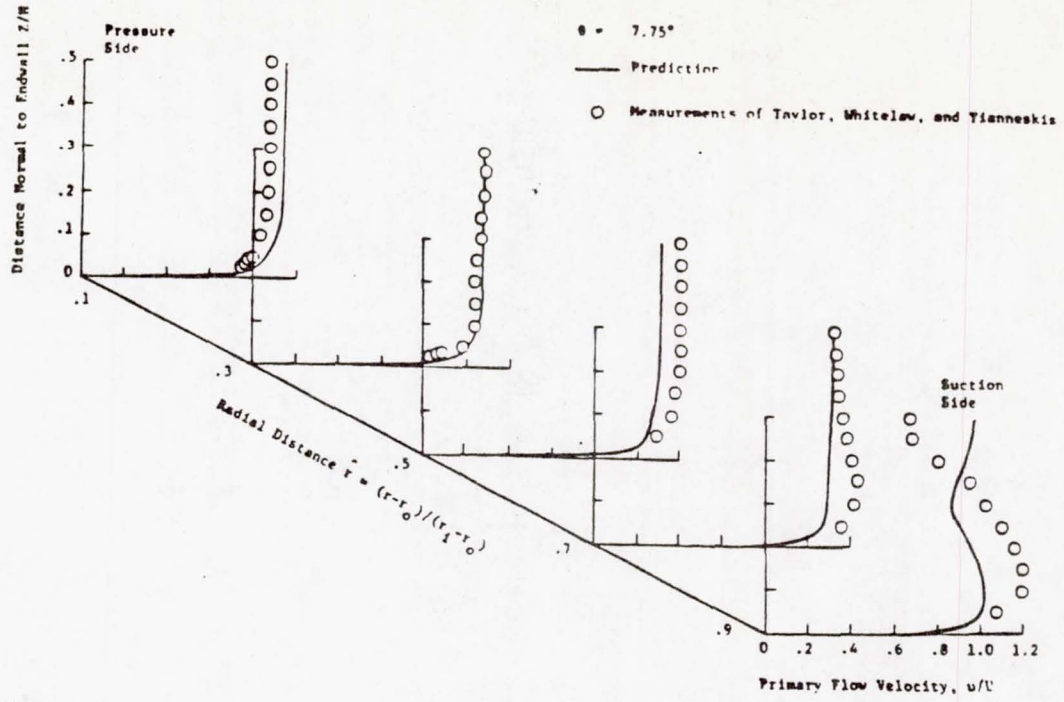

FIG. 35 - BRILEY - COMPUTED AND MEASURED AXIAL VELOCITY PROFILES AFTER 77.5° TURNING IN CIRCULAR ARC SQUARE DUCT

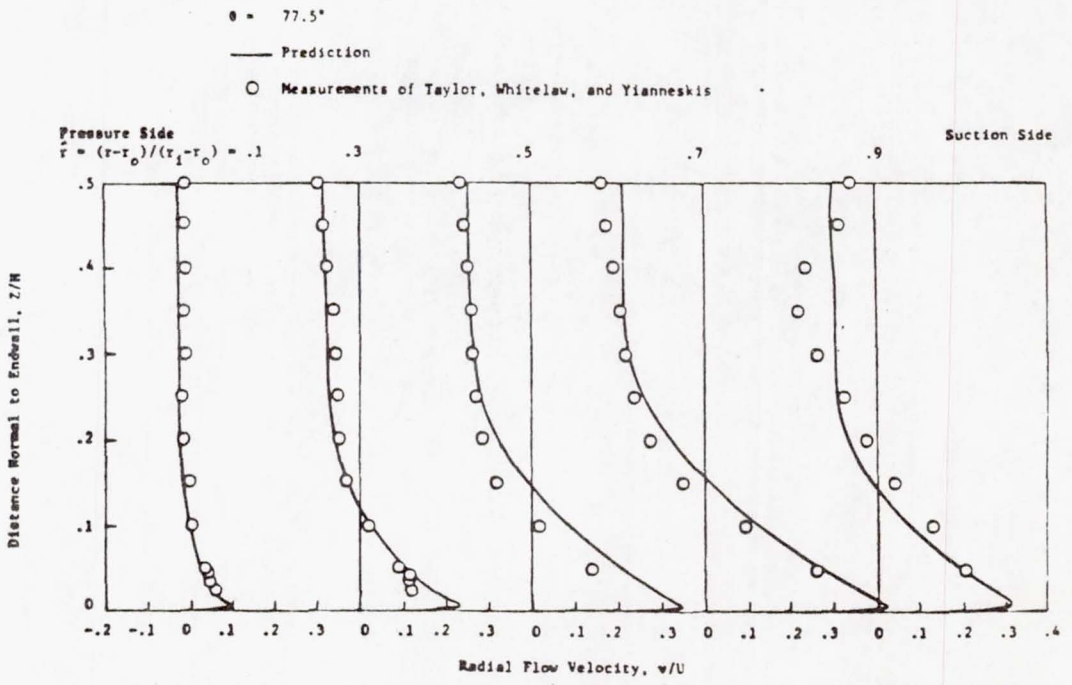

FIG. 36 - BRILEY - COMPUTED AND MEASURED RADIAL FLOW VELOCITY PROFILES AFTER 77.5° TURNING IN CIRCULAR ARC SQUARE DUCT

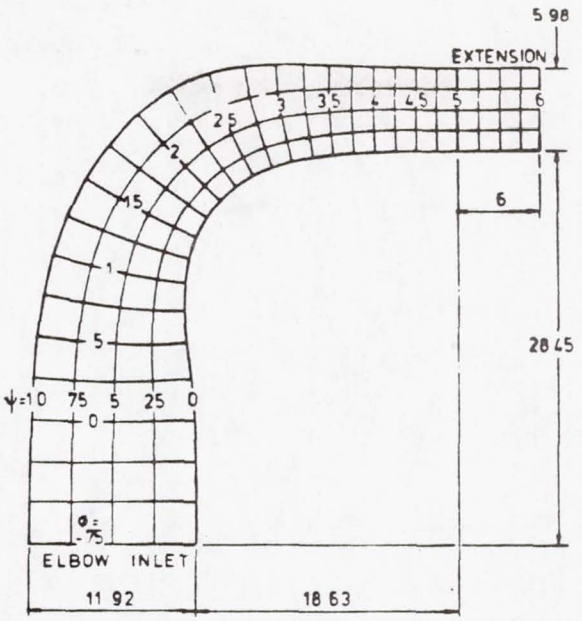

FIG. 37 - STANITZ RECTANGULAR ELBOW WITH STREAMLINES AND POTENTIAL LINES

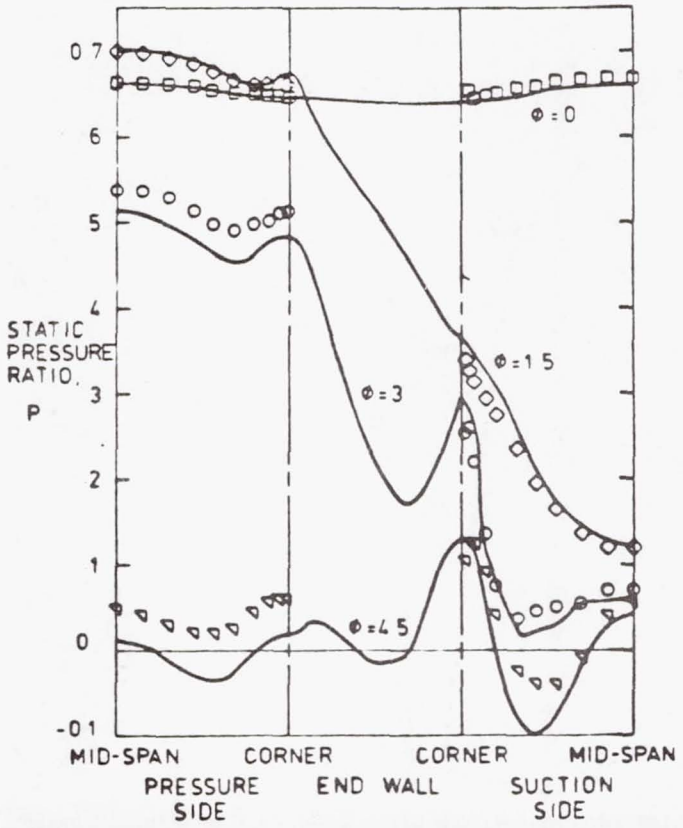

FIG. 38 - MOORE - CALCULATED AND MEASURED WALL STATIC PRESSURE ON SUCTION, PRESSURE AND END WALL SURFACES OF STANITZ ELBOW

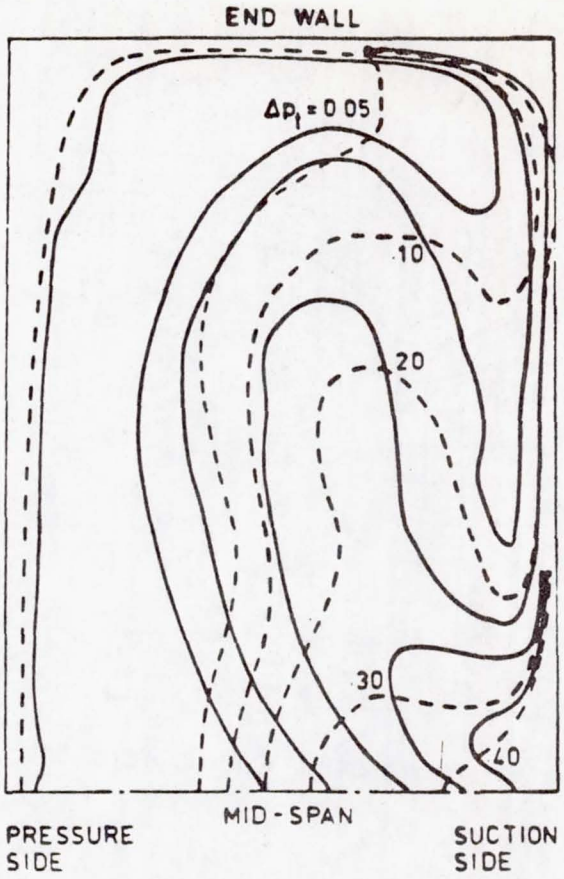

FIG. 39 - MOORE - CALCULATED AND MEASURED TOTAL PRESSURE LOSS CONTOURS AT EXIT OF STANITZ ELBOW

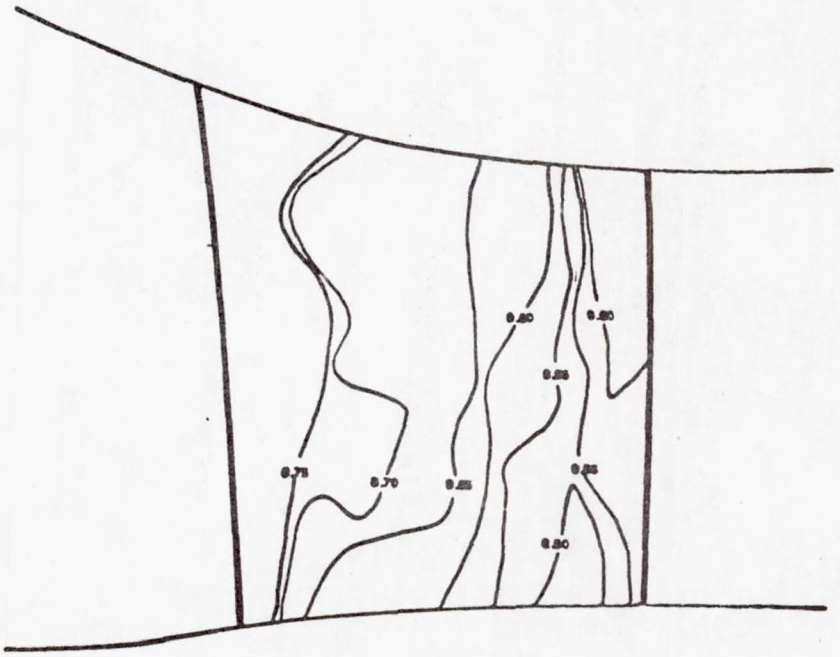

FIG. 40 - DODGE - COMPUTED STATIC PRESSURE ON SUCTION SURFACE OF HIGHLY LOADED TURBINE STATOR

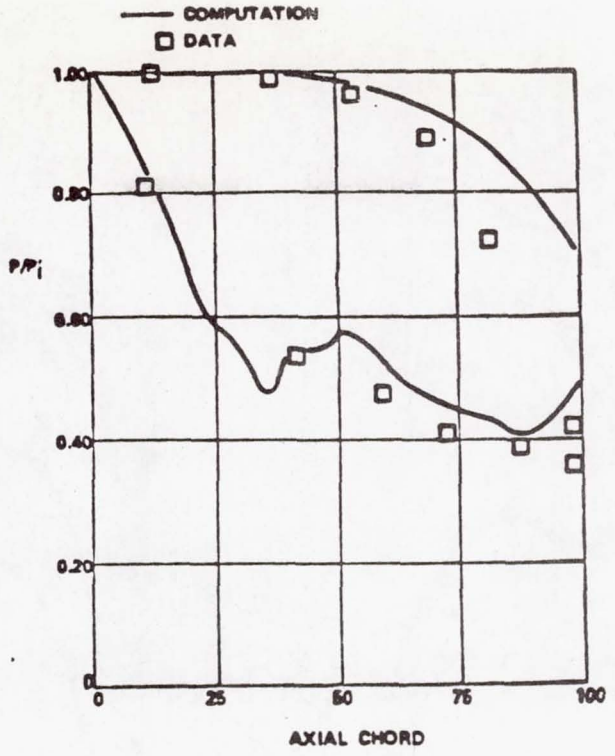

FIG. 41 - DODGE - CALCULATED AND MEASURED STATIC PRESSURES FOR TURBINE STATOR HUB SECTION

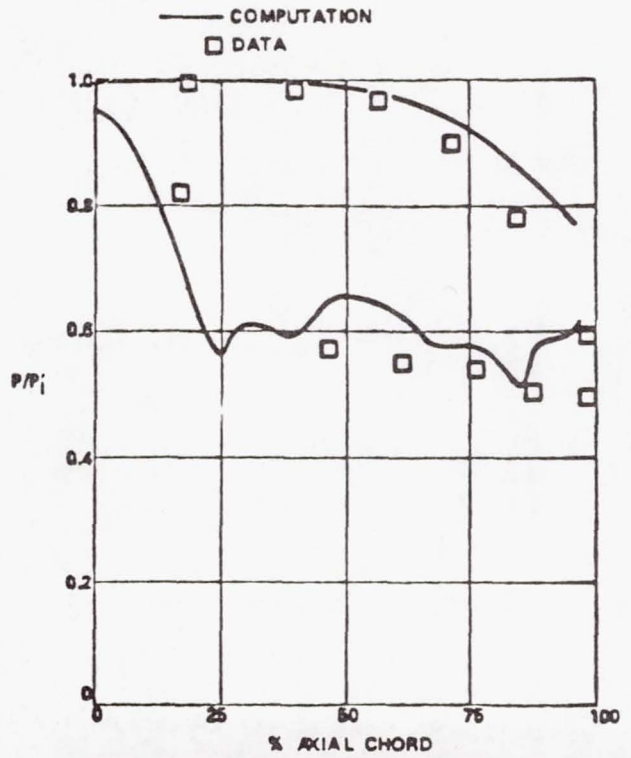

FIG. 42 - DODGE - CALCULATED AND MEASURED STATIC PRESSURES FOR TURBINE STATOR TIP SECTION

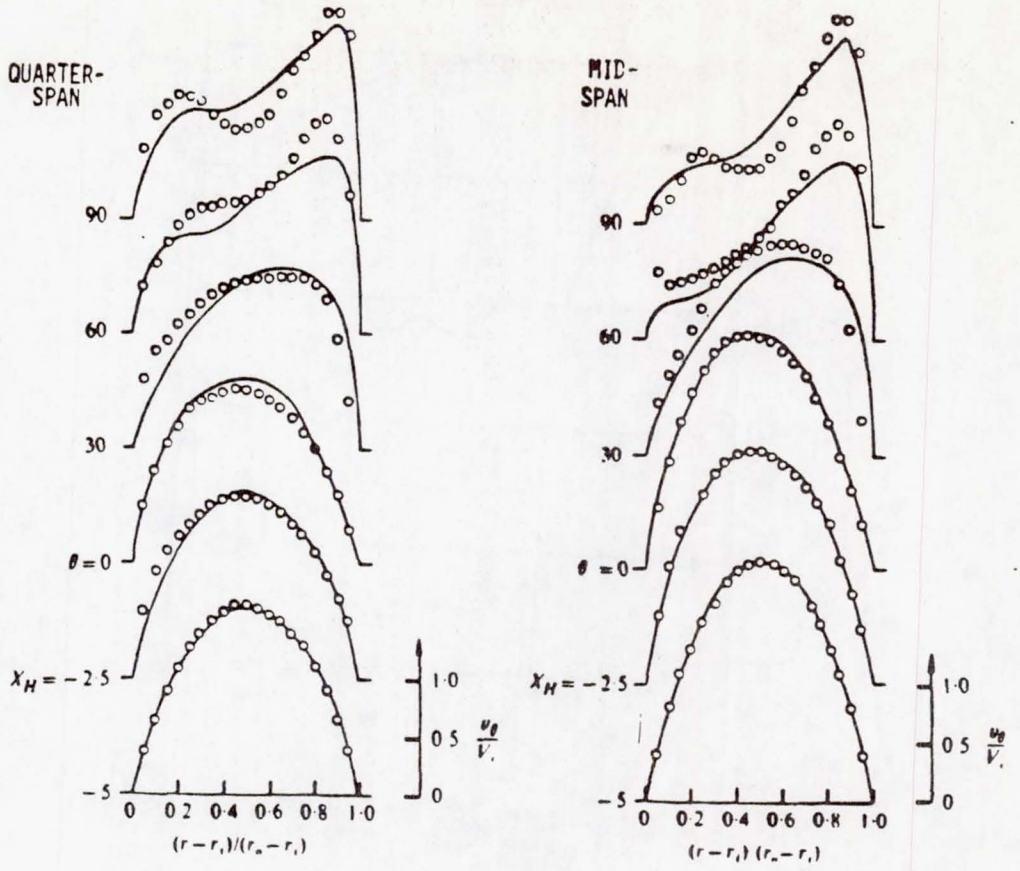

FIG. 43 - HUMPHREY - CALCULATED AND MEASURED PROFILES AT MID-SPAN AND QUARTER-SPAN AROUND CURVED RECTANGULAR DUCT

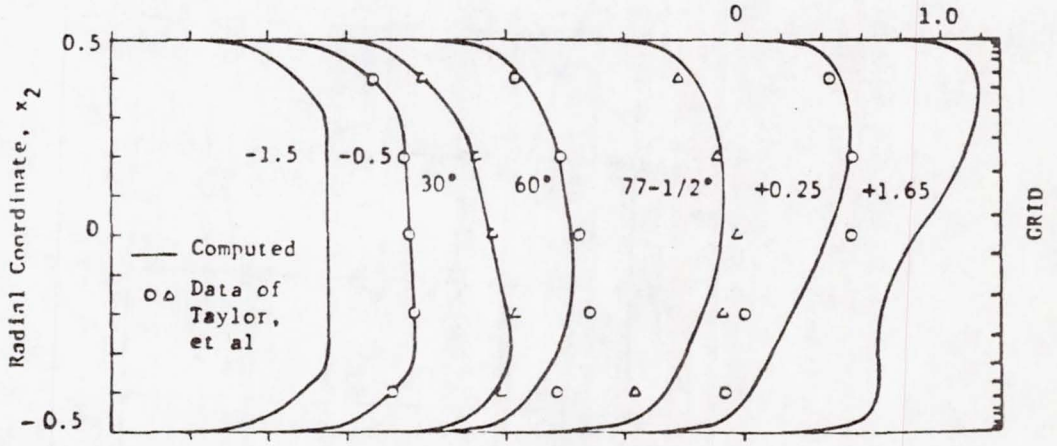

FIG. 44 - BRILEY - COMPUTED AND MEASURED AXIAL VELOCITY PROFILES ALONG SYMMETRY PLANE OF CURVED SQUARE DUCT

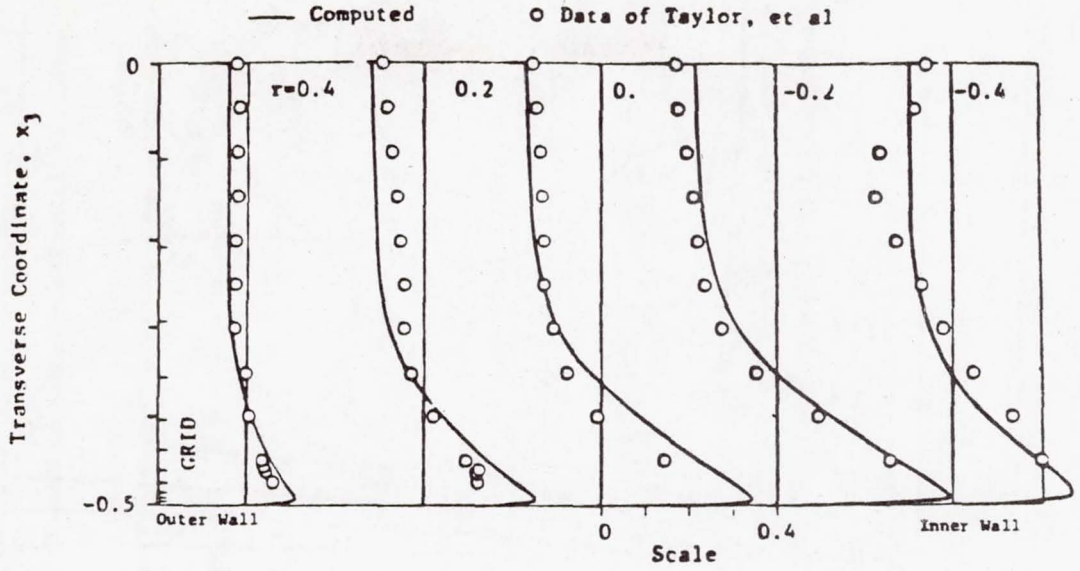

FIG. 45 - BRILEY - COMPUTED AND MEASURED RADIAL FLOW VELOCITY PROFILES AFTER 77.5° TURNING IN CIRCULAR ARC SQUARE DUCT

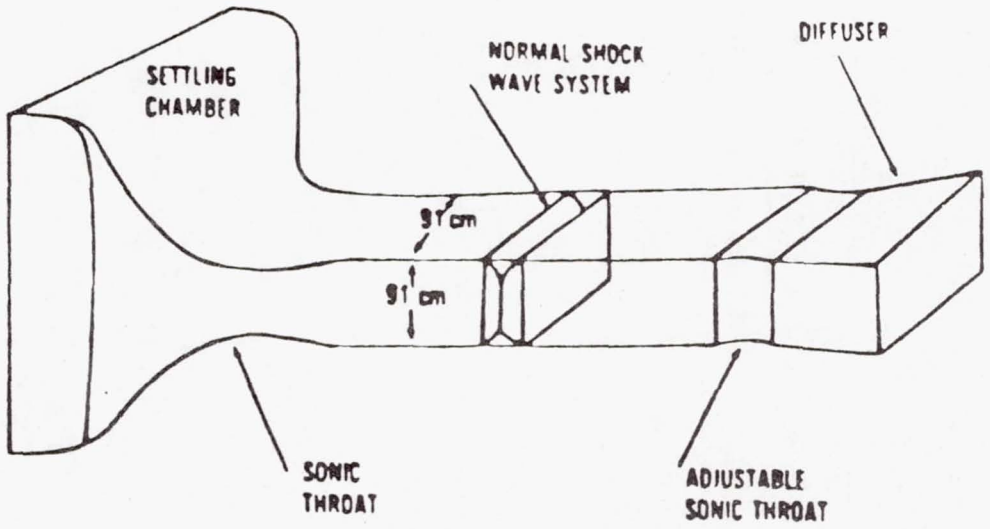

FIG. 46 - SUPERSONIC WIND TUNNEL WITH NORMAL SHOCK WAVE

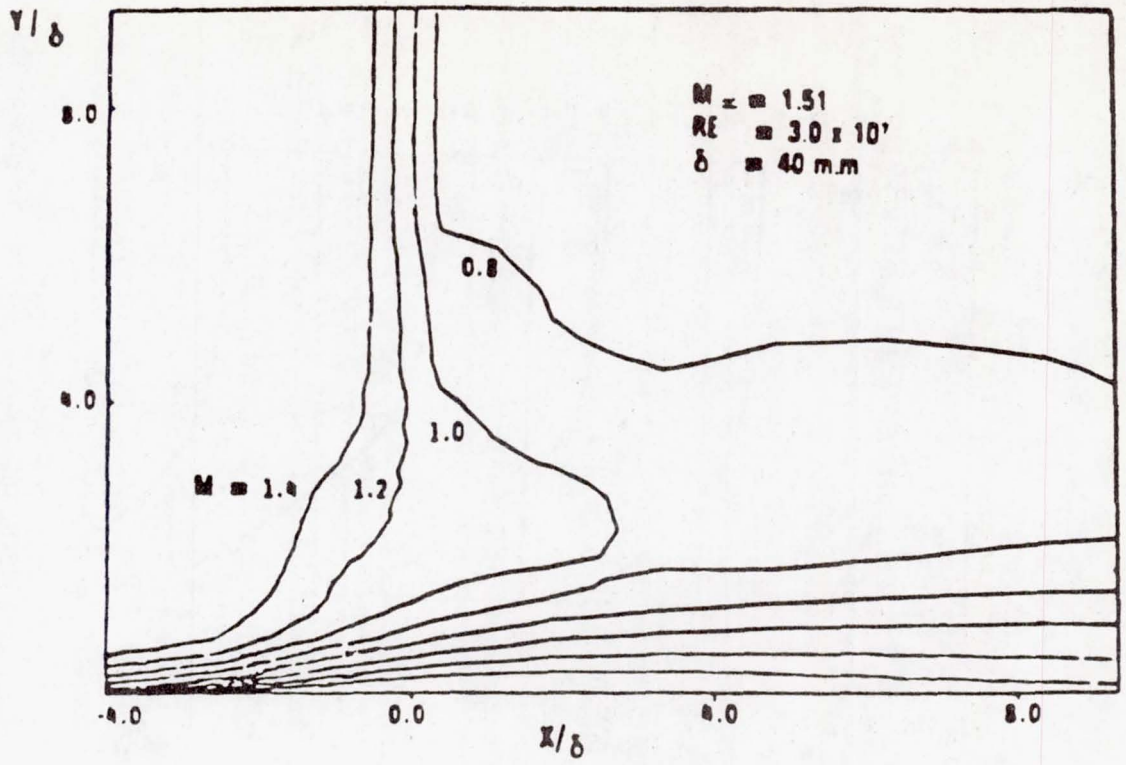

FIG. 47 - SHANG - COMPUTED MACH NUMBER CONTOURS IN PLANE OF SYMMETRY

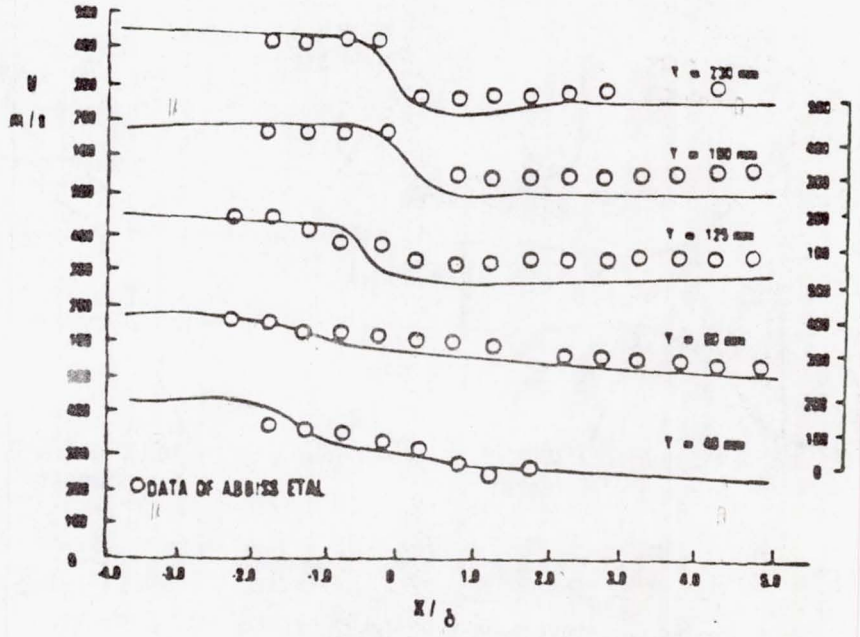

FIG. 48 - SHANG - COMPUTED AND MEASURED VELOCITY IN SYMMETRY PLANE THROUGH INTERACTION REGION

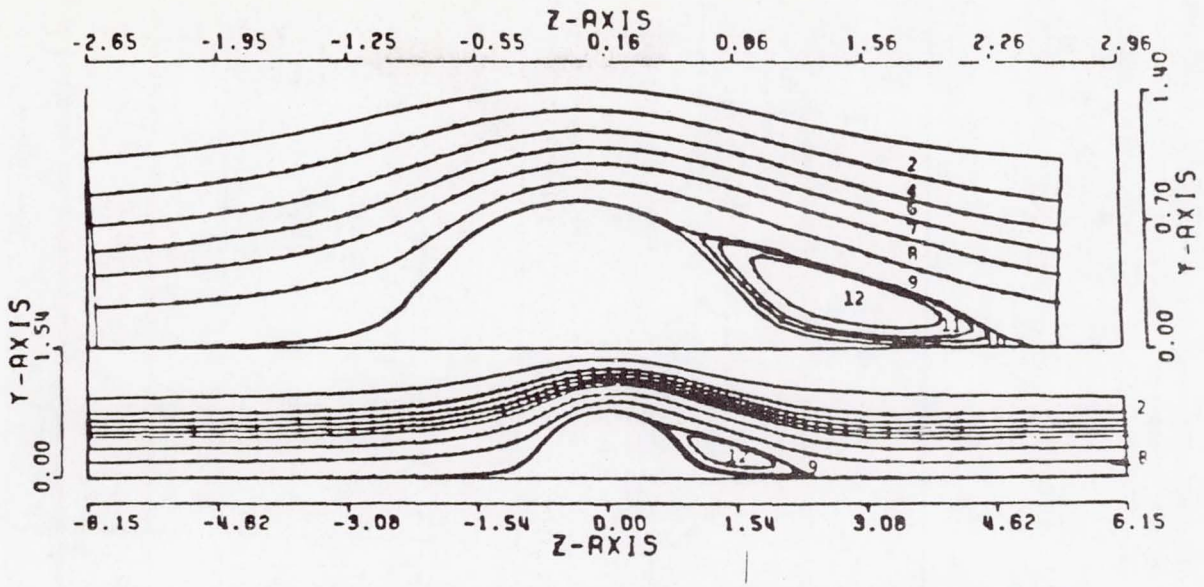

FIG. 49 - GHIA - COMPUTED STREAMLINE CONTOURS FOR CHANNEL WITH CONSTRICTION
RE = 100

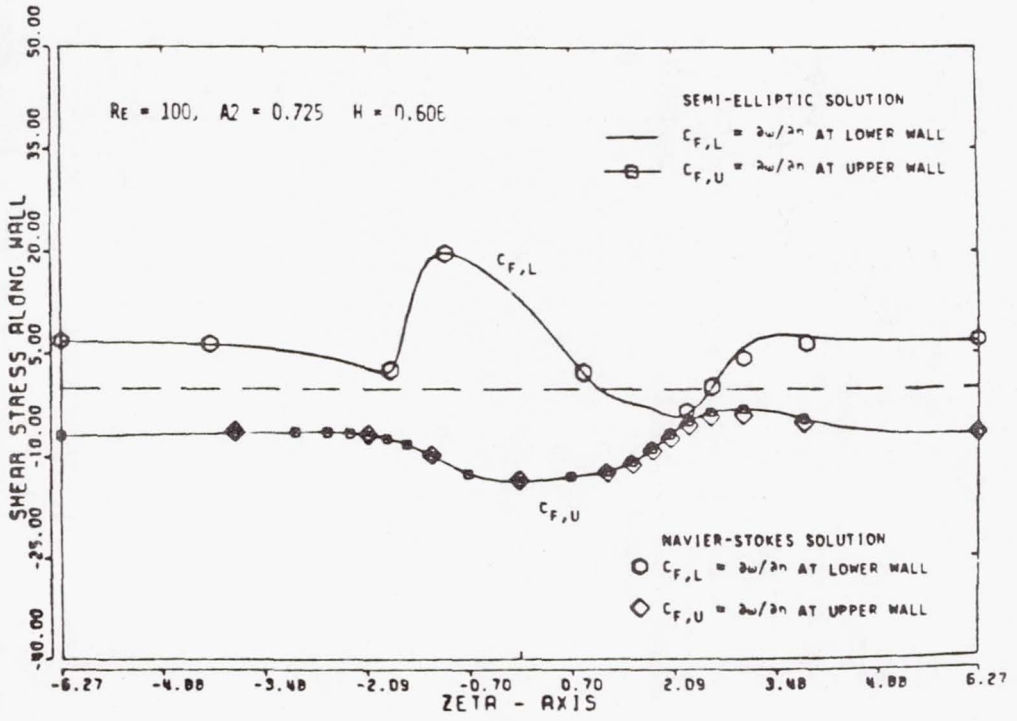

FIG. 50 - GHIA - COMPARISON OF SEMI-ELLIPTIC AND ELLIPTIC COMPUTATIONS FOR WALL SHEAR

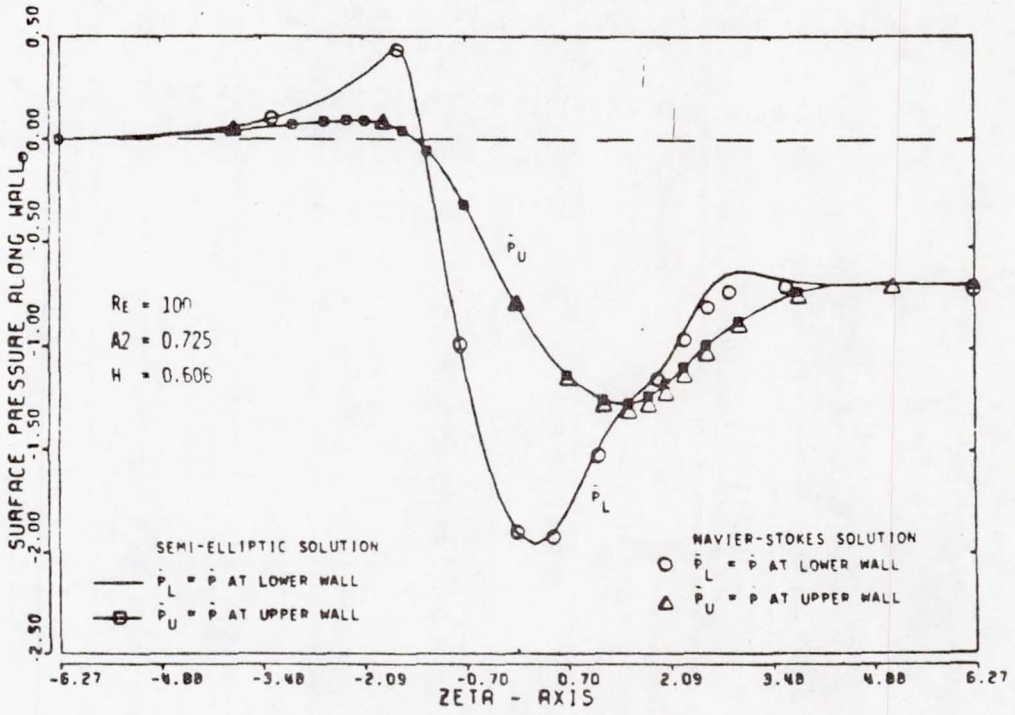

FIG. 51 - GHIA - COMPARISON OF SEMI-ELLIPTIC AND ELLIPTIC COMPUTATIONS FOR WALL STATIC PRESSURE

1. Report No	2. Government Accession No	3. Recipient's Catalog No
NASA TM-82764		

4. Title and Subtitle	5. Report Date
COMPUTATIONAL METHODS FOR INTERNAL FLOWS WITH EMPHASIS ON TURBOMACHINERY	6. Performing Organization Code 505-32-52

7. Author(s)	8. Performing Organization Report No.
William D. McNally and Peter M. Sockol	E-1085

9. Performing Organization Name and Address	10. Work Unit No.
National Aeronautics and Space Administration Lewis Research Center Cleveland, Ohio 44135	11. Contract or Grant No.

12. Sponsoring Agency Name and Address	13. Type of Report and Period Covered
National Aeronautics and Space Administration Washington, D.C. 20546	Technical Memorandum
	14. Sponsoring Agency Code

15. Supplementary Notes

Presented at the Symposium on Computers in Flow Predictions and Fluid Dynamics Experiments at the ASME Winter Annual Meeting, Washington, D.C., November 15-20, 1981.

16. Abstract

A review is given of current computational methods for analyzing flows in turbomachinery and other related internal propulsion components. The methods are divided primarily into two classes, inviscid and viscous. The inviscid methods deal specifically with turbomachinery applications. Viscous methods, on the other hand, due to the state of the art, deal with generalized duct flows as well as flows in turbomachinery passages. Inviscid methods are categorized into the potential, stream function, and Euler approaches. Viscous methods are treated in terms of parabolic, partially parabolic, and elliptic procedures. Various grids used in association with these procedures are also discussed.

17. Key Words (Suggested by Author(s))	18. Distribution Statement
Turbomachinery flows; Duct flows; Inviscid methods; Viscous methods; Stream function; Full potential; Euler equations; Parabolic marching; Elliptic Navier-Stokes	Unclassified - unlimited STAR Category 02

19. Security Classif. (of this report)	20. Security Classif. (of this page)	21. No. of Pages	22. Price*
Unclassified	Unclassified		

* For sale by the National Technical Information Service, Springfield Virginia 22161

National Aeronautics and
Space Administration

Washington, D.C.
20546

Official Business
Penalty for Private Use, $300

SPECIAL FOURTH CLASS MAIL
BOOK

NASA-451

U.S.MAIL

NASA

POSTMASTER: If Undeliverable (Section 158 Postal Manual) Do Not Return